P-13-27

Äspö Hard Rock Laboratory

Difference flow logging in boreholes KA3011A01 and KA3065A01

Eemeli Hurmerinta, Janne Pekkanen
Pöyry Finland Oy

March 2013

Svensk Kärnbränslehantering AB
Swedish Nuclear Fuel
and Waste Management Co

Box 250, SE-101 24 Stockholm
Phone +46 8 459 84 00

ISSN 1651-4416
SKB P-13-27
ID 1351800

Äspö Hard Rock Laboratory

Difference flow logging in boreholes KA3011A01 and KA3065A01

Eemeli Hurmerinta, Janne Pekkanen
Pöyry Finland Oy

March 2013

Keywords: Äspö, Hydrogeology, Hydraulic tests, Difference flow measurements, KA3011A01, KA3065A01, AP TD TUDP002-11-075, Äspö Hard Rock Laboratory.

Abstract

The Posiva Flow Log, Difference Flow Method (PFL DIFF) uses a flowmeter that incorporates a flow guide and can be used for relatively quick determinations of hydraulic conductivity and hydraulic head in fractures/fractured zones in cored boreholes. This report presents the main principles of the methods as well as the results of measurements carried out in underground boreholes KA3011A01 and KA3065A01 at the Äspö Hard Rock Laboratory, Sweden, in January 2012.

The flow logging measurements were done with a 1 m test section by moving the measurement tool in 0.1 m steps. This method was used to flow log the entire measurable part of the boreholes. Each borehole was partially closed during the measurements. Pressure in the borehole was controlled by adjusting flow from the partially closed borehole. The flow measurements were carried out in two different pressure states in the borehole.

The electrical conductivity (EC) and temperature of borehole water were also measured. The EC measurements were used to study the occurrence of saline water in the borehole.

The outflow from the borehole was measured when the borehole was open and when it was partially closed for the measurements.

Sammanfattning

Posiva Flow Log, Differensflödesloggning (PFL DIFF) är en snabb metod för bestämning av transmissiviteten och hydraulisk tryckhöjd i borrhålssektioner och sprickor/sprickzoner i kärnborrhål. Denna rapport presenterar huvudprinciperna för metoden och resultat av mätningar utförda i borrhål KA3011A01 och KA3065A01 inom Äspölaboratoriet, Sverige, i januari 2012.

Flödesmätningarna gjordes med en 1 m lång testsektion som förflyttades successivt i steg om 0,1 m i den mätbara delen av borrhålet. Borrhålet var delvis stängt under mätningarna. Tryck i borrhålet förändrades genom att justera flödet från borrhålet. Flödesmätningarna utfördes i två tryckförhållanden i borrhålet.

Elektrisk konduktivitet (EC) och temperatur på borrhålsvattnet mättes också. EC-mätningarna användes för att studera förekomsten av saltvatten i borrhålet.

Utflödet från borrhålet mättes under tiden detta var öppet eller delvis öppet för mätningarna.

Contents

1 Introduction

Core drilled boreholes KA3011A01 and KA3065A01 at Äspö, Sweden were measured using the Posiva Flow Log, Difference Flow Method (PFL DIFF) which provides a swift, multifaceted characterization of a borehole. The measurements were conducted between January 19 and January 24, 2012. The boreholes are located in the Äspö tunnel at the Äspö Hard Rock Laboratory (HRL).

KA3011A01 is 100.15 m long and its inclination at its reference point at –397.94 m.a.s.l. is –0.9° from the horizontal plane. KA3065A01 is 125.25 m long and its inclination at its reference point at –406.63 m.a.s.l. is –0.65° from the horizontal plane. The boreholes are cased within interval –0.38 m–2.17 m in KA3011A01 and within interval –0.47 m–2.04 m in KA3065A01. The inner diameter of the casing tube is 80 mm. The rest of the boreholes is core drilled with a diameter of c. 76 mm.

The locations of KA3011A01 and KA3065A01 at the Äspö tunnel are illustrated in Figure 1-1.

The field work and the subsequent data interpretation were conducted by Pöyry Finland Oy. PFL DIFF has previously been employed in Posiva's site characterisation programme in Finland as well as at the Äspö HRL, Sweden. The commissions at the latter site included measurements in the 1,700 m long cored borehole KLX02 at Laxemar together with a methodology study (Ludvigson et al. 2002). PFL DIFF was also employed in SKB's site characterisation programme at Laxemar and Forsmark.

The measurements were carried out in accordance to SKB's internal controlling document AP TD TDUP002-11-075. The controlling documents for performing according to this Activity Plan are listed in Table 1-1. The list of the controlling documents excludes the assignment-specific quality plans. Both the Activity Plan and the Method Descriptions are SKB's internal controlling documents. The measurement data and the results were delivered to the SKB site characterization database SICADA and are traceable by the Activity Plan number.

Table 1-1. SKB's internal controlling documents for the activities concerning this report.

Activity Plan	Number	Version
Difference flow logging in borehole KA3011A01 and KA3065A01	AP TD TDUP002-11-075	1.0

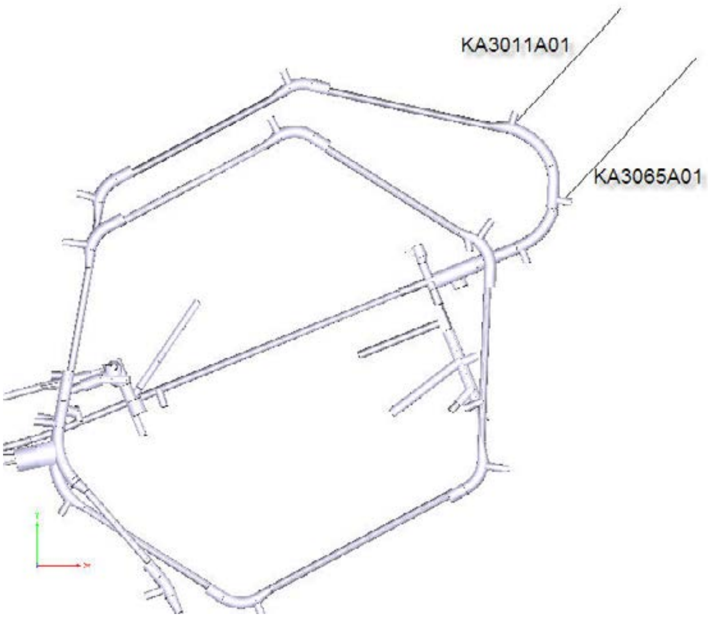

Figure 1-1. *Locations of boreholes KA3011A01 and KA3065A01 in the Äspö tunnel at about –400 m.a.s.l.*

2 Objective and scope

The main objective of the PFL DIFF measurements in KA3011A01 and KA3065A01 is to characterize the rock with respect of its hydraulic properties.

Besides difference flow logging, the measurement programme also included supporting measurements. These measurements included the electrical conductivity (EC) and the temperature of the borehole fluid as well as the single-point resistance of the borehole wall. The flow measurement and the single-point resistance measurement can be used to locate flowing fractures and for depth synchronizing with other methods. Furthermore, the flow rate out from the open or partially closed borehole was recorded.

A high-resolution absolute pressure sensor was used to measure the total pressure along the borehole. These measurements were carried out together with the flow measurements. The results are used in calculation of hydraulic head along the borehole.

3 Principles of measurement and interpretation

3.1 Measurements

Unlike conventional borehole flowmeters which measure the total cumulative flow rate along a borehole, PFL DIFF probe measures the flow rate into or out of defined borehole sections. The advantage that follows from measuring the flow rate in isolated sections is improved detection of incremental changes of flow along the borehole. As these are generally very small, they can easily be missed when using conventional flowmeters.

Rubber sealing disks located at the top and bottom of the probe are used to isolate the flow of water in the test section from the flow in the rest of the borehole, see Figure 3-1. Flow inside the test section is directed through the flow sensor. Flow along the borehole is directed around the test section by means of a bypass pipe and is discharged at either the upper or lower end of the probe. The entire structure is called the flow guide.

Generally two separate measurements with two different section lengths (e.g. 5 m and 1 m) are used. The 5 m setup is usually used first to obtain a general picture of the flow anomalies. It is also good for measuring larger (less than 5 m in length) fractured zones. The 1 m section setup can separate anomalies which are close to each other. There are also many other advantages to using different section lengths.

Flow rates into or out of the test section are monitored using thermistors, which track both the dilution (cooling) of a thermal pulse and its transfer by the moving water (Öhberg and Rouhiainen 2000, pp 11–13). The thermal dilution method is used in measuring flow rates because it is faster than the thermal pulse method, and the latter is used only to determine flow direction within a given time frame. Both methods are used simultaneously at each measurement location.

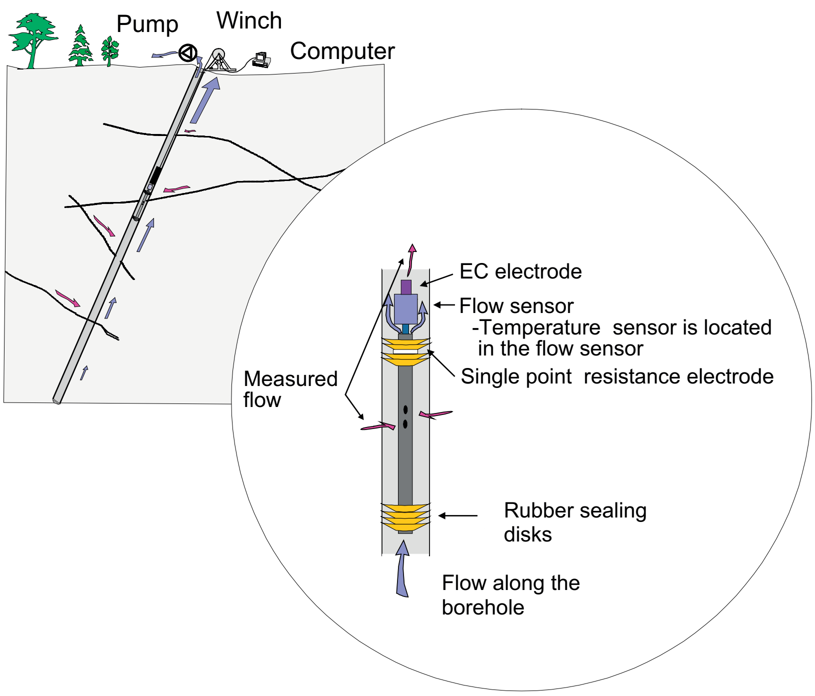

Figure 3-1. *Schematic of the probe used in the PFL DIFF.*

In addition to incremental changes in flow, the PFL DIFF probe can also be used to measure:

- The electrical conductivity (EC) of both borehole water and fracture-specific water. The electrode used in EC measurements is located at the top of the flow sensor, see Figure 3-1.
- The single point resistance (SPR) of the borehole wall (grounding resistance). The electrode used for SPR measurements is located between the uppermost rubber sealing disks, see Figure 3-1, and is used for the high-resolution depth determination of fractures and geological structures.
- The prevailing water pressure profile in the borehole. Located inside the watertight electronics assembly, the pressure sensor transducer is connected to the borehole water through a tube, see Figure 3-2.
- The temperature of the water in the borehole. The temperature sensor is part of the flow sensor, see Figure 3-1.

The principles behind PFL DIFF flow measurements are shown in Figure 3-3. The flow sensor consists of three thermistors (Figure 3-3 a). The central thermistor, A, is used both as a heating element and to register temperature changes (Figures 3-3 b and c). The side thermistors, B1 and B2, serve as detectors of the moving thermal pulse caused by the heating of A.

Flow rate is measured by monitoring heat transients after constant power heating in thermistor A. The measurement begins by constant power (P_1) heating. After the power is cut off the flow rate is measured by monitoring transient thermal dilution (Figure 3-3 c). If the measured flow rate exceeds a certain limit, another constant power heating (P_2) period is started after which the flow rate is re-measured from the following heat transient.

Flows are measured when the probe is at rest. After transferring the probe to a new position, a waiting period (which can be adjusted according to the prevailing circumstances) is allowed to elapse before the heat pulse (Figure 3-3 b) is applied. The measurement period after the constant-power thermal pulse (normally 100 s each time the probe has moved a distance equal to the test section length and 10 s in every other location) can also be adjusted. The longer (100 s) measurement time is used to allow the direction of even the smallest measurable flows to be visible.

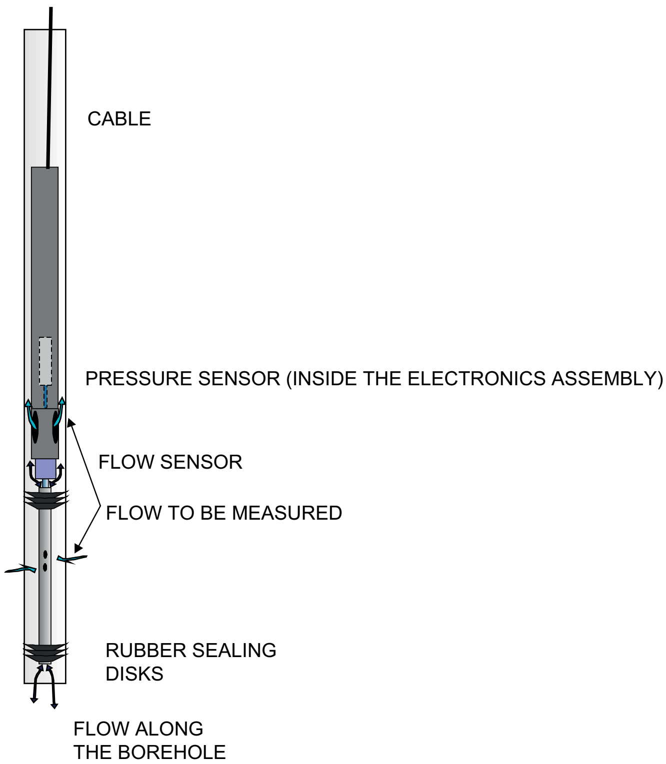

Figure 3-2. *The absolute pressure sensor is located inside the electronics assembly and connected to the borehole water through a tube.*

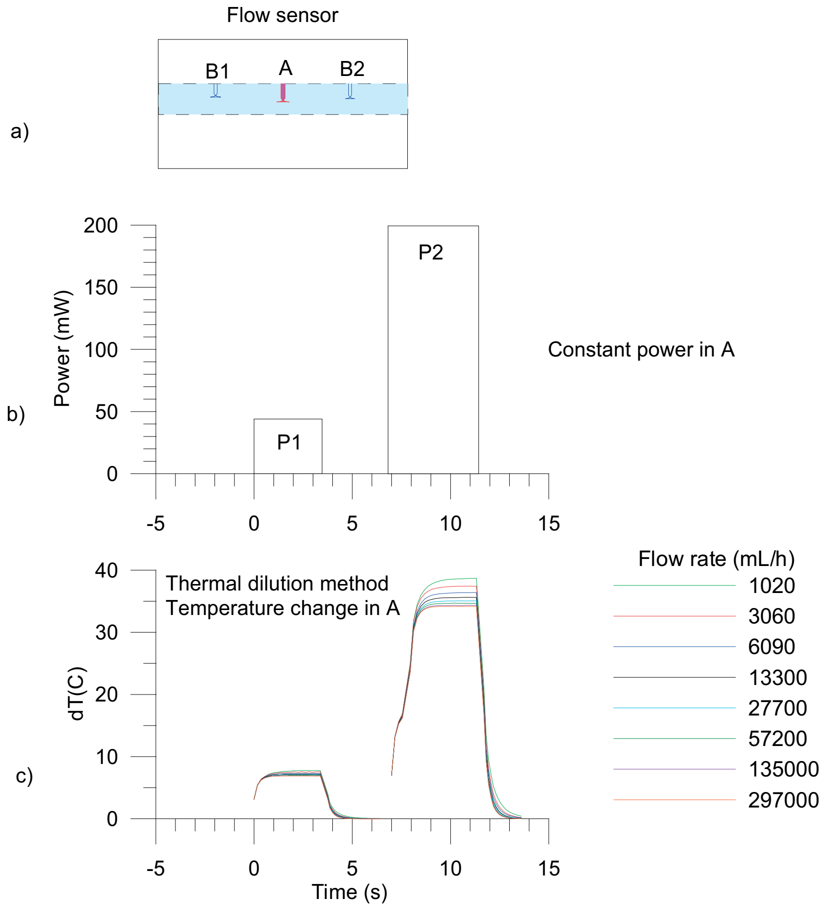

Figure 3-3. *Flow rate measurement.*

The flow rate measurement range is 30 mL/h–300,000 mL/h. The lower limit of measurement for the thermal dilution method is the theoretical lowest measurable value. Depending on conditions in the borehole, these flow limits may not always prevail. Examples of possible disturbances are drilling debris entrained in the borehole water, bubbles of gas in the water and high flow rates (some 30 L/min, i.e., 1,800,000 mL/h or more) along the borehole. If the disturbances encountered are significant, limits on practical measurements are calculated for each set of data.

The device depth reference point in the PFL DIFF is situated at the upper end of the test section.

3.2 Interpretation

The interpretation of data is based on Thiem's or Dupuit's formula, which describes a steady state and two-dimensional radial flow into the borehole (de Marsily 1986):

$$h_S – h = Q/(T \cdot a) \qquad 3\text{-}1$$

where h is the hydraulic head in the vicinity of the borehole and $h = h_S$ at the radius of influence (R),
Q is the flow rate into the borehole,
T is the transmissivity of the test section,
a is a constant depending on the assumed flow geometry. For cylindrical flow, the constant a is:

$$a = 2 \cdot \pi / \ln(R/r_0) \qquad 3\text{-}2$$

where
r_0 is the radius of the well and
R is the radius of influence, i.e., the zone inside which the effect of pumping is felt.

If measurements of flow rate are carried out using two levels of hydraulic head in the borehole, i.e. natural and pump-induced heads, then the undisturbed (natural) hydraulic head and the transmissivity of the borehole sections tested can be calculated. Equation 3-1 can be reformulated in the following two ways:

$$Q_{S0} = T_S \cdot a \cdot (h_S - h_0) \qquad 3\text{-}3$$

$$Q_{S1} = T_S \cdot a \cdot (h_S - h_1) \qquad 3\text{-}4$$

where

h_0 and h_1 are the hydraulic heads in the borehole at the test levels,

Q_{S0} and Q_{S1} are the measured flow rates in the test section,

T_S is the transmissivity of the test section and

h_S is the undisturbed hydraulic head of the tested zone far from the borehole.

In general, since very little is known about the flow geometry, cylindrical flow without skin zones is assumed. Cylindrical flow geometry is also justified because the borehole is at a constant head, and no strong pressure gradients along the borehole exist except at its ends.

The radial distance R to the undisturbed hydraulic head h_S is not known and must be assumed. Here a value of 500 is selected for the quotient R/r_0.

The hydraulic head and the test section transmissivity can be deduced from the two measurements:

$$h_S = (h_0 - b \cdot h_1)/(1 - b) \qquad 3\text{-}5$$

$$T_S = (1/a)\ (Q_{S0} - Q_{S1})/(h_1 - h_0) \qquad 3\text{-}6$$

where

$b = Q_{S0}/Q_{S1}$

The transmissivity (T_f) and hydraulic head (h_f) of individual fractures can be calculated provided that the flow rates at the individual fractures are known. Similar assumptions to those employed above must be used (a steady-state cylindrical flow regime without skin zones).

$$h_f = (h_0 - b \cdot h_1)/(1 - b) \qquad 3\text{-}7$$

$$T_f = (1/a)\ (Q_{f0} - Q_{f1})/(h_1 - h_0) \qquad 3\text{-}8$$

where

Q_{f0} and Q_{f1} are the flow rates at a fracture and h_f and T_f are the hydraulic head (far away from borehole) and transmissivity of a fracture, respectively.

Since the actual flow geometry and any skin effects are unknown, transmissivity values should only be considered as an indication of the prevailing orders of magnitude. As the calculated hydraulic heads do not depend on geometrical properties but only on the ratio of the flows measured at different heads in the borehole, they should be less sensitive to unknown fracture geometry. A discussion of potential uncertainties in the calculation of transmissivity and hydraulic head can be found in Ludvigson et al. (2002).

4 Equipment specification

In the PFL DIFF method, the flow of groundwater into or out of a borehole section is monitored using a flow guide which employs rubber sealing disks to isolate any such flow from the flow of water along the borehole. This flow guide defines the test section being measured without altering the hydraulic head. Groundwater flowing into or out of the test section is guided to the flow sensor, and flow is measured using the thermal pulse and thermal dilution methods. Measured values are transferred to a computer in digital form.

Type of instrument:	PFL DIFF probe.
Borehole diameters:	56 mm, 66 mm and 76 mm (or larger).
Length of test section:	The flow guide length can be varied.
Method of flow measurement:	Thermal pulse and thermal dilution.
Range and accuracy of measurement:	See Table 4-1.
Additional measurements:	Temperature, Single point resistance, Electrical conductivity of water, Water pressure.
Winch:	Mount Sopris Wna 10, 0.55 kW, conductors, Gerhard-Owen cable head.
Depth determination:	Based on a digital distance counter.
Logging computer:	PC (Windows 7).
Software:	Based on MS Visual Basic.
Total power consumption:	1.5–2.5 kW depending on the type of pump employed.
Calibration of flow probe:	August 2010 (Probe PFL8).

The range and accuracy of the sensors used is shown in Table 4-1.

Table 4-1. Range and accuracy of sensors.

Sensor	Range	Accuracy
Flow	30–300,000 mL/h	± 10% curr.value
Temperature (central thermistor)	0–50°C	0.1°C
Temperature difference (between outer thermistors)	–2 to +2°C	0.0001°C
Electrical conductivity of water (EC)	0.02–11 S/m	± 5% curr.value
Single point resistance (SPR)	5–500,000 Ω	± 10% curr.value
Groundwater level sensor	0–0.1 MPa	± 1% full-scale
Air pressure sensor	800–1,060 hPa	± 5 hPa
Absolute pressure sensor	0–20 MPa	± 0.01% full-scale

5 Execution of measurements

5.1 General

The work commission was performed according to Activity Plan AP TD TDUP002-11-075 following the SKB Method Description 322.011e, Version 2.0 (Method description for Difference Flow Logging), see Table 1-1. The Activity Plan and the Method Description are both SKB's internal controlling documents. Prior to the measurements, the downhole tools and the measurement cable were disinfected. Time was synchronized to local Swedish time, UTC +2 (Central European Summer Time). The activity schedule of the borehole measurements is presented in Table 5-1. The items and activities in Table 5-1 are the same as in the Activity Plan.

Logging cables, wires, and pipe strings are exposed to stretching when lowered into a vertical or sub-vertical borehole. This will introduce a certain error in defining the position of a test tool connected to the end of a logging cable. A linear length calibration was made based on borehole casing length, on the cable counter and on length marks marked into the measurement cable.

The outflow from the open or partially closed borehole was measured during the measurements.

The dummy logging (Item 7) of the borehole is done in order to assure that the measurement tools do not get stuck in the borehole. The dummy also collects solid material from the borehole wall. The solid material in the dummy is used for evaluation whether it is safe to continue with other logging tools.

The overlapping flow logging (Item 8 and Item9) was carried out in the partially closed borehole in a two different difference pressure state with a 1 m section length and in 0.1 m length increments (step length). Different pressure states in the borehole were achieved by adjusting the outflow of the partially closed borehole. The borehole was closed after these measurements.

The electrical conductivity (EC) and temperature of borehole water (Item 8 and Item9) were measured during flow logging measurements.

The measurement arrangements are shown in Figures 5-1 and 5-2. The measurement trailer is mobilised at KA3011A01, see Figure 5-1 and at KA3065A01, see Figure 5-2.

Table 5-1. Flow logging and testing in KA3011A01 and KA3065A01. Activity schedule.

Item	Activity	Explanation	Date
2	Mobilisation at site (KA3065A01)	Unpacking the trailer. Pressure in closed borehole 3,700 kPa.	2012-01-19
7	Dummy logging	Borehole stability/risk evaluation.	2012-01-19
8	Overlapping flow logging – partially closed borehole	Section length L_w=1 m. Step length dL=0.1 m. Measurement depth 123.31 m–1.08 m. Absolute pressure from 1,251 kPa to 1,040 kPa. Dp=2,660 kPa–2,449 kPa.	2012-01-19 – 2012-01-20
9	Overlapping flow logging – partially closed borehole	Section length L_w=1 m. Step length dL=0.1 m. Measurement depth 123.31 m–1.2 m. Absolute pressure from 3,513 kPa to 3,418 kPa. Dp=187 kPa–282 kPa.	2012-01-21 – 2012-01-22
10 and 2	Demobilisation at KA3065A01 and mobilisation at KA3011A01	Packing the trailer and closing the borehole. Moving to KA3011A01. Unpacking the trailer. Pressure in closed borehole KA3011A01 3,700 kPa.	2012-01-23
7	Dummy logging	Borehole stability/risk evaluation.	2012-01-23
9	Overlapping flow logging – partially closed borehole	Section length L_w=1 m. Step length dL=0.1 m. Measurement depth 98.35 m–2.04 m. Absolute pressure from 3,284 kPa to 3,128 kPa. Dp=416 kPa–572 kPa.	2012-01-23 – 2012-01-24
8	Overlapping flow logging – partially closed borehole	Section length L_w=1 m. Step length dL=0.1 m. Measurement depth 98.35 m–1.54 m. Absolute pressure from 2,216 kPa to 1,968 kPa. Dp=1,484 kPa–1,732 kPa.	2012-01-24
10	Demobilisation	Packing the trailer. Closing the borehole.	2012-01-25

Figure 5-1. Measurement trailer mobilised at KA3011A01.

Figure 5-2. Measurement trailer mobilised at KA3065A01.

5.2 Nonconformities

In the first measurement (Item 8 in KA3065A01) the rubber cone installation was unsuccessful. Outflow from the borehole was c. 67–70 l/min, see Figure 5-3, and the flow rate was over the measurement limit at fractures 10.0 m, 23.4 m and 116.3 m. When the rubber cone was opened afterwards the brass adapter (see Figure 5-4) was slipped off from its correct position within the rubber cone. Measurement was not repeated due to the time constraints. The positive side of the high outflow (and low pressure in the borehole) is that the ratio of the flow rates of the two loggings (with high and low outflow) is high. This improves the accuracy of the interpretation of hydraulic head of fractures.

Flow logging measurement (Item 8 in KA3065A01) had stopped at the depth 101.9 m because borehole was opened by SKB's contractor. Water was spraying from the borehole at the top of the measurement trailer and the contractor thought that the measurement devices could get damaged. While the borehole was opened, tension of the cable went below the lower limit and stopped the measurement. This caused a one day delay to the measurements.

It was not physically possible to measure approximately one meter of the bottom of the boreholes. There was a centralizer attached to the measurement device, which reduces the measured distance by c. 0.85 m. The rubber sealing disks in the device must also be flipped before the measurement begins. This reduces the measured distance for approximately 0.10 m. It is possible that there were also drill cuttings at the bottom of the boreholes.

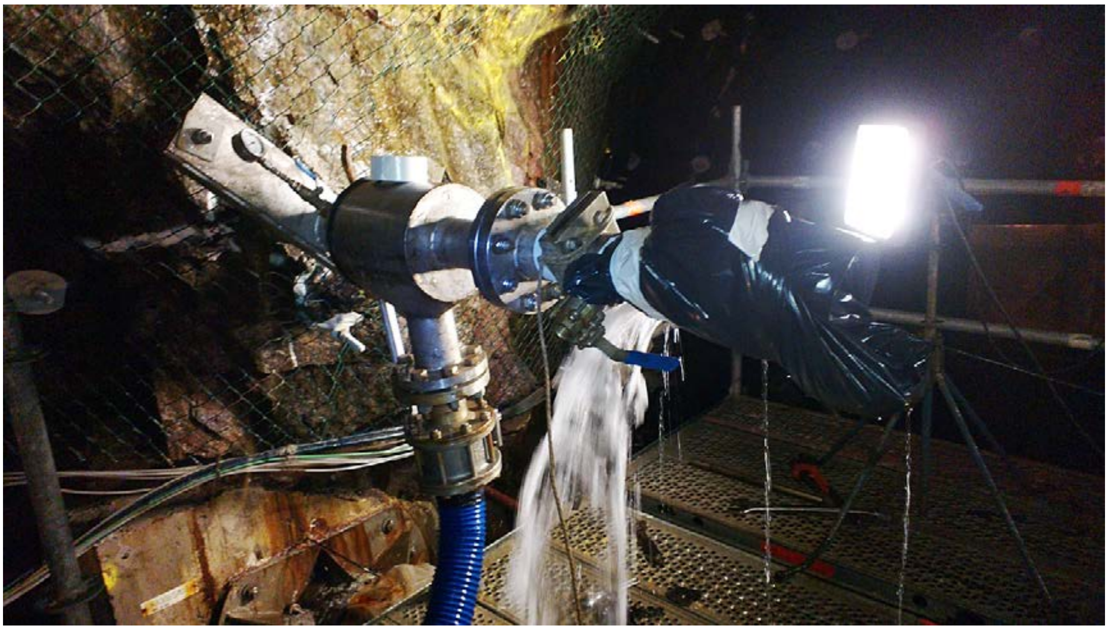

Figure 5-3. *Outflow from the borehole at KA3065A01.*

Figure 5-4. *Brass adapter and rubber cone.*

6 Results

6.1 Length calibration

6.1.1 SPR measurement

An accurate length scale for the measurements is difficult to achieve in long boreholes. The main cause of inaccuracy is the stretching of the logging cable. The stretching depends on the tension on the cable, the magnitude of which in turn depends, among other things, on the inclination of the borehole and the roughness (friction properties) of the borehole wall. The cable tension is larger when the borehole is measured upwards. The cables, especially new cables, may also stretch out permanently.

A linear length calibration was made based on borehole casing length, the cable counter and length marks marked on the measurement cable. The borehole casing length at the upper end of the borehole was detected by single-point resistance (SPR) measurements using the SPR sensor of the PFL DIFF probe. At the end of the borehole measurement length was adjusted using cable length marks. Length corrected SPR results are shown in Appendices 1 and 11.

6.1.2 Estimated error in location of detected fractures

In spite of the length correction in described above, there can still be length errors due to the following reasons:

1. The point interval in the overlapping mode flow measurements is 0.1 m. This could cause an error of ± 0.05 m.
2. The length of the test section is not exact. The specified section length denotes the distance between the nearest upper and lower rubber sealing disks. Effectively, the section length can be larger. At the upper end of the test section there are four rubber sealing disks. The distance between them is 5 cm. This will cause rounded flow anomalies: a flow may be detected already when a fracture is situated between the upper rubber sealing disks. These phenomena can cause an error of ± 0.05 m when the short step length (0.1 m) is used.
3. The cable stretches under tension. When the probe is lifted upwards at c. 1,000 m the tension can be c. 175 kg. When it is lowered at the same length, the tension can be c. 75 kg. This difference could cause a depth difference of c. 3 m between the measurements at depth of c. 1,000 m. The tension values here are estimates and can vary greatly depending on the device setup and hole properties.
4. The total error in the worst case can be estimated. With a 0.1 m point interval in the borehole without a length marks the error would be:

   $E = 0.\ 1 + d \cdot 0.002$

   where E (m) is the total estimated error and d (m) is the cable length in the borehole shown by the cable counter of the winch. For a 100 m long borehole E would be ± 0.3 m. Note that this is only a rough estimate and it is subject to change. It should also be noted that this is only one way of estimating the error. There are no length marks in boreholes KA3011A01 and KA3065A01.

Fractures nearly parallel with the borehole may also be problematic. Fracture location may be difficult to define accurately in such cases.

6.2 Electrical conductivity and temperature

6.2.1 Electrical conductivity and temperature of borehole water

The electrical conductivity of the borehole water (borehole EC) was measured during the flow logging measurements. The measurement was performed upwards, see Appendices 2.1, 12.1 (linear scale), 2.2 and 12.2 (logarithmic scale).

Borehole EC profile was relatively constant during measurements in different borehole pressure states. In KA3011A01 borehole EC was about 0.8 S/m–0.9 S/m except at the fracture area c. 35 m where borehole EC increased to about 1.0 S/m, see Appendix 2.1.

In KA3065A01 borehole EC was lower at the bottom of the borehole – c. 25 m, value varied from about 0.75 S/m to about 0.9 S/m. During the high flow measurement there was a positive EC anomaly (1.3 S/m) at about 25 m and a negative EC anomaly (0.7 S/m) at about 10 m, see Appendix 12.1.

The temperature of the borehole water was measured simultaneously with the EC and flow measurements. The EC values are temperature corrected to 25°C to make them more comparable with other EC measurements (Heikkonen et al. 2002). There is increase of temperature at the high flow fractures at about 35 m and 81 m in KA3011A01, see Appendix 2.3. There is also increase of temperature at the high flow fractures at 10 m and 25 m in KA3065A01, see Appendix 12.3.

6.3 Absolute pressure and outflow measurements

Absolute pressure was registered together with the other measurements in Items 8–9. The pressure sensor measures the sum of hydrostatic pressure in the borehole and air pressure. The hydraulic head along the borehole at natural and pumped conditions is determined in the following way. First, the monitored air pressure at the site is subtracted from the measured absolute pressure. The hydraulic head (h) at a certain elevation (z) is calculated according to the following expression according to:

$$h = (p_{abs} - p_b)/(\rho_{fw} \cdot g) + z \qquad \text{6-1}$$

where

h is the hydraulic head (m.a.s.l.) according to the RHB 70 reference system,

p_{abs} is the absolute pressure (Pa),

p_b is the barometric (air) pressure (Pa),

ρ_{fw} is the unit density, 1,000 kg/m^3

g is the standard gravity, 9.80665 m/s^2 and

z is the elevation of measurement (m.a.s.l.) according to the RHB 70 reference system.

A sensor-specific offset of 6.9 kPa is added to absolute pressure results.

The calculated head distributions are presented in Appendices 10.1–10.3 and 20.1–20.3. The exact z-coordinates are important in head calculation. A 10 cm error in the z-coordinate means a 10 cm error in the head.

Borehole outflow was measured manually during the measurements. The results are shown in Appendices 10.3 and 20.3. Two different pressure states in the boreholes were achieved by adjusting the partially closed borehole outflow. After the measurements the boreholes were closed.

In KA3065A01 borehole pressure was also monitored with manual pressure meter which was mounted to the casing tube by SKB's personnel. Results are plotted in Appendix 20.3 (green dots).

6.4 Flow logging

6.4.1 General comments on results

The measuring programme contained several flow logging sequences. The results were plotted on the same diagram with single-point resistance (right hand side), see Appendices 3.1–3.5 and 13.1–13.6. SPR has a lower value on a fracture where flow is detected. Many other resistance anomalies result from other fractures and geological features. As the electrode of the SPR tool is located within the upper rubber sealing disks of the probe, the locations of resistance anomalies associated with leaky fractures coincide with the lower end of the flow anomalies.

The flow logging was performed with a 1 m section length and with 0.1 m length increments. The method (overlapping flow logging) gives the length and the thickness of conductive zones with a length resolution of 0.1 m.

The direction of small flows (< 100 mL/h) cannot be detected in the normal overlapping mode (thermal dilution method). Therefore the measurement time was longer (so that the thermal pulse method could be used) at every 1 metre interval.

The test section length determines the width of a flow anomaly of a single fracture. If the distance between flow yielding fractures is less than the section length, the anomalies will overlap, resulting in a stepwise flow data plot. The overlapping flow logging was repeated using a 1 m long test section and 0.1 m length increments.

The positions (borehole length) of the detected fractures are shown on the length scale together with their positions. They are interpreted on the basis of the flow curves and therefore represent flowing fractures. A long line represents the location of a leaky fracture; a short line denotes that the existence of a leaky fracture is uncertain. The short line is used if the flow rate is less than 30 mL/h or the flow anomalies are overlapping or unclear because of noise.

The coloured triangles show the magnitude and direction of the measured flows. The triangles have the same colour than the corresponding curves.

The explanations to the tables in Appendices 5.1–5.3, 7.1, 7.2, 15.1–15.5, 17.1 and 17.2 are given in Appendices 4 and 14.

6.4.2 Transmissivity of borehole sections

The entire borehole was flow logged with a 1 m section length and with 0.1 m length increments in a two different pressure states. In the first measurement at KA3011A01 absolute pressure was from 3,284 kPa (head –64 m in RHB 70 scale) to 3,128 kPa (head –79 m in RHB 70 scale) and in the second measurement from 2,216 kPa (head –173 m in RHB 70 scale) to 1,968 kPa (head –197 m in RHB 70 scale), see Appendix 10.2.

In the first measurement at KA3065A01 absolute pressure was from 1,251 kPa (head –280 m in RHB 70 scale) to 1,040 kPa (head –301 m in RHB 70 scale) and in the second measurement from 3,513 kPa (head –49 m in RHB 70 scale) to 3,418 kPa (head –59 m in RHB 70 scale), see Appendix 20.2.

Two sets of flow measurements are needed for calculation of transmissivity as described in Section 3, Equation 3-6. In this case the borehole was all the time partially closed in a different outflow and pressure state. Head in the open borehole is the water level at the top of the borehole (–397.94 m in KA3011A01 and –406.63 in KA3065A01 in RHB 70 scale).

The results of the flow logging measurements with a 1 m section length are presented in tables of Appendices 5.1–5.3 and 15.1–15.5. Only the results with 1 m length increments are used. All borehole sections are shown in Appendices 3.1–3.5 and 13.1–13.6. Secup and Seclow in Appendices 5.1–5.3 and 15.1–15.5 are the distances along the borehole from the reference level (tunnel wall) to the upper end of the test section and to the lower end of the test section, respectively.

Pressure was measured and calculated as described in Section 6.3. h_{1FW} and h_{2FW} in Appendices 5.1–5.3 and 15.1–15.5 represent heads in the borehole in different pressure states. The head in the borehole and calculated heads of formations or fractures are given in RHB 70 scale.

The flow rates are positive if the flow direction is from the bedrock into the borehole and negative to the other direction. 38 sections in KA3011A01 and 45 sections in KA3065A01 were flow yielding in the measurement where borehole outflow was the highest. All of the flows were positive. 28 sections in KA3011A01 were flow yielding in the measurement where borehole outflow was the lowest. All of the flows were positive. 40 sections in KA3065A01 were flow yielding in the measurement where borehole outflow was the lowest, seven of which had a flow direction from the borehole into the bedrock.

The flow data is presented as a plot, see Appendices 6.1 and 16.1. The left-hand plot in each diagram represents flow from the borehole into the bedrock for the respective test sections, while the right-hand plot represents flow from the bedrock into the borehole. If flow could not be detected (zero flow), no corresponding point will be visible on the logarithmic plots in the appendices.

The lower and upper measurement limits of the flow are also presented in the plot (Appendices 6.1 and 16.1) and in the tables (see Appendices 5.1–5.3 and 15.1–15.5). There are theoretical and practical lower limits of flow, see Section 6.4.4.

The hydraulic head and transmissivity (T_D) of borehole sections can be calculated from the flow data using the method described in Chapter 3. The results are illustrated in Appendices 6.2 and 16.2. The hydraulic head of sections is presented in the plots if none of the two flow values at the same length is equal to zero. Transmissivity is presented if none or just one of the flows is equal to zero.

In KA3011A01 the sum of all the detected flows (Q_1) was $2.1 \cdot 10^{-4}$ m^3/s (12.5 L/min). Manually measured outflow from the borehole was approximately 12.4–13.0 L/min during the measurement. The sum of all the detected flows (Q_2) was $5.0 \cdot 10^{-5}$ m^3/s (3.0 L/min). The manually measured outflow from the borehole was approximately 2.0–3.2 L/min during the measurement. Sum of detected flows and manually measured flow are consistent.

In KA3065A01 the sum of all the detected flows (Q_1) was $6.3 \cdot 10^{-4}$ m^3/s (38.0 L/min). Manually measured outflow from the borehole was approximately 67.0–70.0 L/min during the measurement. The sum of all the detected flows (Q_2) was $4.9 \cdot 10^{-5}$ m^3/s (2.9 L/min). The manually measured outflow from the borehole was approximately 2.0–3.6 L/min during the measurement. Sum of detected flows (Q_2) and manually measured flow are consistent. Sum of detected flows (Q_1) and manually measured flow correspond to each other poorly. The sum of the measured flow was uncertain because the measurement limit was exceeded and there may be flowing fractures at the immeasurable part of the borehole at the bottom.

6.4.3 Transmissivity of fractures

An attempt was made to evaluate the magnitude of fracture-specific flow rates. The results for a 1 m section length and 0.1 m length increments were used for this purpose. The first step in this procedure was to identify the locations of individual flowing fractures and then evaluate their flow rates.

In cases where the fracture distance is less than one metre, it may be difficult to evaluate the flow rate. There are such cases for instance in Appendix 3.2. In these cases a stepwise increase or decrease in the flow data plot equals the flow rate of a specific fracture (filled triangles in the appendices).

The total amount of detected flowing fractures was 43 in KA3011A01 and 59 in KA3065A01. These fractures were used for transmissivity estimations. Transmissivity of fractures is presented in Appendices 7.1–7.2, 8, 17.1–17.2 and 18.

Some fracture-specific results were classified to be "uncertain." The basis for this classification is either a minor flow rate (< 30 mL/h) or unclear fracture anomalies. Anomalies are considered unclear if the distance between them is less than 1 m or their nature is unclear because of noise.

Fracture-specific transmissivities were compared with transmissivities of sections in Appendices 9 and 19. All fracture-specific transmissivities within each 1 m interval were first summed together to make them comparable with transmissivities of sections. Transmissivities of sections were calculated from the flow rates of 1 m depth increments.

There is nearly perfect fit of the two transmissivities. The explanation is that both of them are interpreted from the same data set. This plot was used in the iterative process of interpreting fracture flow rates. A deviation of transmissivity in this plot would mean that there is something wrong in the interpreted fracture flow rate. Normally there are measurements in two different section lengths (often 5 m and 1 m) and the usage of this type of plot is different because two separate measurements are then compared.

6.4.4 Theoretical and practical measurement limits of flow and transmissivity

The theoretical minimum for measurable flow rate is some 30 mL/h. The upper limit of flow measurement is 300,000 mL/h. As these upper and lower limits are determined by flow calibration, it is assumed that flows can be reliably detected between the upper and lower theoretical limits in favorable borehole conditions.

In practice, the minimum measurable flow rate may be much higher. Borehole conditions may have an influence on the flow base level (i.e. noise level). Noise levels can be evaluated in intervals along the borehole where there are no flowing fractures or other complicating structures, and may vary along a borehole.

There are several known reasons for increased noise in the flow:

1) Roughness of the borehole wall.
2) Solid particles such as clay or drilling debris in the water.
3) Gas bubbles entrained in the water.
4) High flow rate along the borehole.

Roughness in the borehole wall always results in high levels of noise, not only in the flow results, but also in the SPR results. The flow curve and SPR curves are typically spiky when the borehole wall is rough.

Drilling debris usually increases noise levels. This kind of noise is typical for both natural (un-pumped) and pumped conditions.

Pressure of flowing water is released when it enters into the borehole. This may lead to the release of dissolved gas and increase the quantity of gas bubbles entrained in the water. Some fractures may produce more gas than others. Sometimes, when the borehole is being measured upwards, increased noise levels are observed just above certain fractures. The reason for this is assumed to be gas bubbles.

The effect of a high flow rate along the borehole can often be seen above fractures with a high flow. Any minor leakage in the seal provided by the lower rubber sealing disks will appear in the measurement as increased levels of noise.

A high level of noise in a flow will mask the "real" flow if this is smaller than the noise. Real flows are registered correctly if they are about ten times larger than the noise but are totally invisible if they are some ten times smaller than the noise. Experience indicates that real flows between one-tenth of the noise level and 10 times the noise level are summed with the noise. Noise levels could therefore be subtracted from measured flows to get real flows. This correction has not yet been carried out because the cases to which it is applicable are unclear.

The practical minimum for measurable flow rate is presented in Appendices 3.1–3.5 and 13.1–13.6 using a grey dashed line (Lower limit of flow rate). The practical minimum level of the measurable flow was evaluated using the flow data obtained in the 1 m section length measurements with higher outflow. The limit is an approximation. It is evaluated to obtain a limit below which there may be fractures or structures that remain undetected.

The noise level was 30 mL/h in KA3011A01 and varied between 30 mL/h and 400 mL/h in KA3065A01. In good conditions it may be possible to detect flow anomalies below the limit of the thermal dilution method (30 mL/h). Nevertheless the noise line (grey dashed line) is chosen to be 30 mL/h and anomalies below 30 mL/h are considered to be uncertain.

In some boreholes the upper limit of flow measurement (300,000 mL/h) may be exceeded. Such fractures or structures hardly remain undetected (as the fractures below the lower limit). There were such fractures detected in KA3065A01 during this campaign.

The practical minimum for measurable flow rate is also presented in Appendices 5.1–5.3 and 15.1–15.5 (Q-lower limit P) and is obtained from the plots in Appendices 3.1–3.5 and 13.1–13.6 (Lower limit of flow rate). The practical minimum of measurable transmissivity can be evaluated using

Q-lower limit and the assumed head difference at each measurement location, see Appendices 5.1–5.3 and 15.1–15.5 (T_D-measl$_{LP}$). The theoretical minimum for measurable transmissivity (T_D-measl$_{LT}$) is evaluated using a Q value of 30 mL/h (the minimum theoretical flow rate using the thermal dilution method). The upper measurement limit for transmissivity can be evaluated using the maximum flow rate (300,000 mL/h) and the assumed head difference as above, see Appendices 5.1–5.3 and 15.1–15.5 (T_D-measl$_U$). These transmissivity limits are only qualitative because of the assumptions described in Section 6.4.2.

All three flow limits are plotted with the measured flow rates, see Appendices 6.1 and 16.1. The three transmissivity limits are also presented graphically, see Appendices 6.2 and 16.2.

Similar flow and transmissivity limits are not provided for the fracture-specific results as the limits for these are harder to define. The situation is similar for the upper flow limit. If several high-flowing fractures are positioned closer to one another than a distance of 1 m, the upper flow limit will depend on the sum of these flows, and this must be below 300,000 mL/h.

6.4.5 The flow rate estimations in KA3065A01

In borehole KA3065A01 the sum of all detected flows (Q_1) was remarkable smaller than the manually measured outflow during the measurement with higher flow rate. There were three very transmissive fractures that were over the measurable flow limit. These also had exceptionally low flow ratio (Q_1/Q_2). There was also one possible flowing fracture at the bottom that had a flow rate that could not be reliably interpreted, see Figure 6.1. The difference between the sum of the flows and manually measured flows was c. 32 L/min. The aim was to estimate these four flows so that the sum of all flows would correspond to the manual flow measurement from the top of the borehole.

For the evaluation of corrected flows it was assumed that the four mentioned flows were too small with the same factor (k). Factor k can be estimated as follows:

$k = (Q_m - (Q_s - Q_i))/Q_i$ 6-1

$Q_n = k \times Q_1$ 6-2

where

k is the factor for flow

Q_m is the manually measured outflow (70 L/min)

Q_s is the sum of all flowing fractures

Q_i is the sum of flows of the four fractures which are under the evaluation (sum of Q_1 in Table 6-1)

Q_n is the evaluated flow

Q_1 is flow measured with the PFL probe

Factor k was solved from the equations above (k=2.4). Evaluated flows, transmissivities and fracture heads are presented in the Table 6-1 and in Appendix 18 (red crosses).

With the evaluated flow rates the flow balance in the borehole is better and also the resulted hydraulic head for these four fractures looks more realistic. Therefore the evaluated fracture heads ($h_{i\,n-2}$), transsmissivities ($T_{D\,n-2}$) and flows (Q_n) are possibly closer to the real values than the original values. The evaluated values are still highly speculative and therefore they are not reported in the Sicada tables.

Table 6-1. Inferred flow anomalies from overlapping flow logging and evaluated flow, transmissivity and head.

Length to flow anom. L (m)	h_{1FW} (m.a.s.l.)	Q_1 (mL/h)	h_{2FW} (m.a.s.l.)	Q_2 (mL/h)	h_{nFW} (m.a.s.l.)	Q_n (mL/h)	$T_{D\,1-2}$ (m^2/s)	$h_{i\,1-2}$ (m.a.s.l.)	$T_{D\,n-2}$ (m^2/s)	$h_{i\,n-2}$ (m.a.s.l.)
10	–297.65	403,000	–51.05	–54,300	–297.65	982,779	5.10E–07	–80.33	1.16E–06	–63.96
24.3	–297.61	409,000	–52.36	21,300	–297.61	997,411	4.34E–07	–38.89	1.09E–06	–47.00
116.3	–285.96	462,000	–56.95	107,000	–285.96	1,126,660	4.26E–07	12.08	1.22E–06	–32.92
124.4*	–279.75	36,100	–58.72	6,940	–279.75	88,035	3.62E–08	–6.12	1.01E–07	–39.80

* Uncertain fracture.

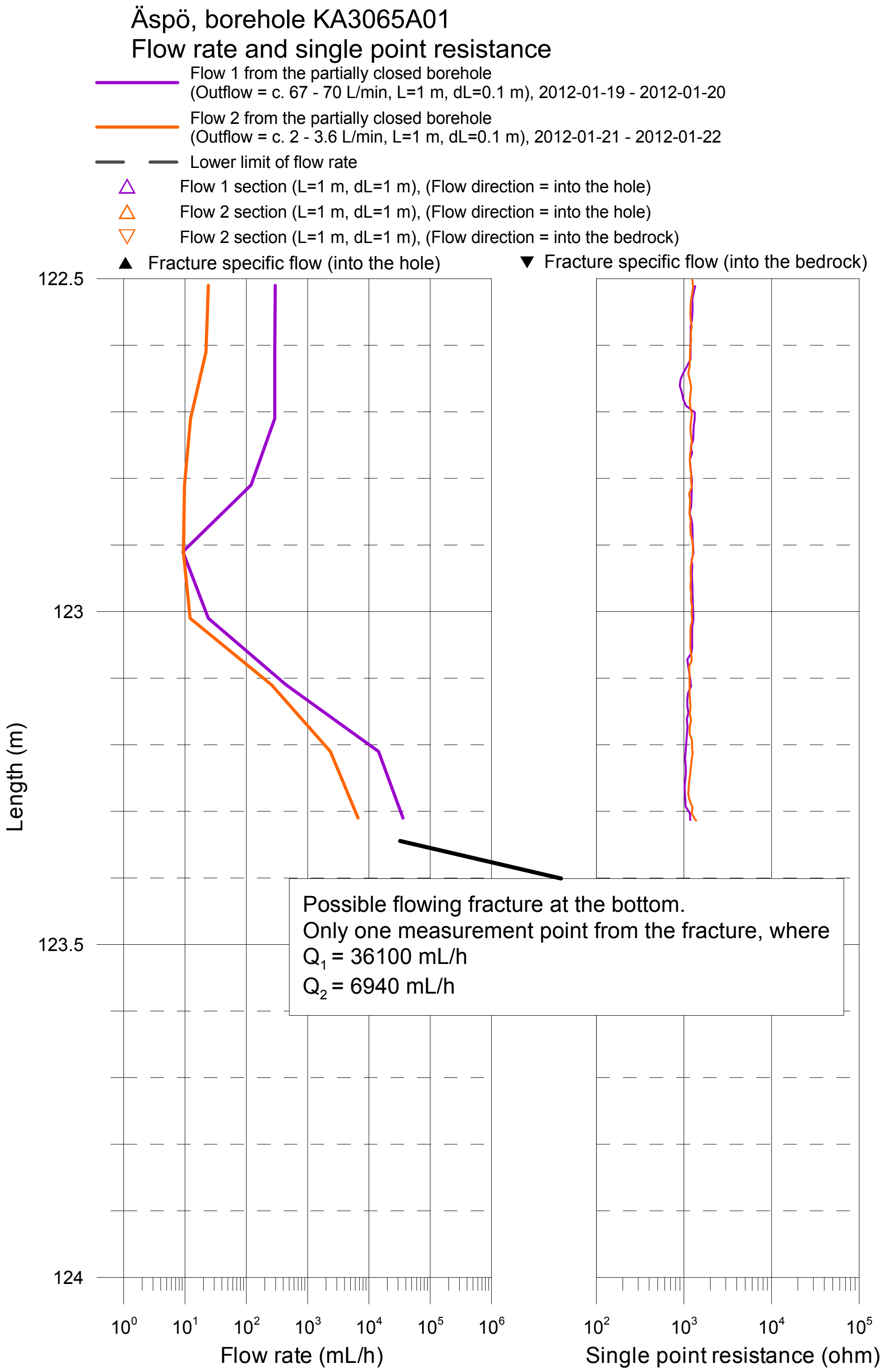

Figure 6-1. *Possible flowing fracture at the bottom of the borehole.*

7 Summary

In this study, the Posiva Flow Log, Difference Flow Method has been used to determine the location and flow rate of flowing fractures or structures in boreholes KA3011A01 and KA3065A01 in the Äspö HRL, Sweden. A 1 m section length with 0.1 m length increments was used in the measurements. The borehole was partially closed during the measurements. The whole borehole was measured twice with different pressure states by adjusting the partially closed borehole's outflow.

It is possible to interpret transmissivity and hydraulic head of fractures if the borehole is measured in two different pressure conditions. The prerequisites to a reliable interpretation are among others that the measured flow rates are within the limits of measurements and that the ratio of the measured flow rates is large enough when measured at the same depth. These prerequisites were not completely fulfilled for technical reasons and for the tight time schedule.

Length calibration was made by using the borehole's casing lower end as a depth mark, the cable counter and the cable's length marks. The single point resistance was measured simultaneously with the flow measurements, and thus all flow results could be length synchronized by synchronizing the single-point resistance logs.

Electrical conductivity and temperature of the borehole water were also logged during the flow measurements.

References

SKB's (Svensk Kärnbränslehantering AB) publications can be found at www.skb.se/publications.

de Marsily G, 1986. Quantitative hydrogeology: groundwater hydrology for engineers. London: Academic Press.

Heikkonen J, Heikkinen E, Mäntynen M, 2002. Pohjaveden sähkönjohtavuuden lämpötilakorjauksen matemaattinen mallinnus synteettisten vesinäytteiden mittauksista (Mathematical modelling of temperature adjustment algorithm for groundwater electrical conductivity on basis of synthetic water sample analysis). Posiva Työraportti 2002-10, Posiva Oy, Finland. (In Finnish.)

Ludvigson J-E, Hansson K, Rouhiainen P, 2002. Methodology study of Posiva difference flow meter in borehole KLX02 at Laxemar. SKB R-01-52, Svensk Kärnbränslehantering AB.

Öhberg A, Rouhiainen P, 2000. Posiva groundwater flow measuring techniques. Posiva 2000-12, Posiva Oy, Finland.

SPR results after length correction

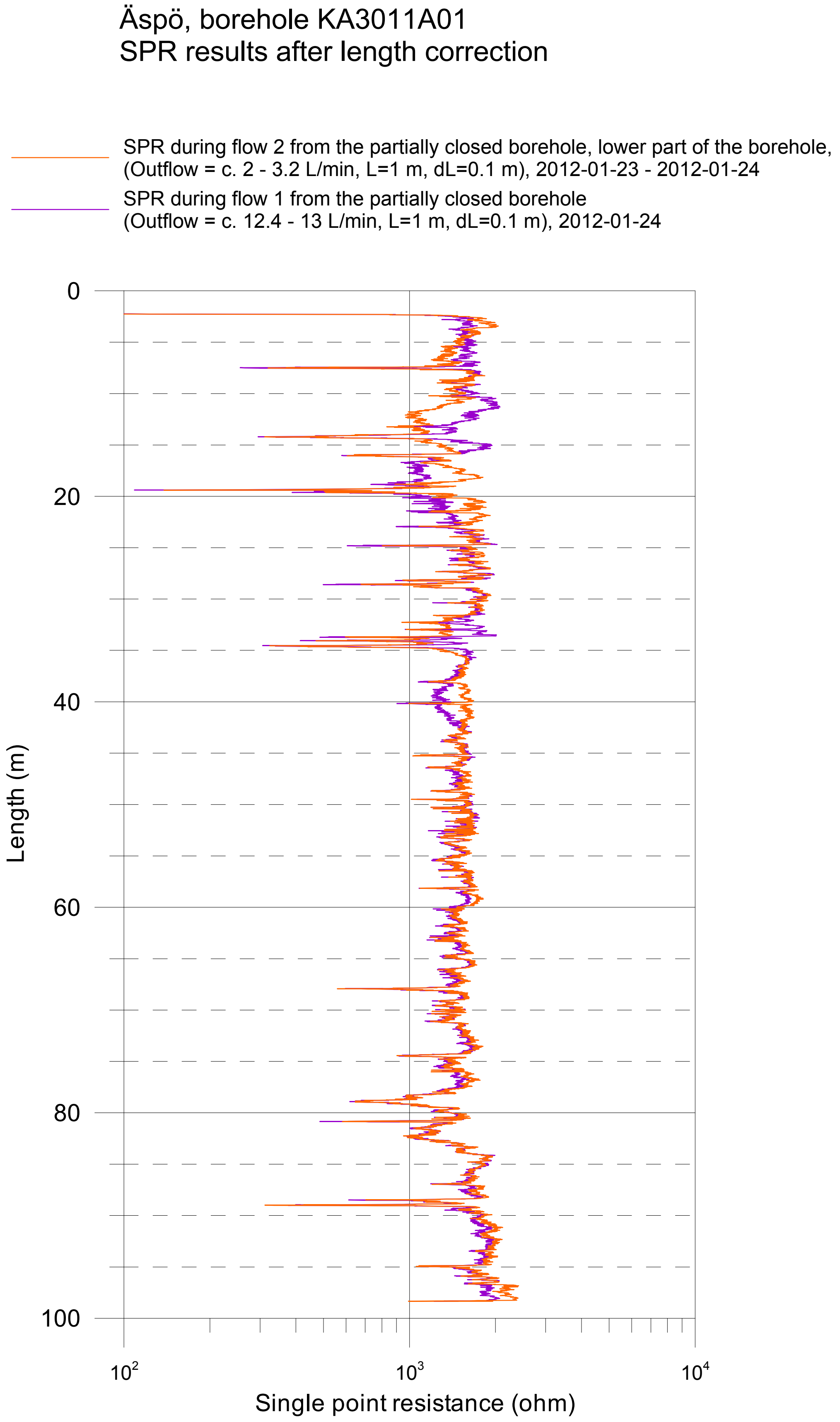

Electrical conductivity of borehole water

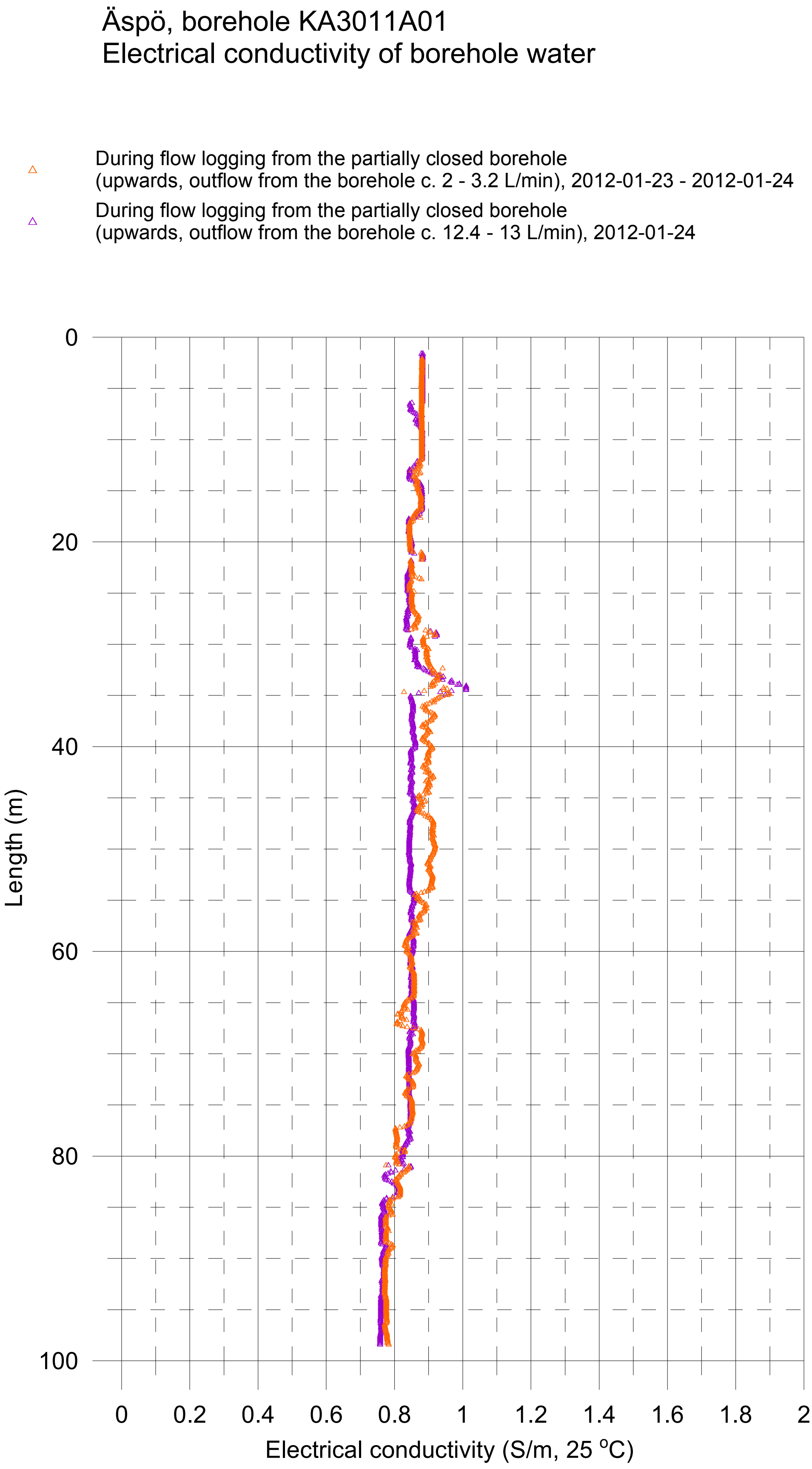

Appendix 2.2

Electrical conductivity of borehole water

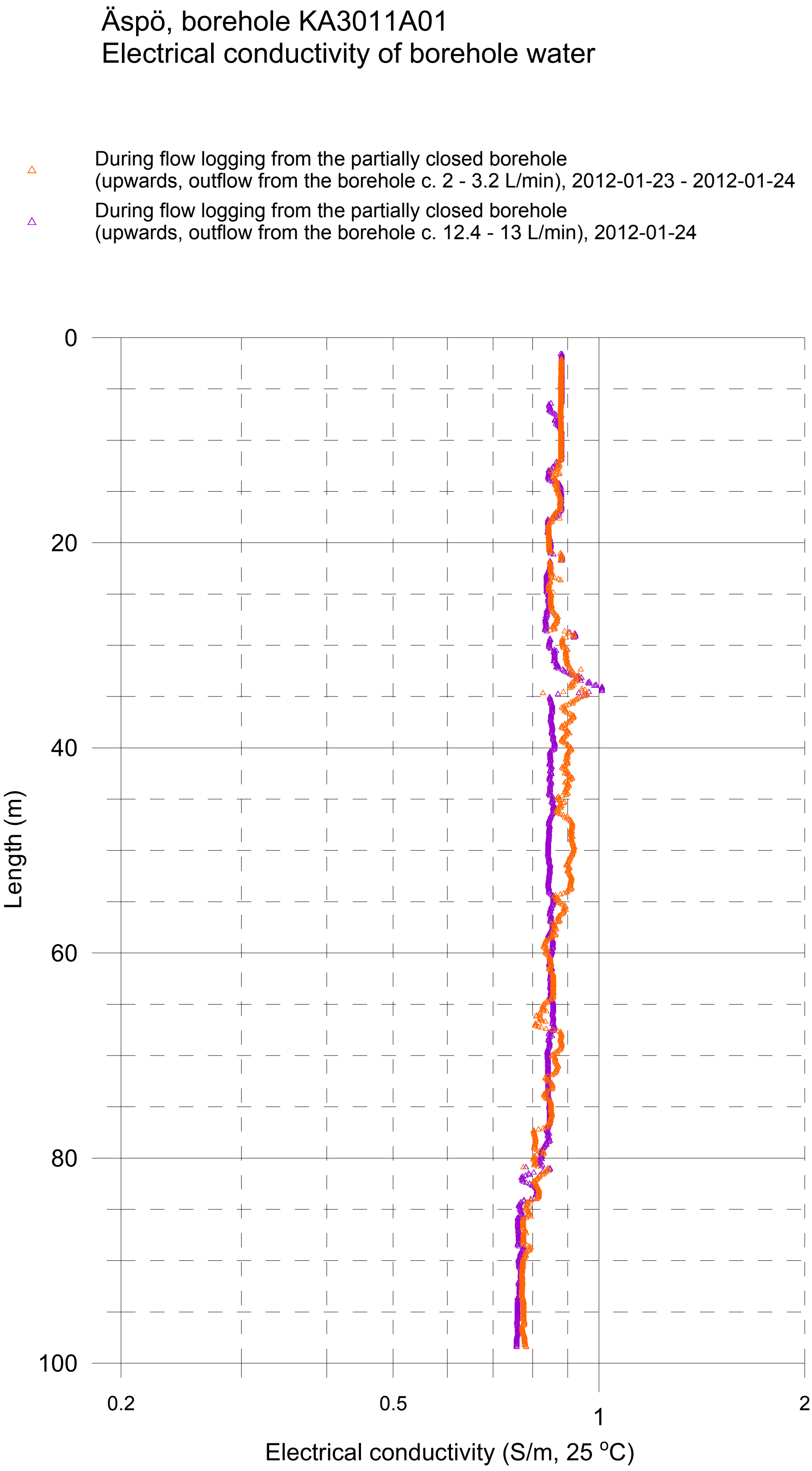

Temperature of borehole water

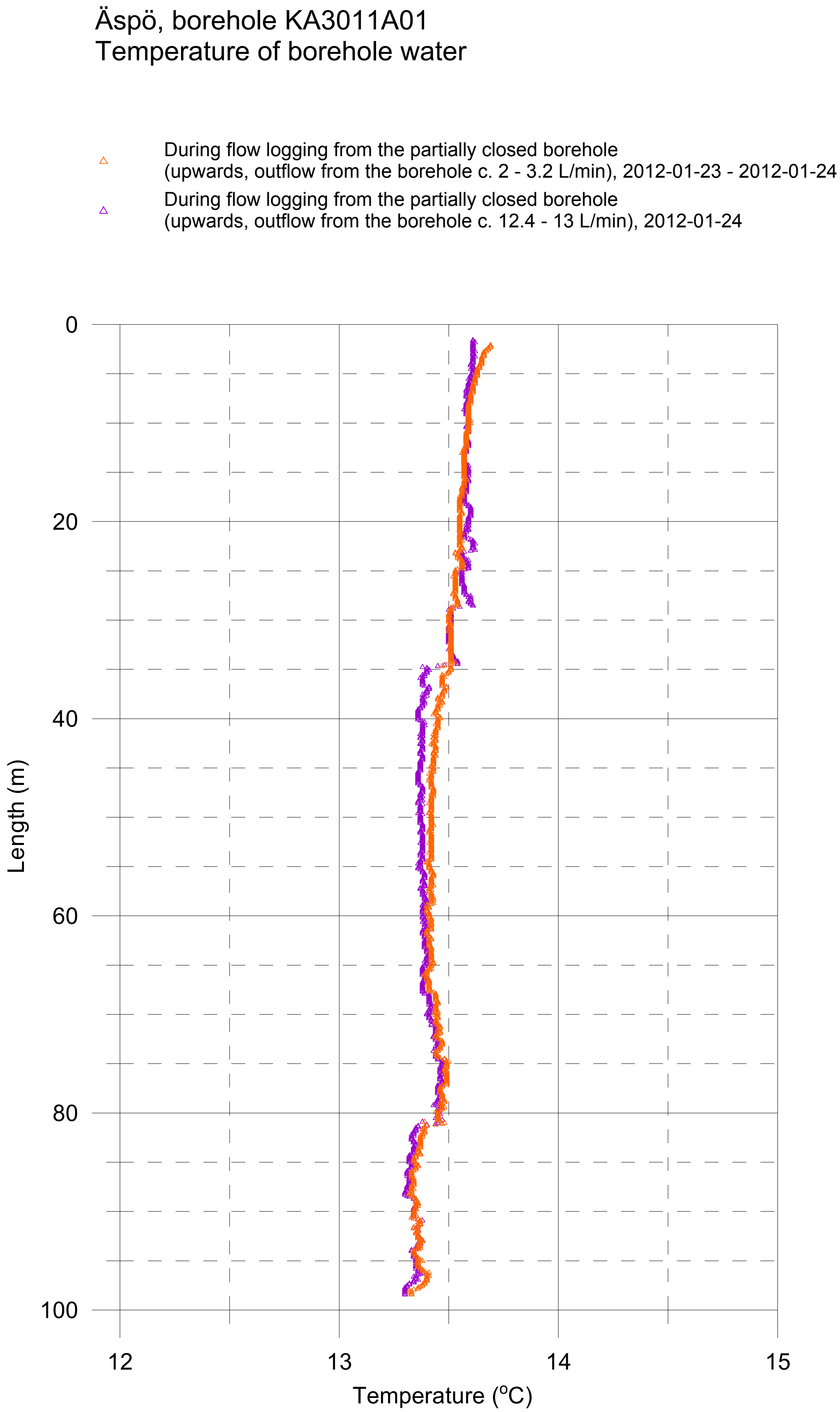

Flow rate and single point resistance

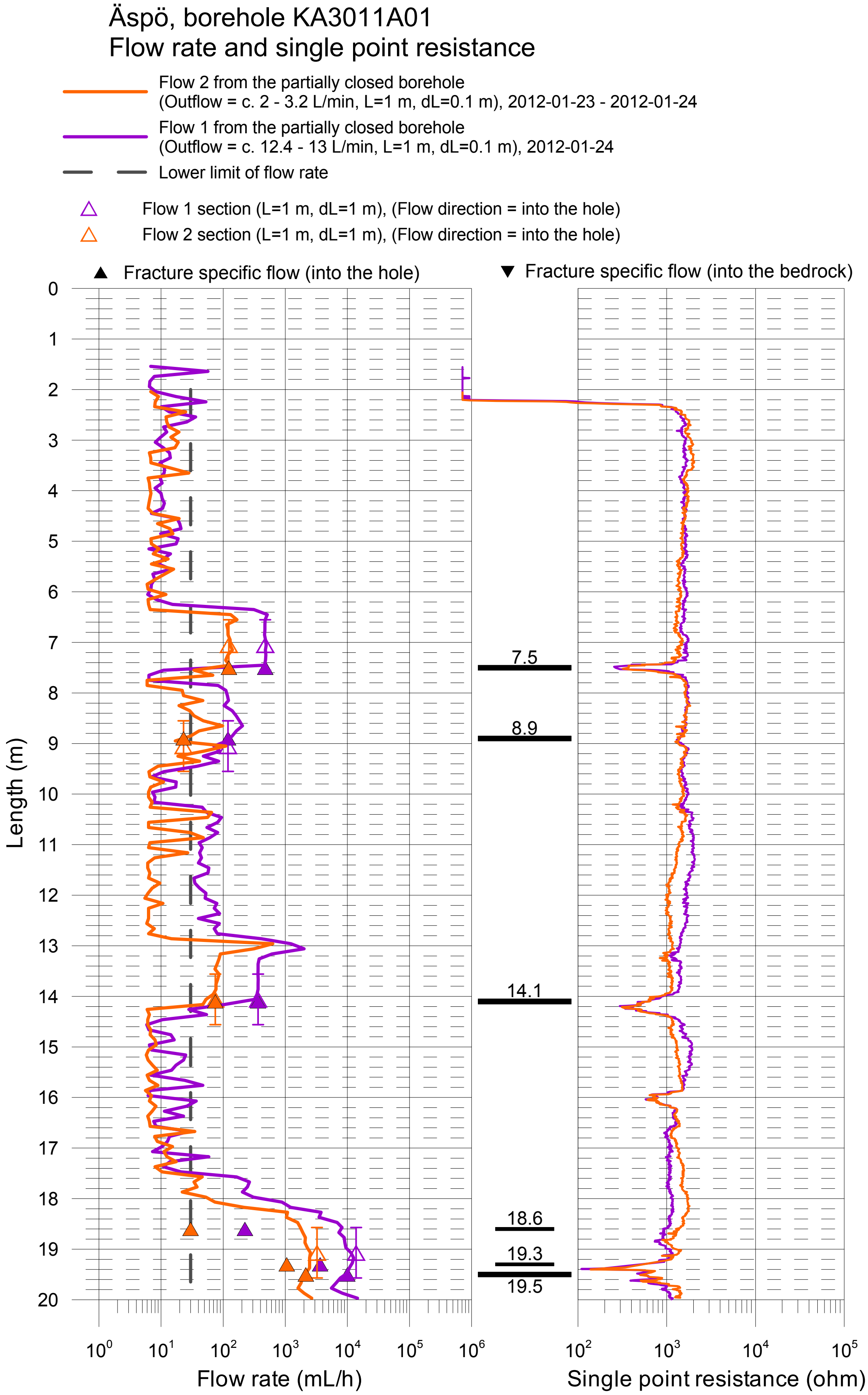

Flow rate and single point resistance

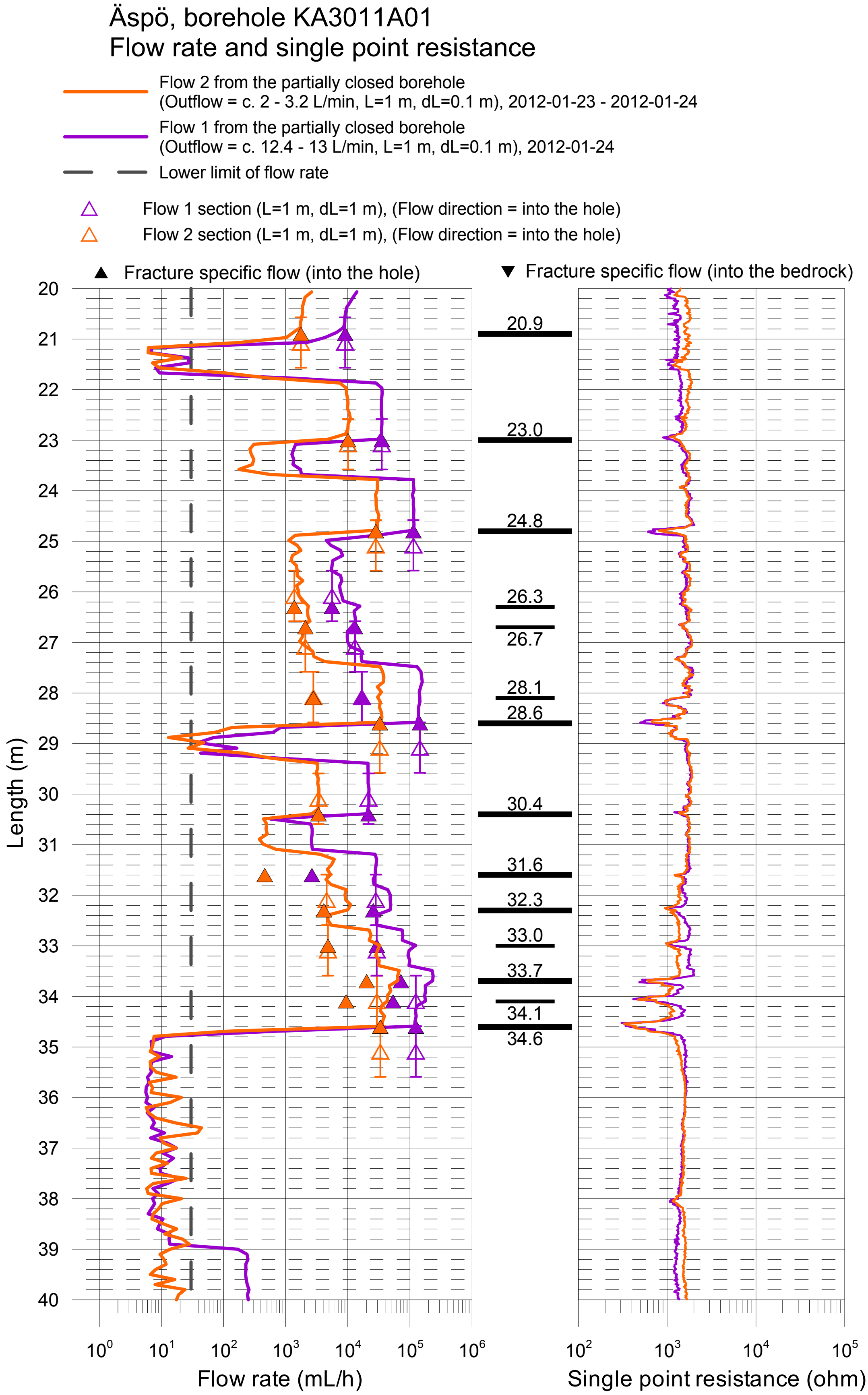

Flow rate and single point resistance

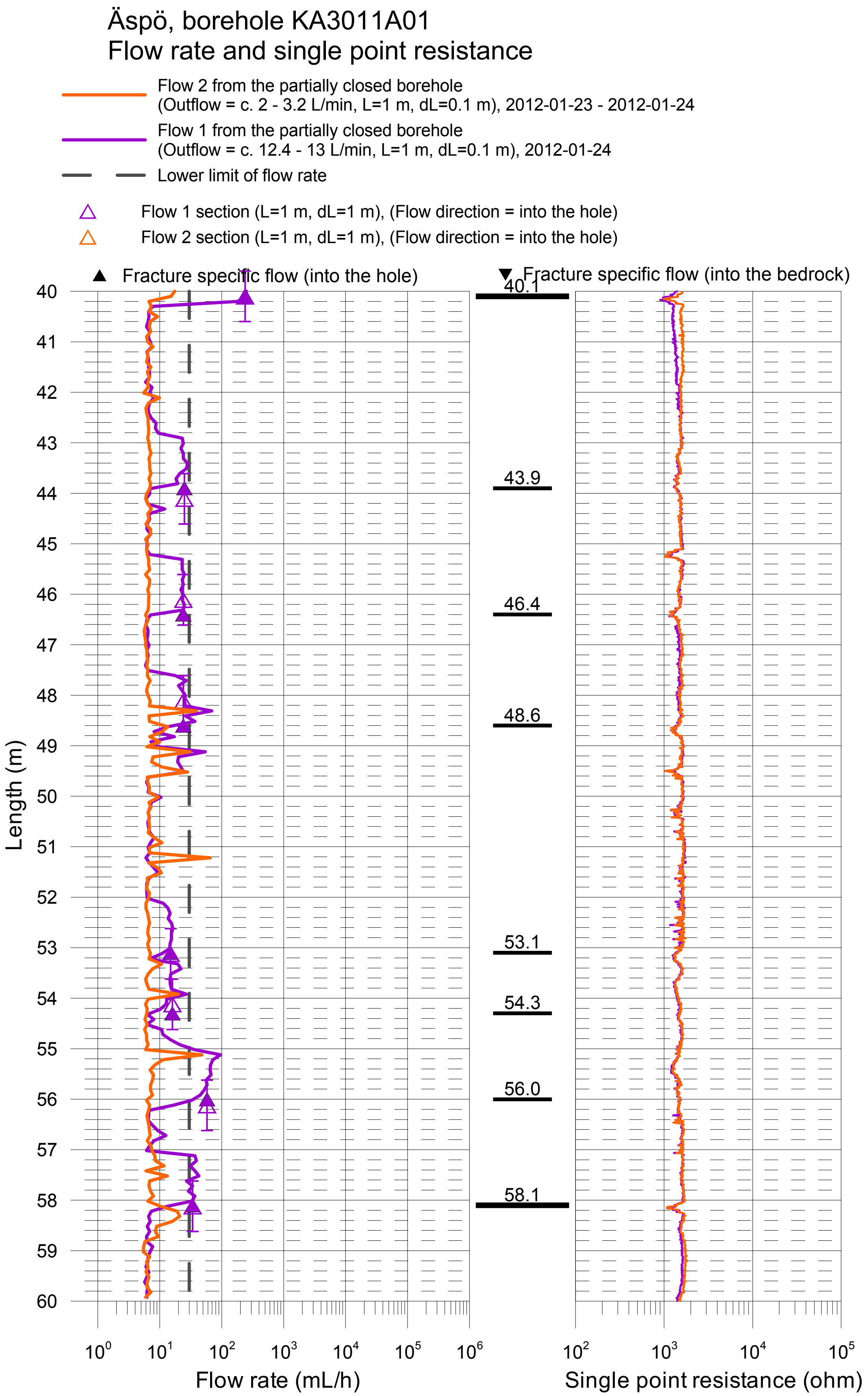

Flow rate and single point resistance

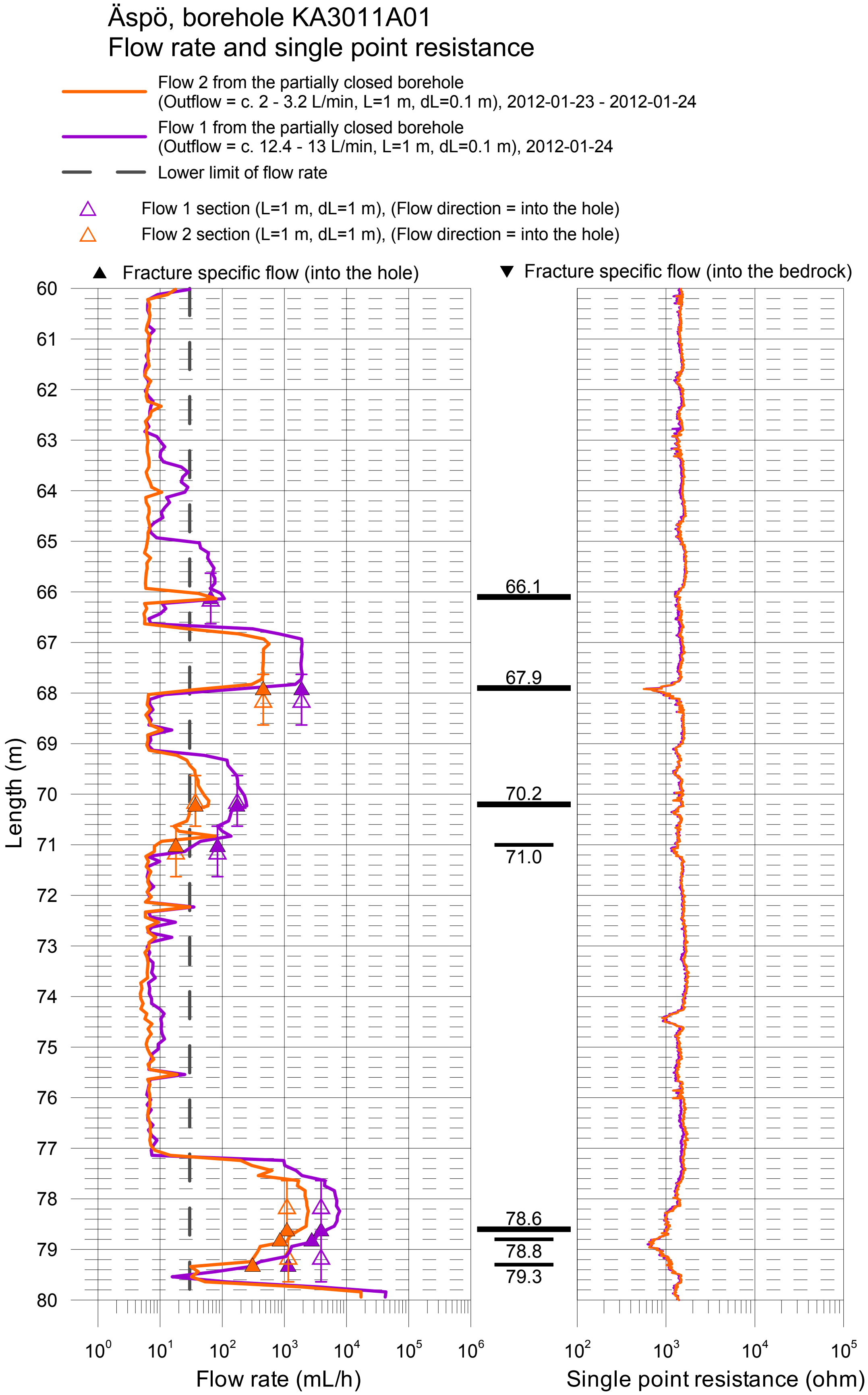

Flow rate and single point resistance

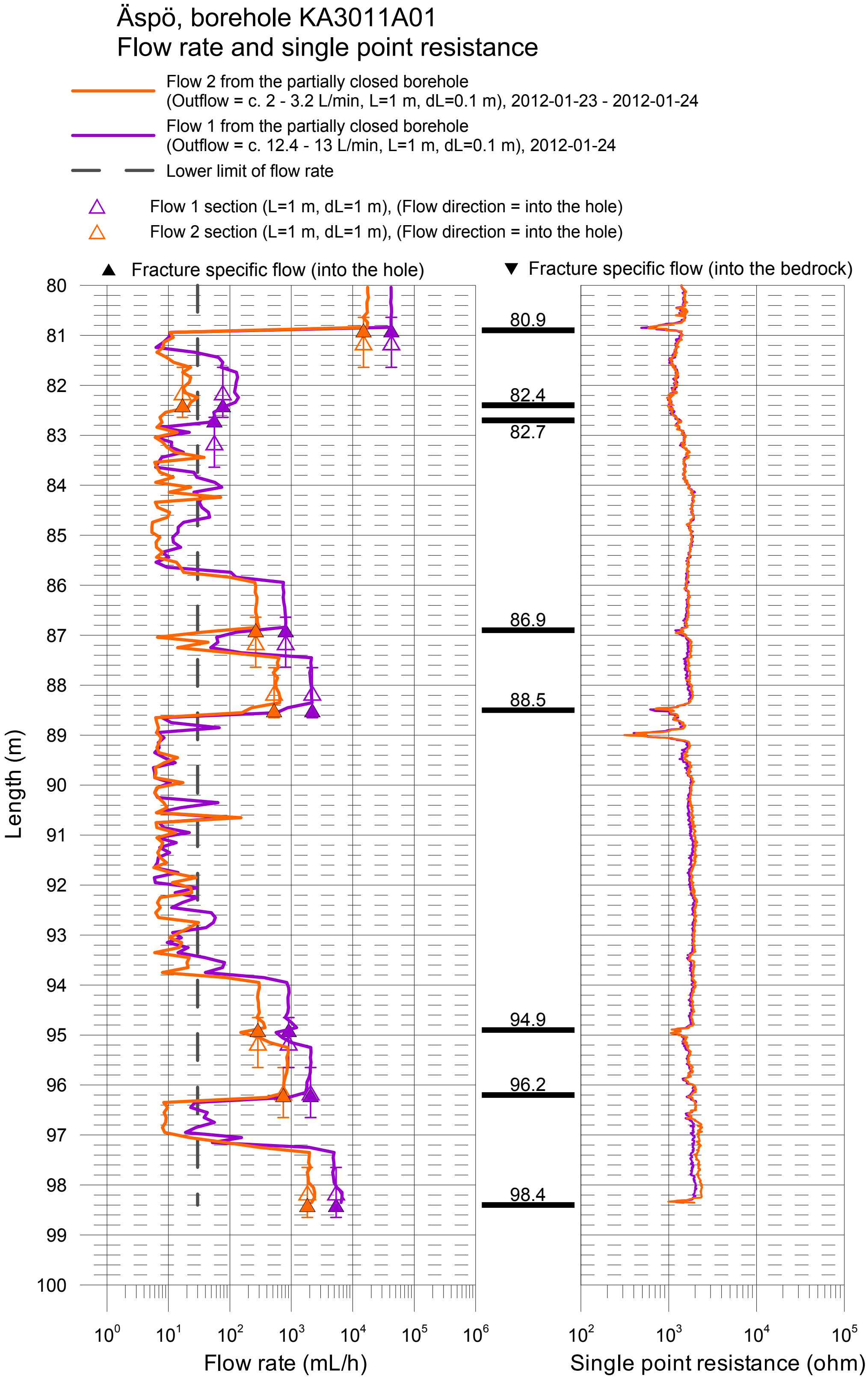

Appendix 4

Explanations for the tables in Appendices 5 and 7

Header	Unit	Explanations
Borehole		ID for borehole
Secup	m	Length along the borehole for the upper limit of the test section (based on corrected length L).
Seclow	m	Length along the borehole for the lower limit of the test section (based on corrected length L).
L	m	Corrected length along borehole based on SKB procedures for length correction.
Length to flow anom.	m	Length along the borehole to inferred flow anomaly during overlapping flow logging.
Test type (1–6)	(–)	1A: Pumping test – wire-line eq., 1B:Pumping test-submersible pump, 1C: Pumping test-airlift pumping, 2: Interference test, 3: Injection test, 4: Slug test, 5A: Difference flow logging – PFL-DIFF-Sequential, 5B: Difference flow logging – PFL-DIFF-Overlapping, 6: Flow logging-Impeller.
Date of test, start	YY-MM-DD	Date for start of pumping..
Time of test, start	hh:mm	Time for start of pumping
Date of flowl., start .	YY-MM-DD	Date for start of the flow logging.
Time of flowl., start	hh:mm	Time for start of the flow logging.
Date of test, stop	YY-MM-DD	Date for stop of the test.
Time of test, stop	hh:mm	Time for stop of the test.
L_w	m	Section length used in the difference flow logging.
dL	m	Step length (increment) used in the difference flow logging.
Q_{p1}	m^3/s	Flow rate at surface by the end of the first pumping period of the flow logging.
Q_{p2}	m^3/s	Flow rate at surface by the end of the second pumping period of the flow logging.
t_{p1}	s	Duration of the first pumping period.
t_{p2}	s	Duration of the second pumping period.
t_{F1}	s	Duration of the first recovery period.
t_{F2}	s	Duration of the second recovery period.
h_0	m.a.s.l.	Initial hydraulic head before pumping. Elevation of water level in open borehole in the local co-ordinates system with z=0 m.
h_1	m.a.s.l.	Stabilized hydraulic head during the first pumping period. Elevation of water level in open borehole in the local co-ordinates system with z=0 m.
h_2	m.a.s.l.	Stabilized hydraulic head during the second pumping period. Elevation of water level in open borehole in the local co-ordinates system with z=0 m.
s_1	m	Drawdown of the water level in the borehole during first pumping period. Difference between the actual hydraulic head and the initial head (s_1= h_1–h_0).
s_2	m	Drawdown of the water level in the borehole during second pumping period. Difference between the actual hydraulic head and the initial head (s_2=h_2–h_0).
T	m^2/s	Transmissivity of the entire borehole.
Q_0	m^3/s	Measured flow rate through the test section or flow anomaly under natural conditions (no pumping) with h=h_0 in the open borehole.
Q_1	m^3/s	Measured flow rate through the test section or flow anomaly during the first pumping period.
Q_2	m^3/s	Measured flow rate through the test section or flow anomaly during the second pumping period.
h_{0FW}	m.a.s.l.	Corrected initial hydraulic head along the hole due to e.g. varying salinity conditions of the borehole fluid before pumping.
h_{1FW}	m.a.s.l.	Corrected hydraulic head along the hole due to e.g. varying salinity conditions of the borehole fluid during the first pumping period.
h_{2FW}	m.a.s.l.	Corrected hydraulic head along the hole due to e.g. varying salinity conditions of the borehole fluid during the second pumping period.
EC_w	S/m	Measured electrical conductivity of the borehole fluid in the test section during difference flow logging.
Te_w	°C	Measured borehole fluid temperature in the test section during difference flow logging.
EC_f	S/m	Measured fracture-specific electrical conductivity of the fluid in flow anomaly during difference flow logging.
Te_f	°C	Measured fracture-specific fluid temperature in flow anomaly during difference flow logging.
T_D	m^2/s	Transmissivity of section or flow anomaly based on 2D model for evaluation of formation properties of the test section based on PFL-DIFF.
T-$measl_{LT}$	m^2/s	Estimated theoretical lower measurement limit for evaluated T_D. If the estimated T_D equals T_D-measlim, the actual T_D is considered to be equal or less than T_D-measlim.
T-$measl_{LP}$	m^2/s	Estimated practical lower measurement limit for evaluated T_D. If the estimated T_D equals T_D-measlim, the actual T_D is considered to be equal or less than T_D-measlim.
T-$measl_U$	m^2/s	Estimated upper measurement limit for evaluated T_D. If the estimated T_D equals T_D-measlim, the actual T_D is considered to be equal or less than T_D-measlim.
h_i	m.a.s.l.	Calculated relative, natural freshwater head for test section or flow anomaly (undisturbed conditions).

Appendix 5.1

Results of sequential flow logging

Borehole ID	Secup L(m)	Seclow L(m)	L_w (m)	Q_1 (m^3/s)	h_{1FW} (m.a.s.l.)	Q_2 (m^3/s)	h_{2FW} (m.a.s.l.)	T_D (m^2/s)	h_i (m.a.s.l.)	Q-lower limit P (mL/h)	T_D-measl$_{LT}$ (m^2/s)	T_D-measl$_{LP}$ (m^2/s)	T_D-measl$_U$ (m^2/s)	Comments
KA3011A01	2.54	3.54	1	–	–184.93	–	–67.03	–	–	30	7.0E–11	7.0E–11	7.0E–07	
KA3011A01	3.55	4.55	1	–	–189.15	–	–71.13	–	–	30	7.0E–11	7.0E–11	7.0E–07	
KA3011A01	4.55	5.55	1	–	–191.16	–	–74.00	–	–	30	7.0E–11	7.0E–11	7.0E–07	
KA3011A01	5.55	6.55	1	–	–197.24	–	–78.93	–	–	30	7.0E–11	7.0E–11	7.0E–07	
KA3011A01	6.55	7.55	1	1.32E–07	–195.50	3.44E–08	–77.34	8.2E–10	–35.60	30	7.0E–11	7.0E–11	7.0E–07	
KA3011A01	7.55	8.55	1	–	–192.86	–	–74.67	–	–	30	7.0E–11	7.0E–11	7.0E–07	
KA3011A01	8.55	9.55	1	3.33E–08	–191.27	6.39E–09	–72.81	2.3E–10	–44.72	30	7.0E–11	7.0E–11	7.0E–07	*
KA3011A01	9.56	10.56	1	–	–190.09	–	–71.82	–	–	30	7.0E–11	7.0E–11	7.0E–07	
KA3011A01	10.56	11.56	1	–	–188.96	–	–70.96	–	–	30	7.0E–11	7.0E–11	7.0E–07	
KA3011A01	11.56	12.56	1	–	–190.09	–	–72.20	–	–	30	7.0E–11	7.0E–11	7.0E–07	
KA3011A01	12.56	13.56	1	–	–191.18	–	–73.20	–	–	30	7.0E–11	7.0E–11	7.0E–07	
KA3011A01	13.56	14.56	1	1.02E–07	–191.44	2.08E–08	–73.94	6.8E–10	–43.66	30	7.0E–11	7.0E–11	7.0E–07	
KA3011A01	14.56	15.56	1	–	–190.98	–	–73.28	–	–	30	7.0E–11	7.0E–11	7.0E–07	
KA3011A01	15.56	16.56	1	–	–193.44	–	–75.68	–	–	30	7.0E–11	7.0E–11	7.0E–07	
KA3011A01	16.57	17.57	1	–	–191.20	–	–73.30	–	–	30	7.0E–11	7.0E–11	7.0E–07	
KA3011A01	17.57	18.57	1	–	–186.47	–	–69.29	–	–	30	7.0E–11	7.0E–11	7.0E–07	
KA3011A01	18.57	19.57	1	3.85E–06	–189.57	9.00E–07	–72.08	2.5E–08	–36.18	30	7.0E–11	7.0E–11	6.9E–07	
KA3011A01	19.57	20.57	1	–	–189.27	–	–71.74	–	–	30	7.0E–11	7.0E–11	7.0E–07	
KA3011A01	20.57	21.57	1	2.51E–06	–186.88	4.89E–07	–69.59	1.7E–08	–41.27	30	7.0E–11	7.0E–11	7.0E–07	
KA3011A01	21.57	22.57	1	–	–190.92	–	–73.80	–	–	30	7.0E–11	7.0E–11	7.0E–07	
KA3011A01	22.58	23.58	1	9.78E–06	–190.63	2.81E–06	–73.16	5.9E–08	–25.89	30	7.0E–11	7.0E–11	6.8E–07	
KA3011A01	23.58	24.58	1	–	–189.06	–	–71.86	–	–	30	7.0E–11	7.0E–11	7.0E–07	
KA3011A01	24.58	25.58	1	3.17E–05	–190.21	7.89E–06	–72.64	2.0E–07	–33.63	30	7.0E–11	7.0E–11	6.3E–07	
KA3011A01	25.58	26.58	1	1.55E–06	–190.19	3.83E–07	–72.58	9.8E–09	–33.94	30	7.0E–11	7.0E–11	7.0E–07	
KA3011A01	26.58	27.58	1	3.64E–06	–186.97	5.78E–07	–69.49	2.6E–08	–47.32	30	7.0E–11	7.0E–11	7.0E–07	
KA3011A01	27.58	28.58	1	4.69E–06	–182.81	7.75E–07	–66.73	3.3E–08	–43.78	30	7.1E–11	7.1E–11	7.0E–07	
KA3011A01	28.58	29.58	1	4.03E–05	–190.77	9.11E–06	–73.59	2.6E–07	–39.33	30	7.0E–11	7.0E–11	6.3E–07	
KA3011A01	29.59	30.59	1	6.00E–06	–192.11	9.36E–07	–74.93	4.3E–08	–53.27	30	7.0E–11	7.0E–11	7.0E–07	
KA3011A01	30.59	31.59	1	–	–191.70	–	–74.50	–	–	30	7.0E–11	7.0E–11	7.0E–07	
KA3011A01	31.59	32.59	1	7.88E–06	–190.53	1.27E–06	–73.59	5.6E–08	–51.12	30	7.0E–11	7.1E–11	6.9E–07	
KA3011A01	32.59	33.59	1	8.14E–06	–190.52	1.33E–06	–73.36	5.8E–08	–50.41	30	7.0E–11	7.0E–11	6.9E–07	

Appendix 5.2

Results of sequential flow logging

Borehole ID	Secup L(m)	Seclow L(m)	L_w (m)	Q_1 (m^3/s)	h_{1FW} (m.a.s.l.)	Q_2 (m^3/s)	h_{2FW} (m.a.s.l.)	T_D (m^2/s)	h_i (m.a.s.l.)	Q-lower limit P (mL/h)	T_D-$measl_{LT}$ (m^2/s)	T_D-$measl_{LP}$ (m^2/s)	T_D-$measl_U$ (m^2/s)	Comments
KA3011A01	33.59	34.59	1	3.47E–05	–187.46	8.19E–06	–70.53	2.2E–07	–34.41	30	7.0E–11	7.1E–11	6.4E–07	
KA3011A01	34.59	35.59	1	3.47E–05	–187.42	9.31E–06	–70.38	2.2E–07	–27.53	30	7.0E–11	7.0E–11	6.3E–07	
KA3011A01	35.60	36.60	1	–	–186.19	–	–69.05	–	–	30	7.0E–11	7.0E–11	7.0E–07	
KA3011A01	36.60	37.60	1	–	–186.14	–	–68.97	–	–	30	7.0E–11	7.0E–11	7.0E–07	
KA3011A01	37.60	38.60	1	–	–185.91	–	–68.71	–	–	30	7.0E–11	7.0E–11	7.0E–07	
KA3011A01	38.60	39.60	1	–	–188.77	–	–71.52	–	–	30	7.0E–11	7.0E–11	7.0E–07	
KA3011A01	39.60	40.60	1	6.61E–08	–188.80	–	–71.71	5.6E–10	–	30	7.0E–11	7.0E–11	7.0E–07	**
KA3011A01	40.60	41.60	1	–	–189.25	–	–72.09	–	–	30	7.0E–11	7.0E–11	7.0E–07	
KA3011A01	41.60	42.60	1	–	–189.04	–	–72.04	–	–	30	7.0E–11	7.1E–11	7.0E–07	
KA3011A01	42.61	43.61	1	–	–189.68	–	–72.46	–	–	30	7.0E–11	7.0E–11	7.0E–07	
KA3011A01	43.61	44.61	1	6.94E–09	–187.14	–	–70.26	5.9E–11	–	30	7.1E–11	7.1E–11	7.1E–07	*, **
KA3011A01	44.61	45.61	1	–	–188.48	–	–71.48	–	–	30	7.0E–11	7.1E–11	7.0E–07	
KA3011A01	45.61	46.61	1	6.67E–09	–187.11	–	–70.26	5.6E–11	–	30	7.1E–11	7.1E–11	7.1E–07	*, **
KA3011A01	46.61	47.61	1	–	–185.82	–	–68.77	–	–	30	7.0E–11	7.0E–11	7.0E–07	
KA3011A01	47.61	48.61	1	6.67E–09	–185.65	–	–68.80	5.6E–11	–	30	7.1E–11	7.1E–11	7.1E–07	*, **
KA3011A01	48.62	49.62	1	–	–188.92	–	–72.25	–	–	30	7.1E–11	7.1E–11	7.1E–07	
KA3011A01	49.62	50.62	1	–	–188.40	–	–71.60	–	–	30	7.1E–11	7.1E–11	7.1E–07	
KA3011A01	50.62	51.62	1	–	–186.94	–	–70.48	–	–	30	7.1E–11	7.1E–11	7.1E–07	
KA3011A01	51.62	52.62	1	–	–187.30	–	–70.72	–	–	30	7.1E–11	7.1E–11	7.1E–07	
KA3011A01	52.62	53.62	1	4.17E–09	–186.76	–	–70.38	3.5E–11	–	30	7.1E–11	7.1E–11	7.1E–07	*, **
KA3011A01	53.62	54.62	1	4.44E–09	–186.48	–	–69.96	3.8E–11	–	30	7.1E–11	7.1E–11	7.1E–07	*, **
KA3011A01	54.62	55.62	1	–	–186.94	–	–70.42	–	–	30	7.1E–11	7.1E–11	7.1E–07	
KA3011A01	55.62	56.62	1	1.61E–08	–185.80	–	–68.88	1.4E–10	–	30	7.1E–11	7.1E–11	7.1E–07	**
KA3011A01	56.62	57.62	1	–	–184.45	–	–67.49	–	–	30	7.0E–11	7.1E–11	7.0E–07	
KA3011A01	57.62	58.62	1	9.44E–09	–184.46	–	–68.50	8.1E–11	–	30	7.1E–11	7.1E–11	7.1E–07	**
KA3011A01	58.62	59.62	1	–	–184.35	–	–68.38	–	–	30	7.1E–11	7.1E–11	7.1E–07	
KA3011A01	59.62	60.62	1	–	–184.76	–	–68.91	–	–	30	7.1E–11	7.1E–11	7.1E–07	
KA3011A01	60.63	61.63	1	–	–183.08	–	–67.48	–	–	30	7.1E–11	7.1E–11	7.1E–07	
KA3011A01	61.63	62.63	1	–	–183.52	–	–67.85	–	–	30	7.1E–11	7.1E–11	7.1E–07	
KA3011A01	62.63	63.63	1	–	–184.31	–	–68.40	–	–	30	7.1E–11	7.1E–11	7.1E–07	
KA3011A01	63.63	64.63	1	–	–183.15	–	–67.20	–	–	30	7.1E–11	7.1E–11	7.1E–07	
KA3011A01	64.63	65.63	1	–	–184.76	–	–69.24	–	–	30	7.1E–11	7.1E–11	7.1E–07	

Results of sequential flow logging

Borehole ID	Secup L(m)	Seclow L(m)	L_w (m)	Q_1 (m^3/s)	h_{1FW} (m.a.s.l.)	Q_2 (m^3/s)	h_{2FW} (m.a.s.l.)	T_D (m^2/s)	h_i (m.a.s.l.)	Q-lower limit P (mL/h)	T_D-measl$_{LT}$ (m^2/s)	T_D-measl$_{LP}$ (m^2/s)	T_D-measl$_U$ (m^2/s)	Comments
KA3011A01	65.63	66.63	1	1.81E–08	–183.03	–	–67.31	1.5E–10	–	30	7.1E–11	7.1E–11	7.1E–07	**
KA3011A01	66.63	67.63	1	–	–183.06	–	–67.03	–	–	30	7.1E–11	7.1E–11	7.1E–07	
KA3011A01	67.63	68.63	1	5.25E–07	–182.89	1.27E–07	–67.17	3.4E–09	–30.37	30	7.1E–11	7.1E–11	7.1E–07	
KA3011A01	68.63	69.63	1	–	–182.41	–	–67.09	–	–	30	7.1E–11	7.2E–11	7.1E–07	
KA3011A01	69.63	70.63	1	4.83E–08	–183.07	1.03E–08	–67.68	3.3E–10	–36.52	30	7.1E–11	7.1E–11	7.1E–07	
KA3011A01	70.63	71.63	1	2.33E–08	–183.42	5.00E–09	–68.26	1.6E–10	–36.85	30	7.2E–11	7.2E–11	7.2E–07	*
KA3011A01	71.63	72.63	1	–	–182.96	–	–68.30	–	–	30	7.2E–11	7.2E–11	7.2E–07	
KA3011A01	72.63	73.63	1	–	–181.82	–	–66.63	–	–	30	7.2E–11	7.2E–11	7.2E–07	
KA3011A01	73.63	74.63	1	–	–179.70	–	–65.49	–	–	30	7.2E–11	7.2E–11	7.2E–07	
KA3011A01	74.64	75.64	1	–	–182.94	–	–68.30	–	–	30	7.2E–11	7.2E–11	7.2E–07	
KA3011A01	75.64	76.64	1	–	–181.87	–	–67.09	–	–	30	7.2E–11	7.2E–11	7.2E–07	
KA3011A01	76.64	77.64	1	–	–178.96	–	–65.62	–	–	30	7.3E–11	7.3E–11	7.3E–07	
KA3011A01	77.64	78.64	1	1.08E–06	–180.41	3.06E–07	–66.36	6.8E–09	–21.55	30	7.2E–11	7.2E–11	7.2E–07	
KA3011A01	78.64	79.64	1	1.08E–06	–180.79	3.21E–07	–67.10	6.6E–09	–19.15	30	7.3E–11	7.3E–11	7.2E–07	
KA3011A01	79.64	80.64	1	–	–181.96	–	–68.16	–	–	30	7.2E–11	7.2E–11	7.2E–07	
KA3011A01	80.64	81.64	1	1.18E–05	–182.18	4.17E–06	–68.55	6.7E–08	–6.57	30	7.3E–11	7.3E–11	6.9E–07	
KA3011A01	81.64	82.64	1	2.14E–08	–182.50	4.72E–09	–69.45	1.5E–10	–37.42	30	7.3E–11	7.3E–11	7.3E–07	*
KA3011A01	82.64	83.64	1	1.56E–08	–182.75	–	–69.17	1.4E–10	–	30	7.3E–11	7.3E–11	7.3E–07	**
KA3011A01	83.64	84.64	1	–	–182.92	–	–69.34	–	–	30	7.3E–11	7.3E–11	7.3E–07	
KA3011A01	84.64	85.64	1	–	–182.71	–	–68.96	–	–	30	7.2E–11	7.3E–11	7.2E–07	
KA3011A01	85.64	86.64	1	–	–183.95	–	–70.28	–	–	30	7.3E–11	7.3E–11	7.3E–07	
KA3011A01	86.64	87.64	1	2.25E–07	–181.56	7.31E–08	–68.90	1.3E–09	–14.73	30	7.3E–11	7.3E–11	7.3E–07	
KA3011A01	87.65	88.65	1	6.11E–07	–180.81	1.45E–07	–67.96	4.1E–09	–32.77	30	7.3E–11	7.3E–11	7.3E–07	
KA3011A01	88.65	89.65	1	–	–180.92	–	–68.31	–	–	30	7.3E–11	7.3E–11	7.3E–07	
KA3011A01	89.65	90.65	1	–	–179.30	–	–66.66	–	–	30	7.3E–11	7.3E–11	7.3E–07	
KA3011A01	90.65	91.65	1	–	–179.54	–	–67.43	–	–	30	7.4E–11	7.4E–11	7.4E–07	
KA3011A01	91.65	92.65	1	–	–179.87	–	–68.29	–	–	30	7.4E–11	7.4E–11	7.4E–07	
KA3011A01	92.65	93.65	1	–	–178.97	–	–68.89	–	–	30	7.5E–11	7.5E–11	7.5E–07	
KA3011A01	93.65	94.65	1	–	–181.13	–	–68.98	–	–	30	7.4E–11	7.4E–11	7.3E–07	
KA3011A01	94.65	95.65	1	2.51E–07	–181.25	7.92E–08	–69.73	1.5E–09	–18.47	30	7.4E–11	7.4E–11	7.4E–07	
KA3011A01	95.65	96.65	1	5.72E–07	–180.70	2.06E–07	–69.48	3.3E–09	–7.13	30	7.4E–11	7.4E–11	7.4E–07	
KA3011A01	96.65	97.65	1	–	–177.37	–	–68.44	–	–	30	7.6E–11	7.6E–11	7.6E–07	
KA3011A01	97.65	98.65	1	1.49E–06	–178.55	5.07E–07	–69.57	8.9E–09	–13.31	30	7.6E–11	7.6E–11	7.5E–07	

* Uncertain = The flow rate Q_1 and/or Q_2 is less than 30 mL/h or the flow anomalies are overlapping or they are unclear because of noise.

** T_D calculation based on assumption that flow rate Q_2 = 0 mL/h.

Plotted flow rates of 1 m sections

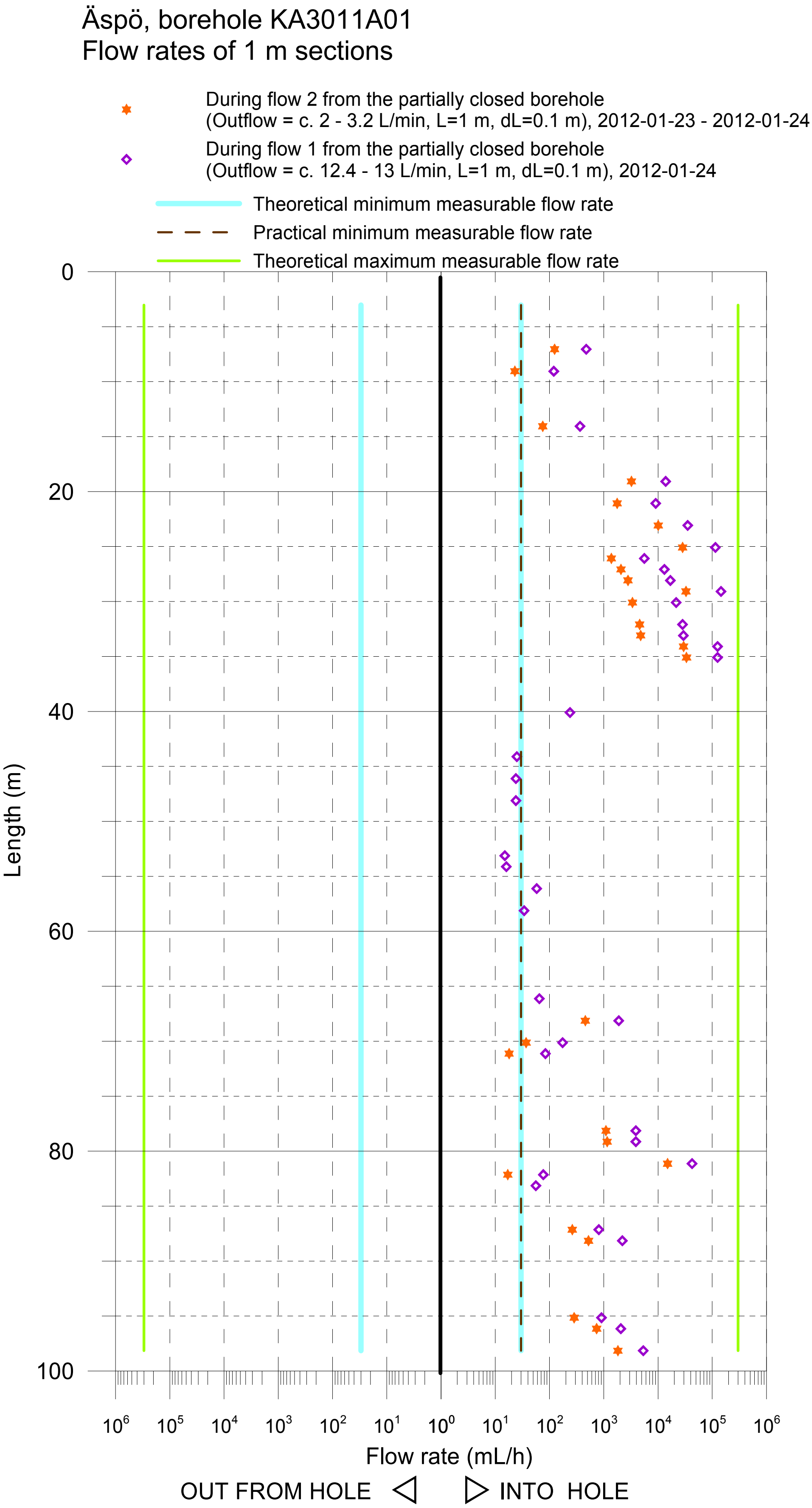

Plotted transmissivity and head of 1 m sections

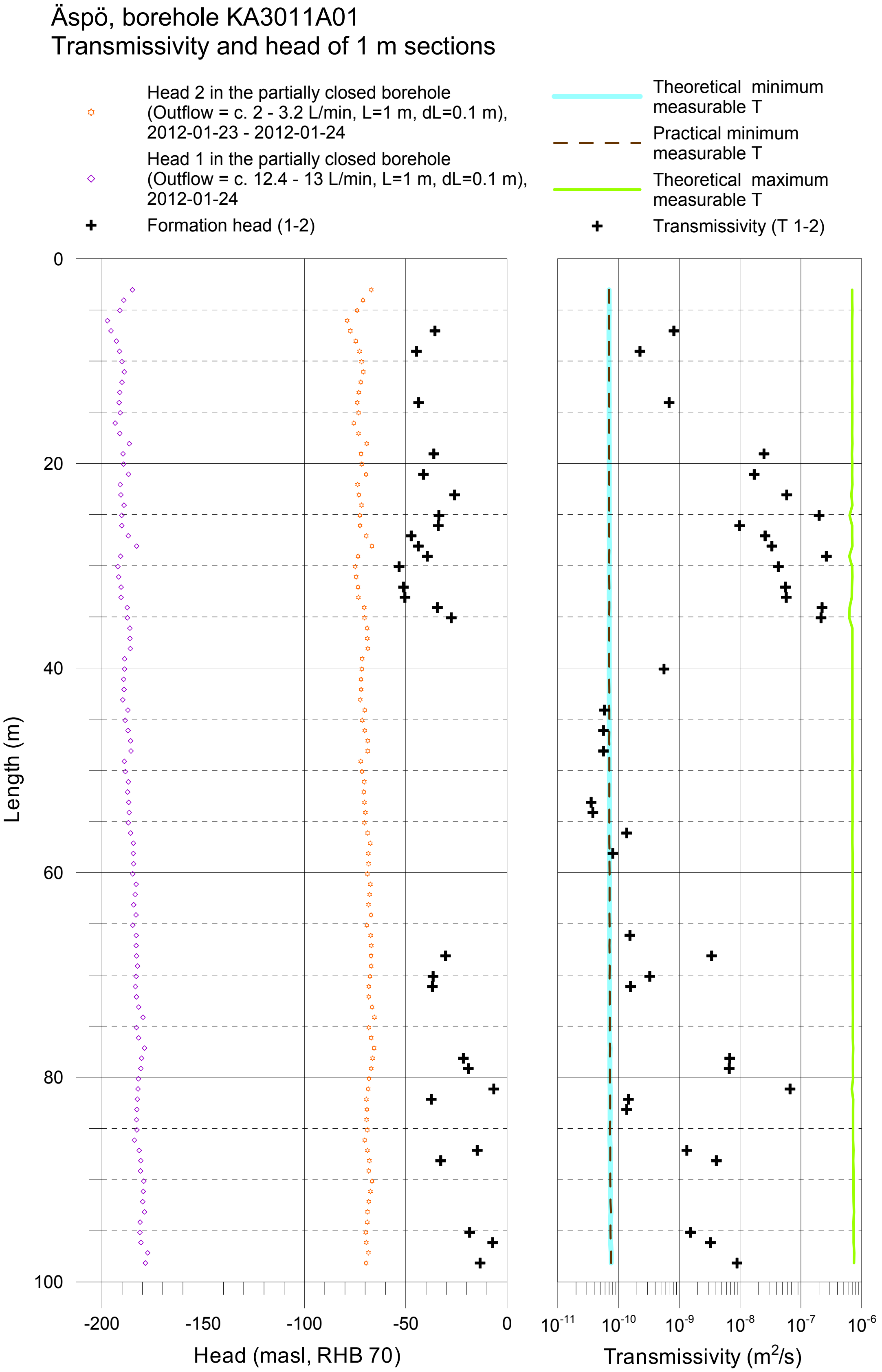

Appendix 7.1

Inferred flow anomalies from overlapping flow logging

Borehole ID	Length to flow anom. L (m)	L_w (m)	dL (m)	Q_1 (m^3/s)	h_{1FW} (m.a.s.l.)	Q_2 (m^3/s)	h_{2FW} (m.a.s.l.)	T_D (m^2/s)	h_i (m.a.s.l.)	Comments
KA3011A01	7.5	1	0.1	1.32E–07	–194.98	3.44E–08	–76.52	8.1E–10	–34.67	
KA3011A01	8.9	1	0.1	3.33E–08	–191.60	6.39E–09	–73.10	2.3E–10	–45.00	
KA3011A01	14.1	1	0.1	1.02E–07	–191.67	2.08E–08	–74.05	6.8E–10	–43.74	
KA3011A01	18.6	1	0.1	6.25E–08	–188.90	8.33E–09	–71.42	4.6E–10	–53.35	*
KA3011A01	19.3	1	0.1	1.01E–06	–189.28	2.94E–07	–71.50	6.0E–09	–23.11	*
KA3011A01	19.5	1	0.1	2.77E–06	–189.14	5.97E–07	–71.25	1.8E–08	–38.88	
KA3011A01	20.9	1	0.1	2.51E–06	–186.96	4.89E–07	–69.83	1.7E–08	–41.55	
KA3011A01	23.0	1	0.1	9.78E–06	–189.59	2.81E–06	–72.35	5.9E–08	–25.17	
KA3011A01	24.8	1	0.1	3.17E–05	–192.10	7.89E–06	–74.42	2.0E–07	–35.38	
KA3011A01	26.3	1	0.1	1.55E–06	–189.18	3.83E–07	–71.60	9.8E–09	–32.97	*
KA3011A01	26.7	1	0.1	3.64E–06	–188.49	5.78E–07	–70.89	2.6E–08	–48.69	*
KA3011A01	28.1	1	0.1	4.69E–06	–183.10	7.75E–07	–66.99	3.3E–08	–44.03	*
KA3011A01	28.6	1	0.1	4.03E–05	–187.36	9.11E–06	–70.72	2.6E–07	–36.62	
KA3011A01	30.4	1	0.1	6.00E–06	–191.49	9.36E–07	–74.40	4.3E–08	–52.75	
KA3011A01	31.6	1	0.1	7.36E–07	–190.84	1.28E–07	–73.63	5.1E–09	–49.01	
KA3011A01	32.3	1	0.1	7.14E–06	–191.51	1.14E–06	–74.42	5.1E–08	–52.13	
KA3011A01	33.0	1	0.1	8.14E–06	–190.28	1.33E–06	–73.14	5.8E–08	–50.19	*
KA3011A01	33.7	1	0.1	1.99E–05	–189.67	5.58E–06	–72.45	1.2E–07	–26.61	
KA3011A01	34.1	1	0.1	1.49E–05	–187.46	2.61E–06	–70.53	1.0E–07	–45.61	*
KA3011A01	34.6	1	0.1	3.47E–05	–188.87	9.31E–06	–71.81	2.2E–07	–28.95	
KA3011A01	40.1	1	0.1	6.61E–08	–188.81	–	–71.72	5.6E–10	–	**
KA3011A01	43.9	1	0.1	6.94E–09	–187.97	–	–70.94	5.9E–11	–	*, **
KA3011A01	46.4	1	0.1	6.67E–09	–186.76	–	–69.85	5.6E–11	–	*, **
KA3011A01	48.6	1	0.1	6.67E–09	–184.81	–	–68.26	5.7E–11	–	*, **
KA3011A01	53.1	1	0.1	4.17E–09	–186.60	–	–70.24	3.5E–11	–	*, **
KA3011A01	54.3	1	0.1	4.44E–09	–186.74	–	–69.87	3.8E–11	–	*, **
KA3011A01	56.0	1	0.1	1.61E–08	–186.62	–	–69.71	1.4E–10	–	*, **
KA3011A01	58.1	1	0.1	9.44E–09	–184.31	–	–68.42	8.1E–11	–	**
KA3011A01	66.1	1	0.1	1.81E–08	–183.09	–	–67.32	1.5E–10	–	**
KA3011A01	67.9	1	0.1	5.25E–07	–181.33	1.27E–07	–66.05	3.4E–09	–29.39	
KA3011A01	70.2	1	0.1	4.83E–08	–182.15	1.03E–08	–67.40	3.3E–10	–36.41	
KA3011A01	71.0	1	0.1	2.33E–08	–182.70	5.00E–09	–67.66	1.6E–10	–36.29	*
KA3011A01	78.6	1	0.1	1.08E–06	–180.38	3.06E–07	–66.68	6.8E–09	–22.01	
KA3011A01	78.8	1	0.1	7.64E–07	–181.12	2.36E–07	–67.24	4.6E–09	–16.38	*
KA3011A01	79.3	1	0.1	3.19E–07	–180.62	8.56E–08	–66.42	2.0E–09	–24.65	*
KA3011A01	80.9	1	0.1	1.18E–05	–182.36	4.17E–06	–69.35	6.7E–08	–7.71	
KA3011A01	82.4	1	0.1	2.14E–08	–181.45	4.72E–09	–68.76	1.5E–10	–36.83	
KA3011A01	82.7	1	0.1	1.56E–08	–181.83	–	–68.97	1.4E–10	–	**
KA3011A01	86.9	1	0.1	2.25E–07	–181.88	7.31E–08	–69.00	1.3E–09	–14.73	
KA3011A01	88.5	1	0.1	6.11E–07	–179.73	1.45E–07	–67.32	4.1E–09	–32.26	
KA3011A01	94.9	1	0.1	2.51E–07	–180.85	7.92E–08	–69.86	1.5E–09	–18.84	
KA3011A01	96.2	1	0.1	5.72E–07	–180.28	2.06E–07	–69.13	3.3E–09	–6.82	
KA3011A01	98.4	1	0.1	1.49E–06	–177.42	5.07E–07	–69.85	9.0E–09	–14.32	

* Uncertain = The flow rate Q_1 and/or Q_2 is less than 30 mL/h or the flow anomalies are overlapping or they are unclear because of noise.

** T_D calculation based on assumption that flow rate Q_2 = 0 mL/h.

Inferred flow anomalies from overlapping flow logging

Äspö, borehole KA3011A01
Transmissivity and head of detected fractures

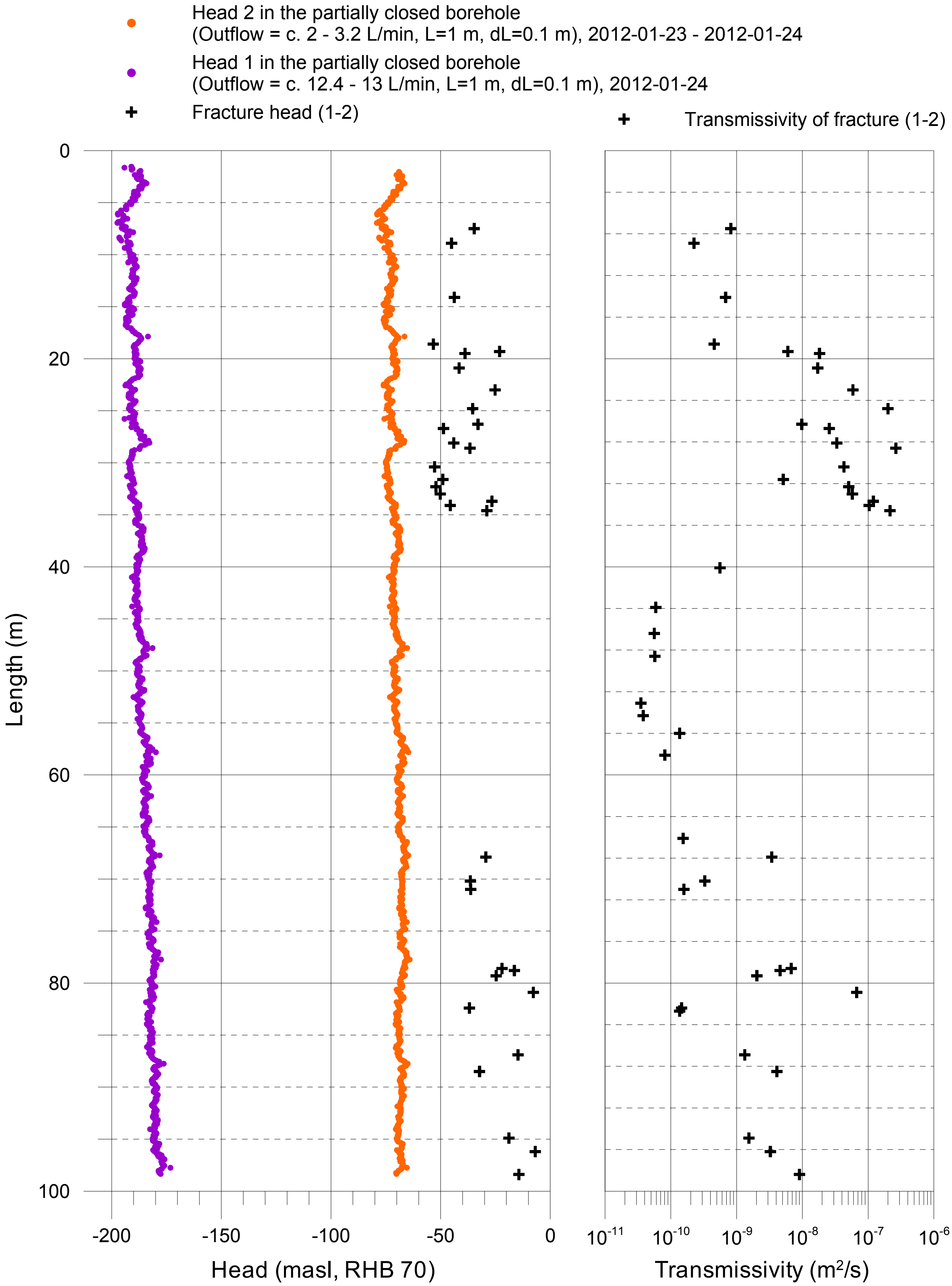

Plotted transmissivity and head of detected fractures

Äspö, borehole KA3011A01
Comparison between section transmissivity and fracture transmissivity

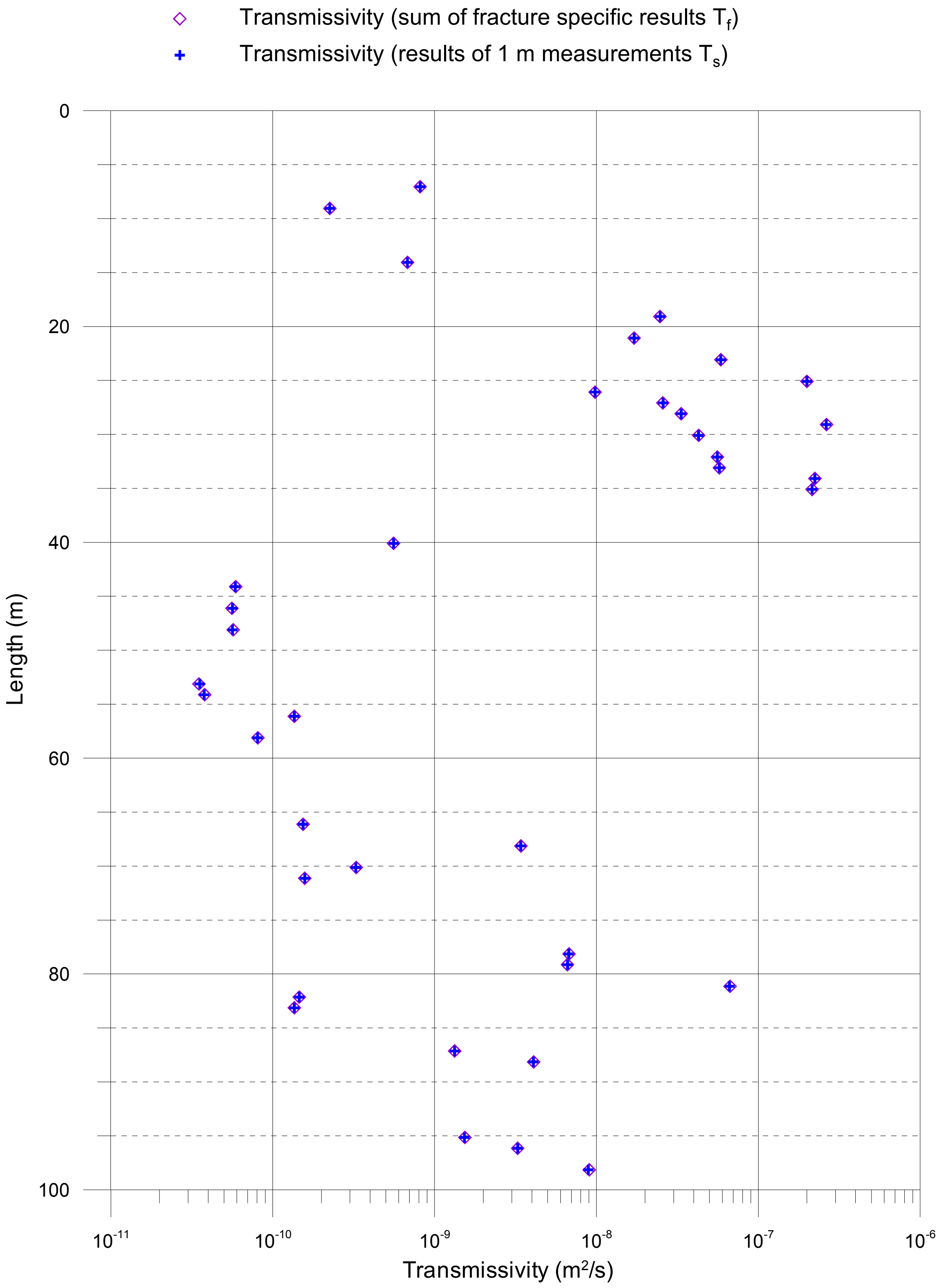

Comparison between section transmissivity and fracture transmissivity

Äspö, borehole KA3011A01
Head in the borehole during flow logging

Head(masl)= (Absolute pressure (Pa) - Airpressure (Pa) + Offset) /(1000 kg/m^3 * 9.80665 m/s^2) + Elevation (m)
Offset = 2600 Pa (Correction for absolute pressure sensor)

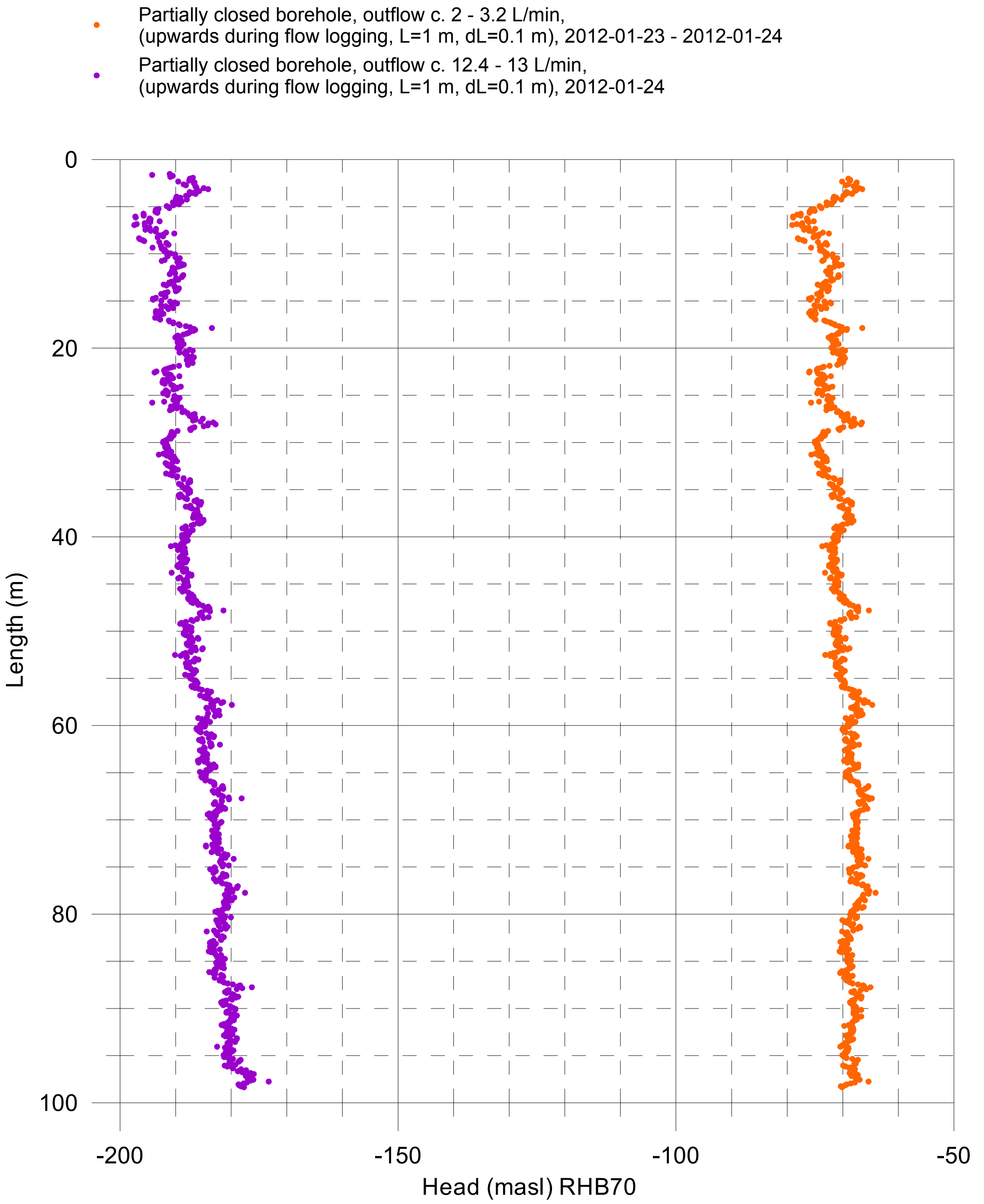

Head in the borehole during flow logging

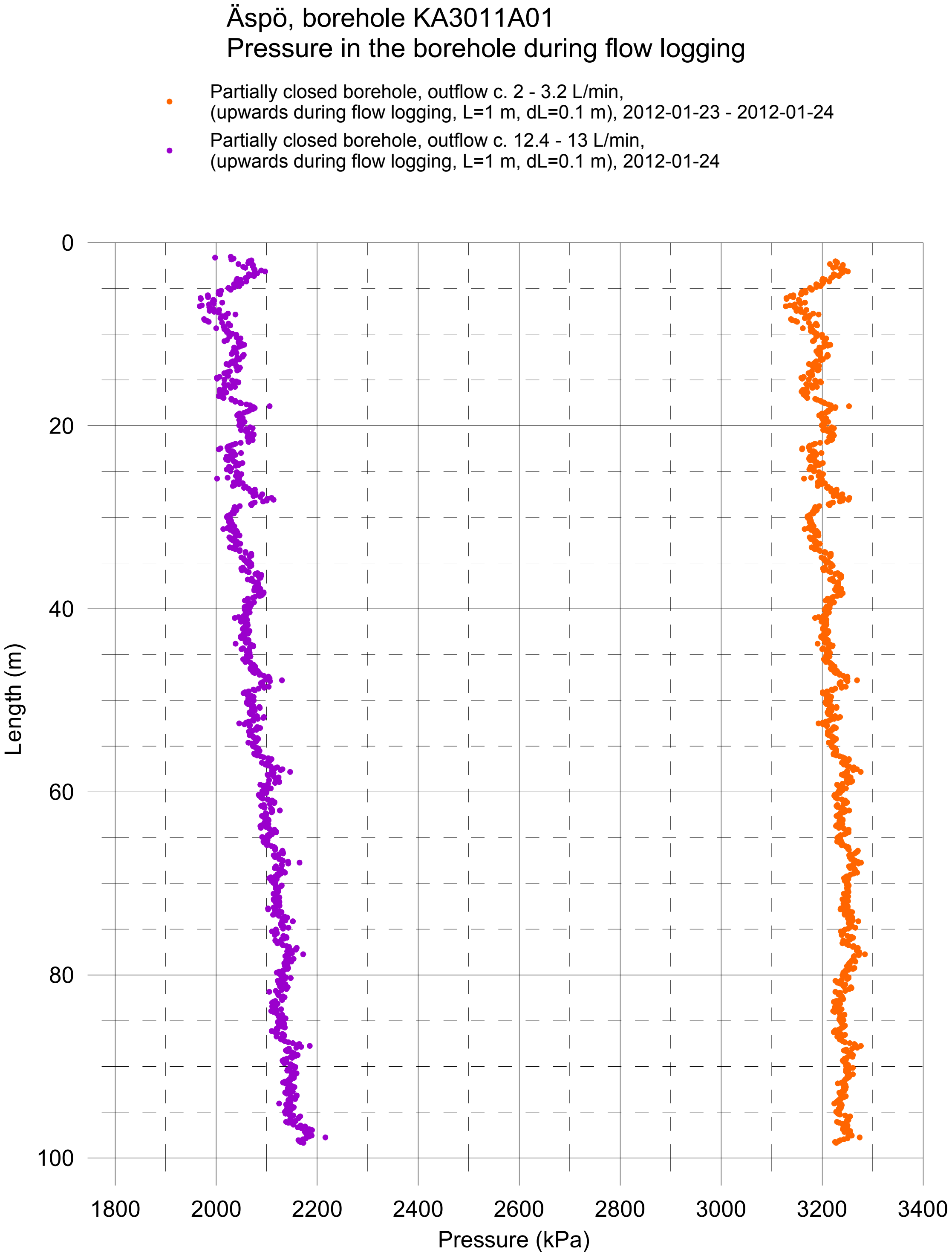

Pressure in the borehole during flow logging

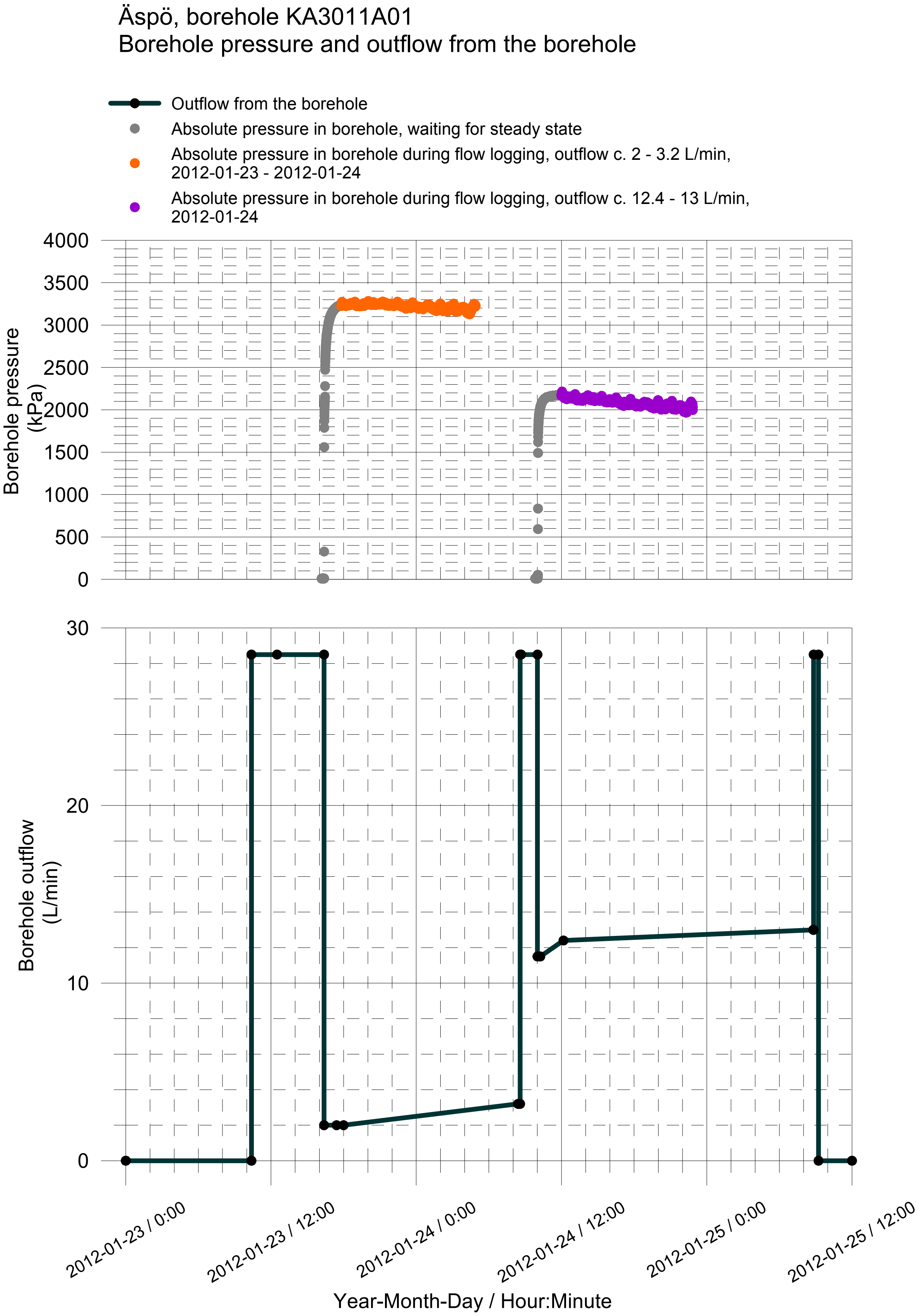

Borehole pressure and outflow from the borehole

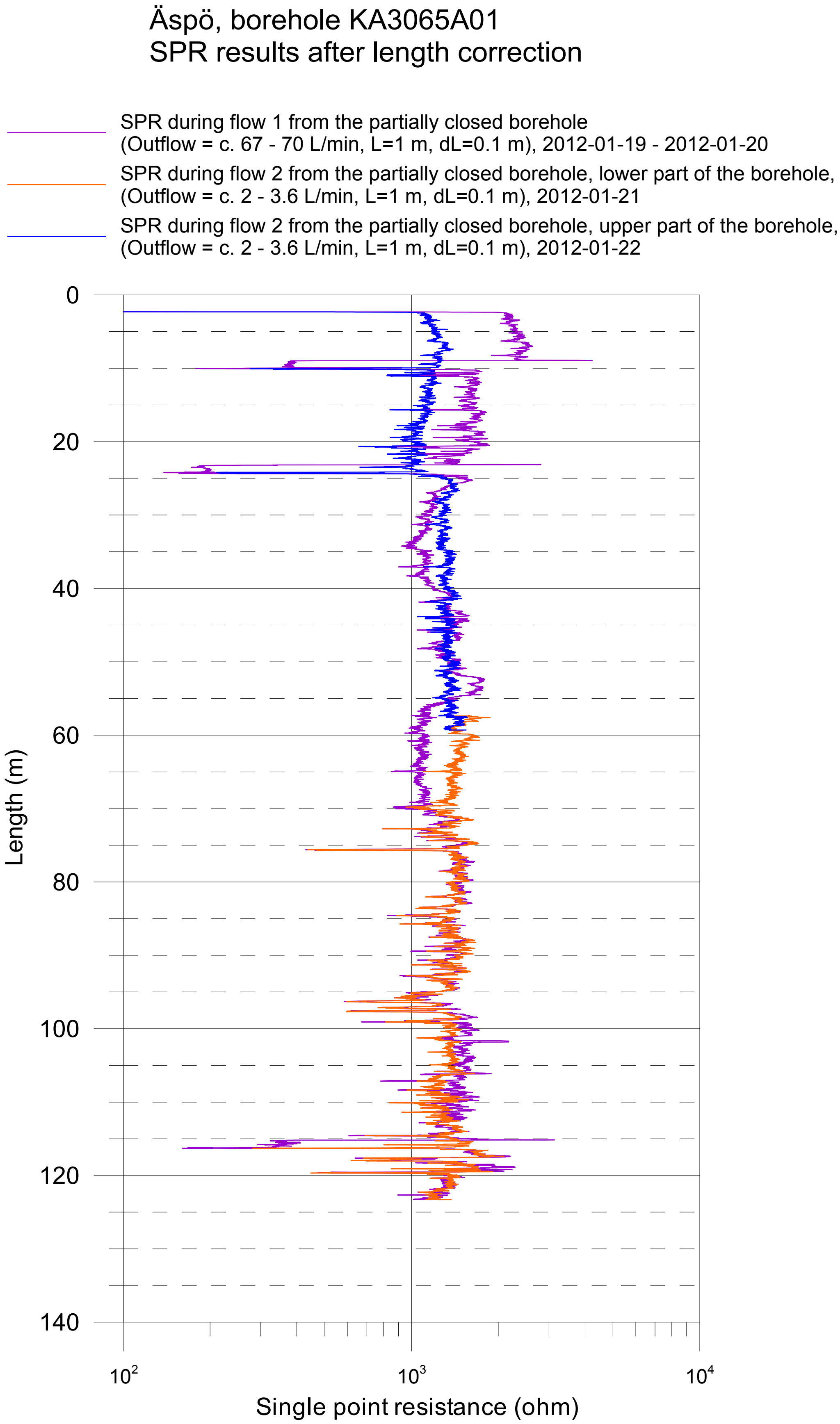

SPR results after length correction

Äspö, borehole KA3065A01
Electrical conductivity of borehole water

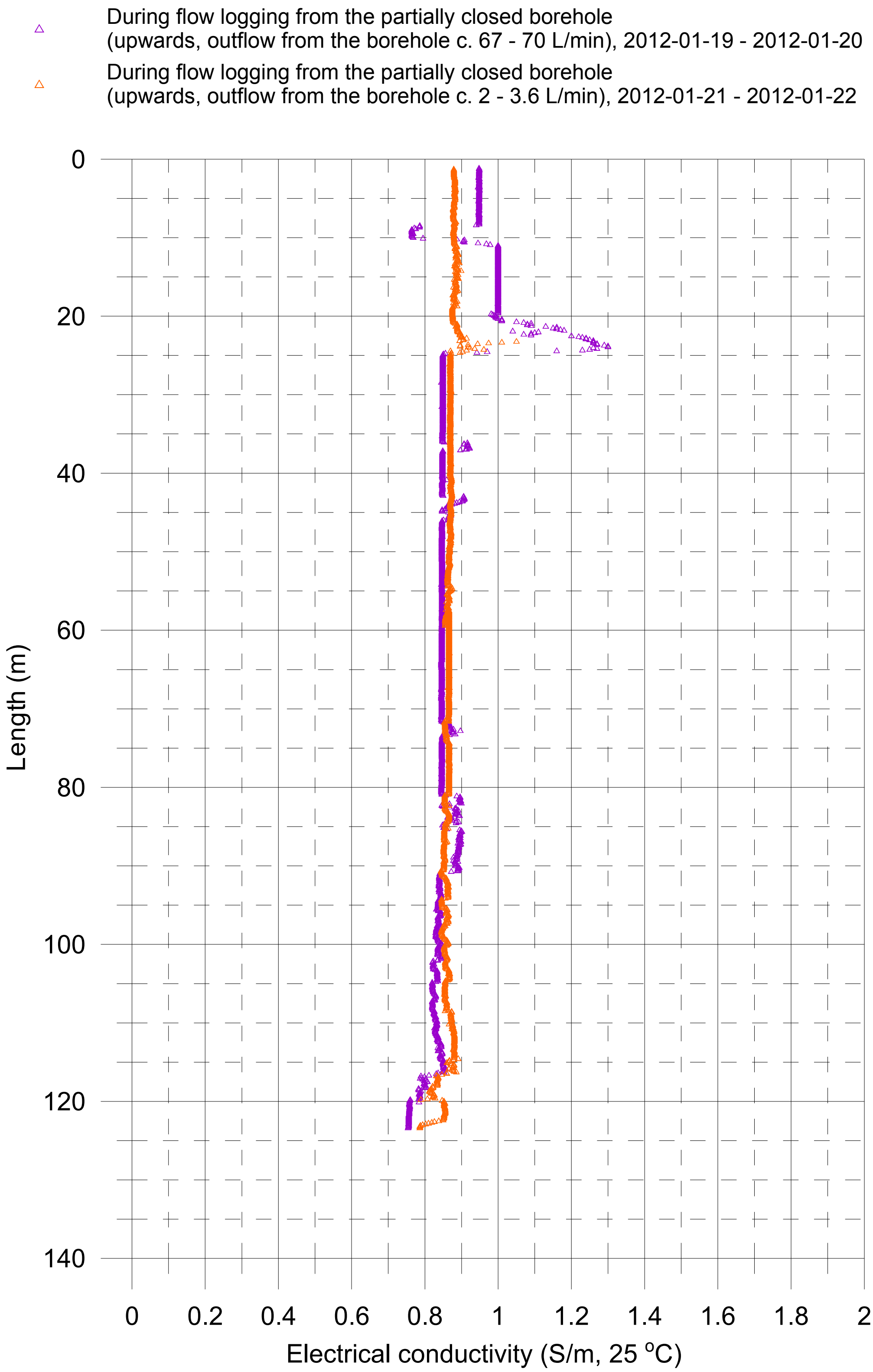

Electrical conductivity of borehole water

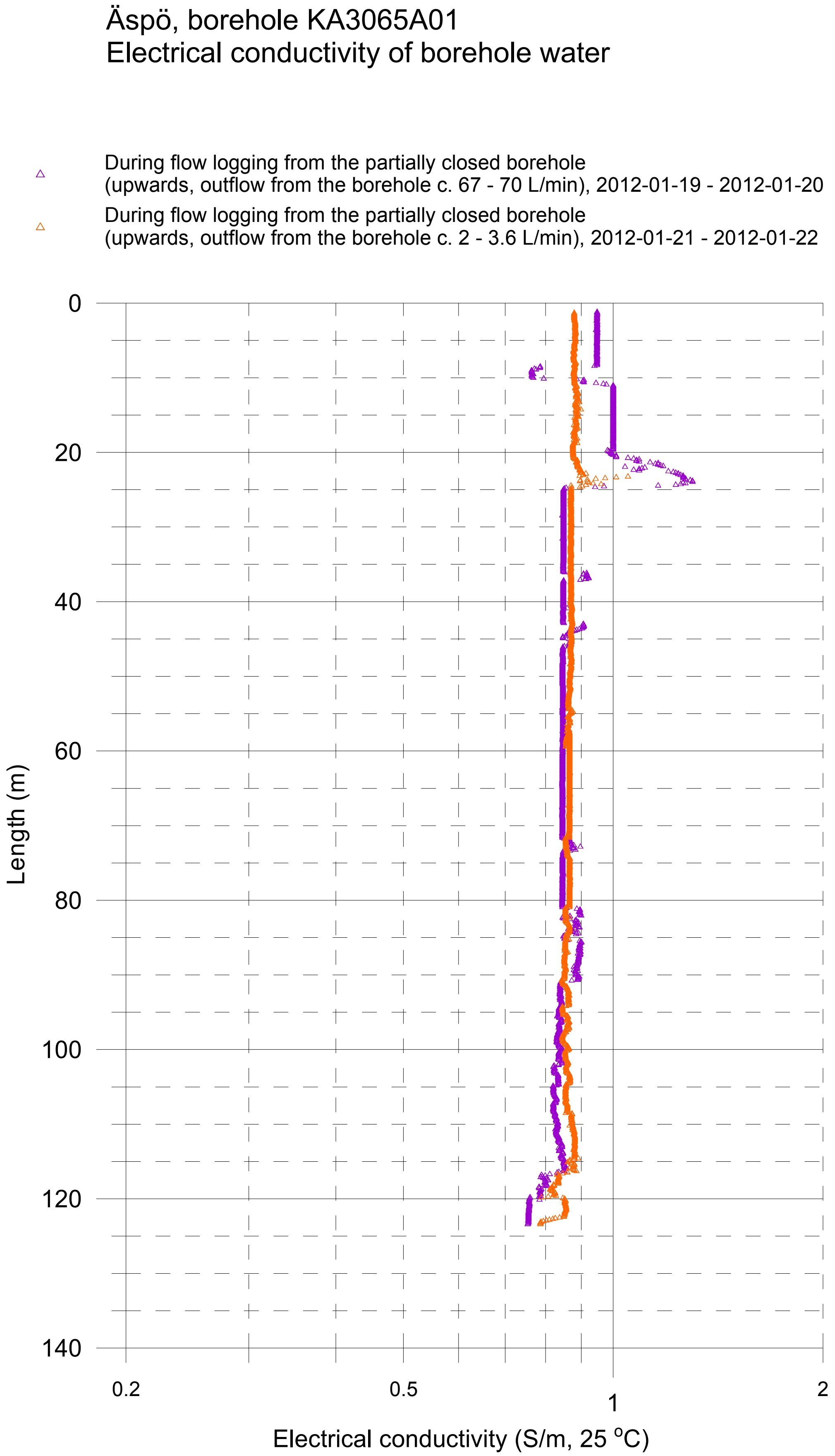

Electrical conductivity of borehole water

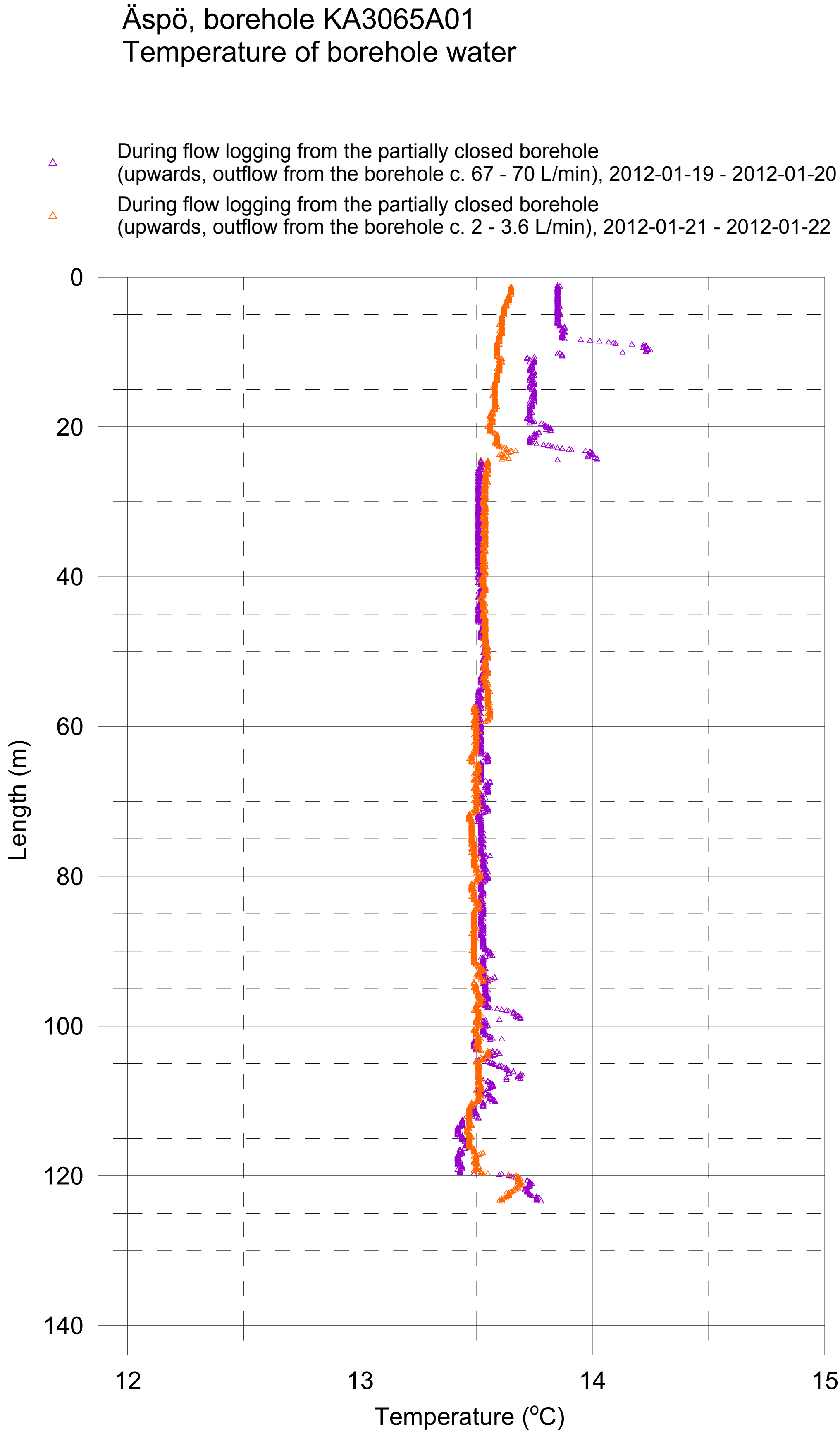

Temperature of borehole water

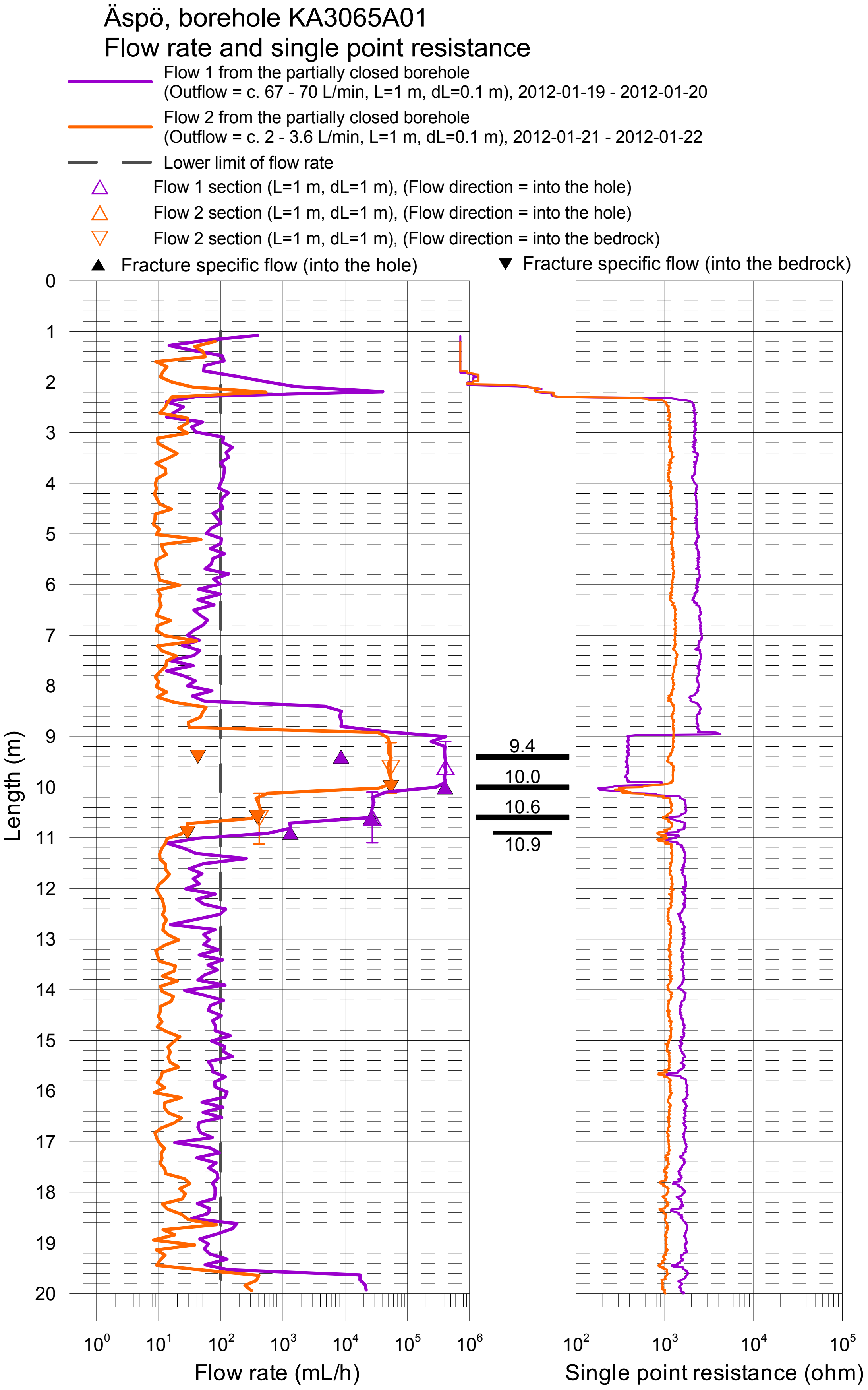

Flow rate and single point resistance

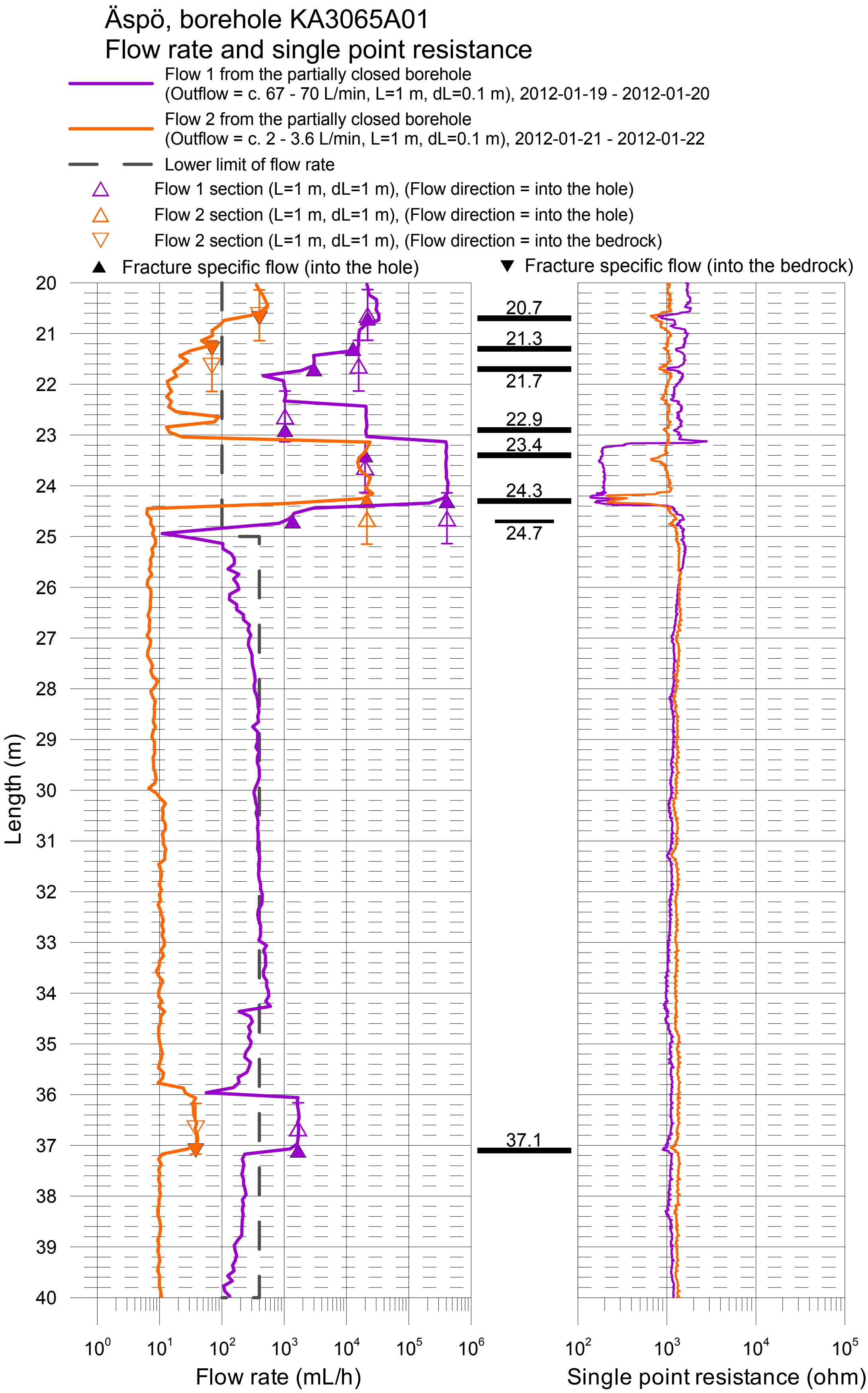

Flow rate and single point resistance

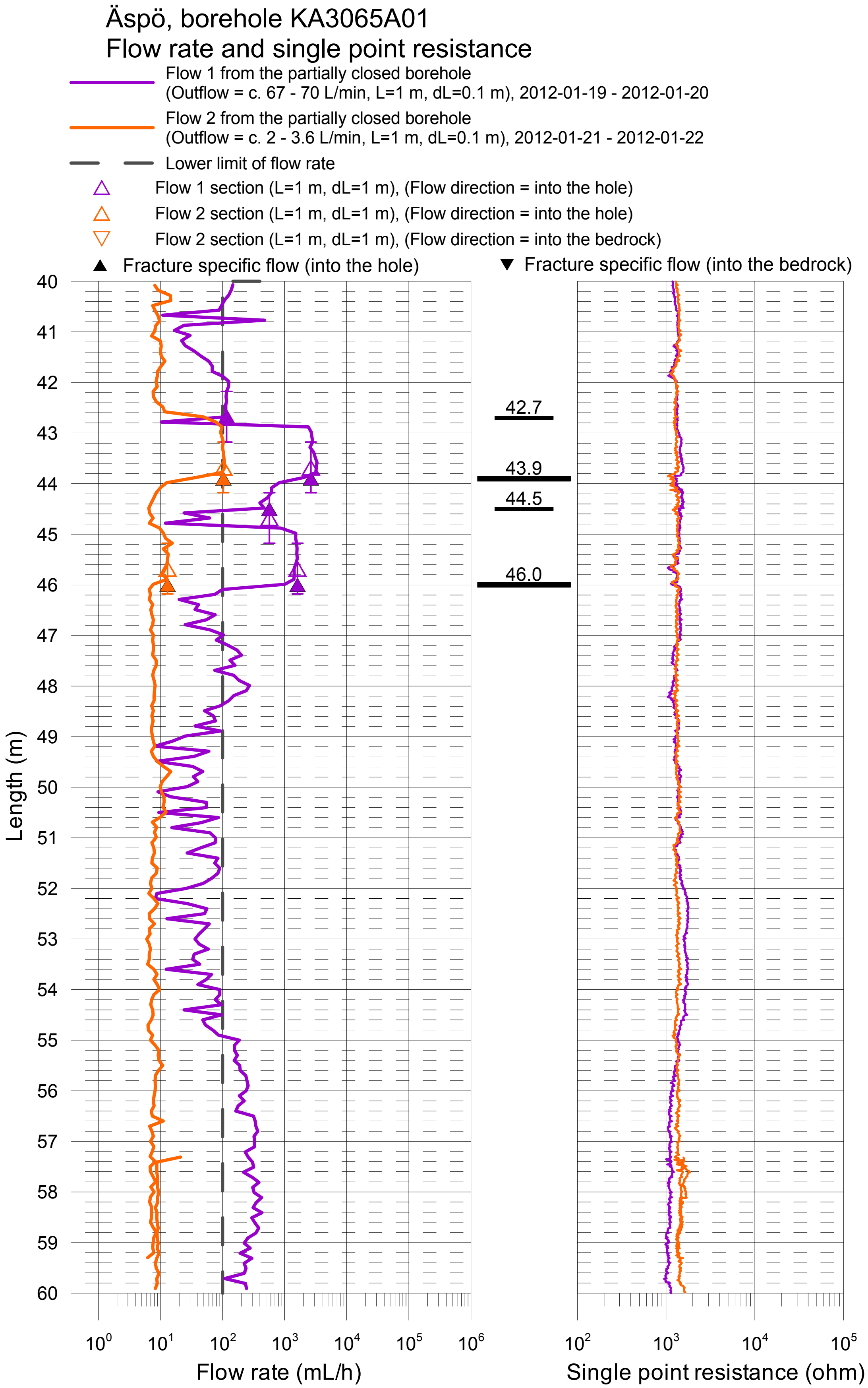

Flow rate and single point resistance

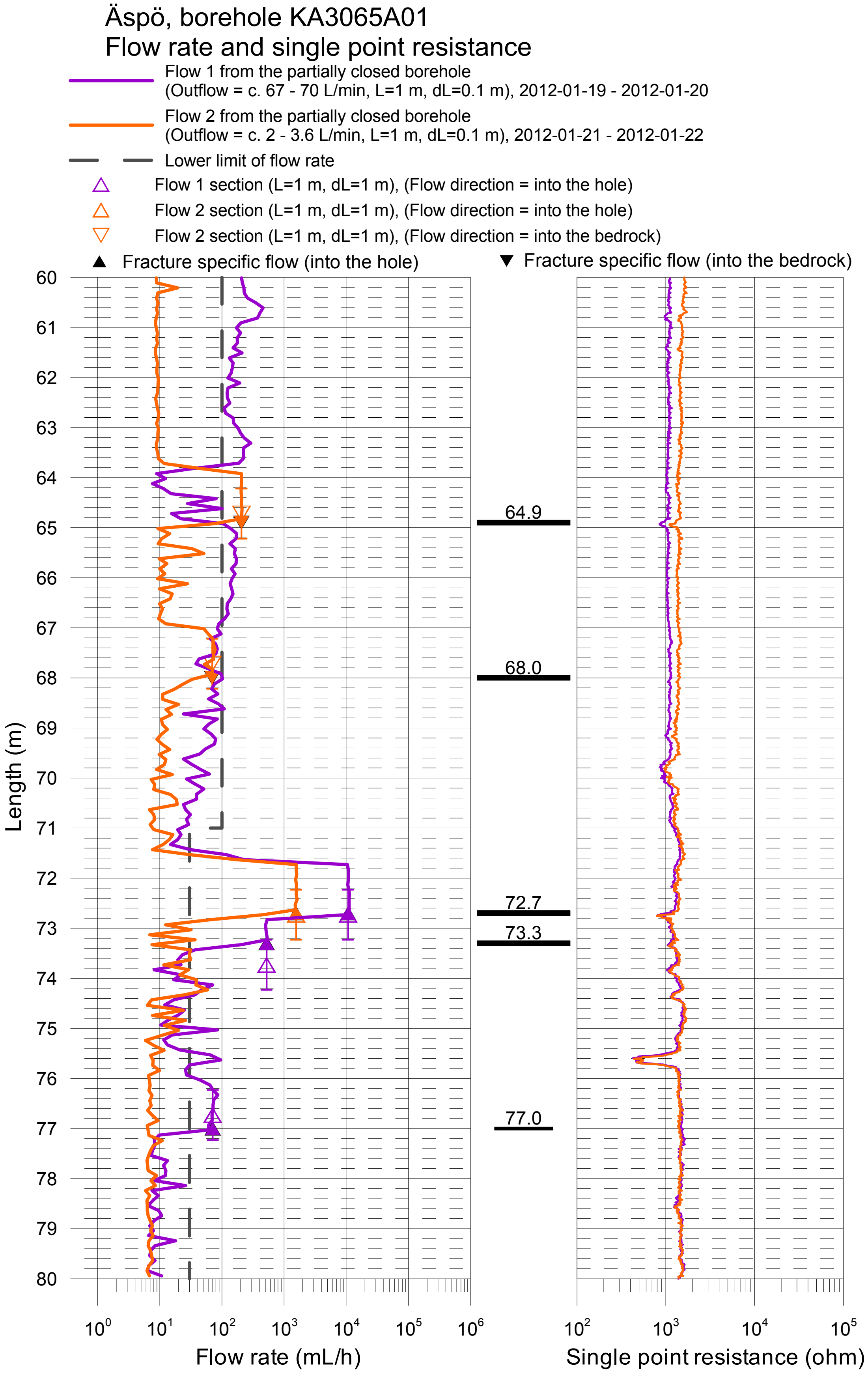

Flow rate and single point resistance

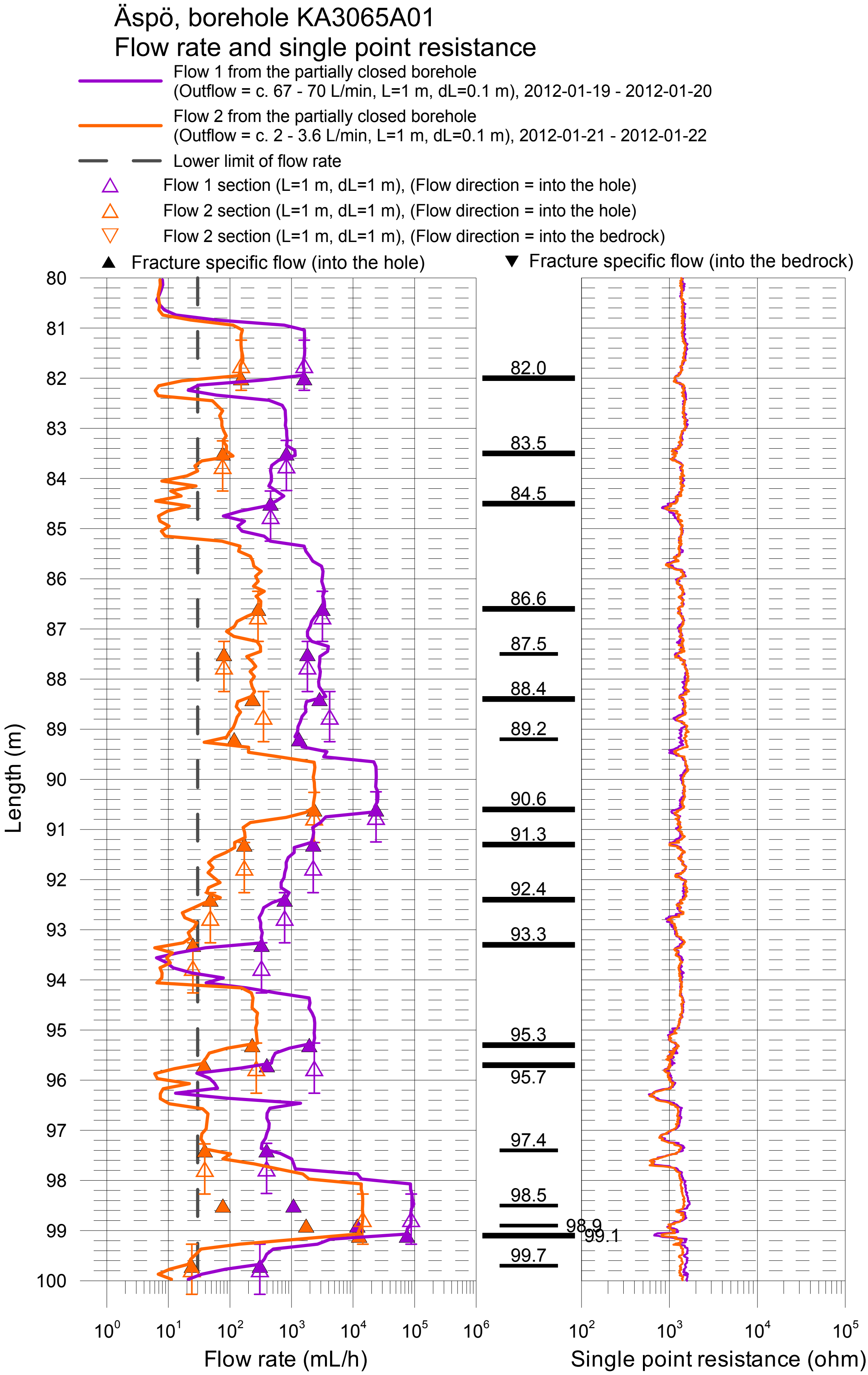

Flow rate and single point resistance

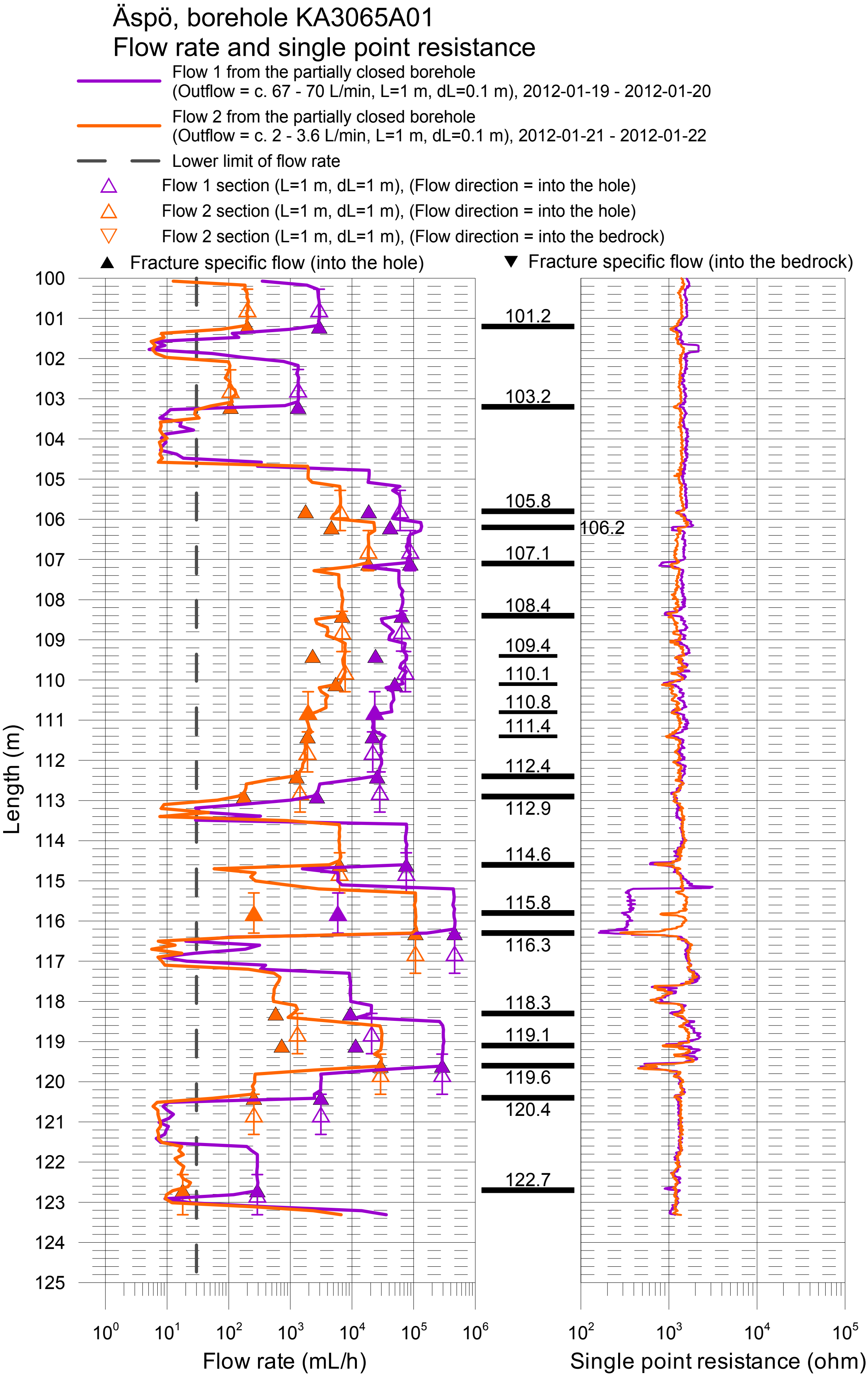

Appendix 14

Explanations for the tables in Appendices 5 and 7

Header	Unit	Explanations
Borehole		ID for borehole
Secup	m	Length along the borehole for the upper limit of the test section (based on corrected length L).
Seclow	m	Length along the borehole for the lower limit of the test section (based on corrected length L).
L	m	Corrected length along borehole based on SKB procedures for length correction.
Length to flow anom.	m	Length along the borehole to inferred flow anomaly during overlapping flow logging.
Test type (1–6)	(–)	1A: Pumping test – wire-line eq., 1B:Pumping test-submersible pump, 1C: Pumping test-airlift pumping, 2: Interference test, 3: Injection test, 4: Slug test, 5A: Difference flow logging – PFL-DIFF-Sequential, 5B: Difference flow logging – PFL-DIFF-Overlapping, 6: Flow logging-Impeller.
Date of test, start	YY-MM-DD	Date for start of pumping..
Time of test, start	hh:mm	Time for start of pumping
Date of flowl., start .	YY-MM-DD	Date for start of the flow logging.
Time of flowl., start	hh:mm	Time for start of the flow logging.
Date of test, stop	YY-MM-DD	Date for stop of the test.
Time of test, stop	hh:mm	Time for stop of the test.
L_w	m	Section length used in the difference flow logging.
dL	m	Step length (increment) used in the difference flow logging.
Q_{p1}	m^3/s	Flow rate at surface by the end of the first pumping period of the flow logging.
Q_{p2}	m^3/s	Flow rate at surface by the end of the second pumping period of the flow logging.
t_{p1}	s	Duration of the first pumping period.
t_{p2}	s	Duration of the second pumping period.
t_{F1}	s	Duration of the first recovery period.
t_{F2}	s	Duration of the second recovery period.
h_0	m.a.s.l.	Initial hydraulic head before pumping. Elevation of water level in open borehole in the local co-ordinates system with z=0 m.
h_1	m.a.s.l.	Stabilized hydraulic head during the first pumping period. Elevation of water level in open borehole in the local co-ordinates system with z=0 m.
h_2	m.a.s.l.	Stabilized hydraulic head during the second pumping period. Elevation of water level in open borehole in the local co-ordinates system with z=0 m.
s_1	m	Drawdown of the water level in the borehole during first pumping period. Difference between the actual hydraulic head and the initial head ($s_1= h_1–h_0$).
s_2	m	Drawdown of the water level in the borehole during second pumping period. Difference between the actual hydraulic head and the initial head ($s_2=h_2–h_0$).
T	m^2/s	Transmissivity of the entire borehole.
Q_0	m^3/s	Measured flow rate through the test section or flow anomaly under natural conditions (no pumping) with $h=h_0$ in the open borehole.
Q_1	m^3/s	Measured flow rate through the test section or flow anomaly during the first pumping period.
Q_2	m^3/s	Measured flow rate through the test section or flow anomaly during the second pumping period.
h_{0FW}	m.a.s.l.	Corrected initial hydraulic head along the hole due to e.g. varying salinity conditions of the borehole fluid before pumping.
h_{1FW}	m.a.s.l.	Corrected hydraulic head along the hole due to e.g. varying salinity conditions of the borehole fluid during the first pumping period.
h_{2FW}	m.a.s.l.	Corrected hydraulic head along the hole due to e.g. varying salinity conditions of the borehole fluid during the second pumping period.
EC_w	S/m	Measured electrical conductivity of the borehole fluid in the test section during difference flow logging.
Te_w	°C	Measured borehole fluid temperature in the test section during difference flow logging.
EC_f	S/m	Measured fracture-specific electrical conductivity of the fluid in flow anomaly during difference flow logging.
Te_f	°C	Measured fracture-specific fluid temperature in flow anomaly during difference flow logging.
T_D	m^2/s	Transmissivity of section or flow anomaly based on 2D model for evaluation of formation properties of the test section based on PFL-DIFF.
T-$measl_{LT}$	m^2/s	Estimated theoretical lower measurement limit for evaluated T_D. If the estimated T_D equals T_D-measlim, the actual T_D is considered to be equal or less than T_D-measlim.
T-$measl_{LP}$	m^2/s	Estimated practical lower measurement limit for evaluated T_D. If the estimated T_D equals T_D-measlim, the actual T_D is considered to be equal or less than T_D-measlim.
T-$measl_U$	m^2/s	Estimated upper measurement limit for evaluated T_D. If the estimated T_D equals T_D-measlim, the actual T_D is considered to be equal or less than T_D-measlim.
h_i	m.a.s.l.	Calculated relative, natural freshwater head for test section or flow anomaly (undisturbed conditions).

Appendix 15.1

Results of sequential flow logging

Borehole ID	Secup L(m)	Seclow L(m)	L_w (m)	Q_1 (m^3/s)	h_{1FW} (m.a.s.l.)	Q_2 (m^3/s)	h_{2FW} (m.a.s.l.)	T_D (m^2/s)	h_i (m.a.s.l.)	Q-lower limit P (mL/h)	T_D-measl$_{LT}$ (m^2/s)	T_D-measl$_{LP}$ (m^2/s)	T_D-measl$_U$ (m^2/s)	Comments
KA3065A01	2.10	3.10	1	–	–296.90	–	–49.83	–	–	100	3.3E–11	1.1E–10	3.3E–07	
KA3065A01	3.10	4.10	1	–	–297.64	–	–50.28	–	–	100	3.3E–11	1.1E–10	3.3E–07	
KA3065A01	4.10	5.10	1	–	–298.90	–	–50.89	–	–	100	3.3E–11	1.1E–10	3.3E–07	
KA3065A01	5.10	6.10	1	–	–299.15	–	–51.04	–	–	100	3.3E–11	1.1E–10	3.3E–07	
KA3065A01	6.10	7.10	1	–	–299.45	–	–51.07	–	–	100	3.3E–11	1.1E–10	3.3E–07	
KA3065A01	7.11	8.11	1	–	–299.70	–	–51.06	–	–	100	3.3E–11	1.1E–10	3.3E–07	
KA3065A01	8.11	9.11	1	–	–300.61	–	–51.20	–	–	100	3.3E–11	1.1E–10	3.3E–07	
KA3065A01	9.11	10.11	1	1.14E–04	–296.93	–1.51E–05	–51.07	5.2E–07	–79.75	100	3.4E–11	1.1E–10	4.0E–07	**
KA3065A01	10.11	11.11	1	7.64E–06	–298.63	–1.16E–07	–50.87	3.1E–08	–54.56	100	3.3E–11	1.1E–10	3.3E–07	
KA3065A01	11.12	12.12	1	–	–298.59	–	–51.04	–	–	100	3.3E–11	1.1E–10	3.3E–07	
KA3065A01	12.12	13.12	1	–	–299.10	–	–51.41	–	–	100	3.3E–11	1.1E–10	3.3E–07	
KA3065A01	13.12	14.12	1	–	–299.39	–	–51.54	–	–	100	3.3E–11	1.1E–10	3.3E–07	
KA3065A01	14.12	15.12	1	–	–298.47	–	–51.37	–	–	100	3.3E–11	1.1E–10	3.3E–07	
KA3065A01	15.13	16.13	1	–	–298.81	–	–51.77	–	–	100	3.3E–11	1.1E–10	3.3E–07	
KA3065A01	16.13	17.13	1	–	–298.86	–	–51.58	–	–	100	3.3E–11	1.1E–10	3.3E–07	
KA3065A01	17.13	18.13	1	–	–298.21	–	–51.43	–	–	100	3.3E–11	1.1E–10	3.3E–07	
KA3065A01	18.13	19.13	1	–	–298.21	–	–51.61	–	–	100	3.3E–11	1.1E–10	3.3E–07	
KA3065A01	19.13	20.13	1	–	–297.85	–	–51.58	–	–	100	3.3E–11	1.1E–10	3.3E–07	
KA3065A01	20.14	21.14	1	6.06E–06	–298.26	–1.11E–07	–51.79	2.5E–08	–56.22	100	3.3E–11	1.1E–10	3.3E–07	
KA3065A01	21.14	22.14	1	4.36E–06	–299.20	–1.92E–08	–52.13	1.8E–08	–53.21	100	3.3E–11	1.1E–10	3.3E–07	
KA3065A01	22.14	23.14	1	2.86E–07	–299.11	–	–52.25	1.2E–09	–	100	3.3E–11	1.1E–10	3.3E–07	¤
KA3065A01	23.14	24.14	1	5.50E–06	–296.66	–	–52.15	2.2E–08	–	100	3.4E–11	1.1E–10	3.4E–07	¤
KA3065A01	24.15	25.15	1	1.14E–04	–298.89	5.92E–06	–52.23	4.3E–07	–38.73	100	3.3E–11	1.1E–10	3.1E–07	**
KA3065A01	25.15	26.15	1	–	–298.63	–	–52.26	–	–	400	3.3E–11	4.5E–10	3.3E–07	
KA3065A01	26.15	27.15	1	–	–298.12	–	–52.19	–	–	400	3.4E–11	4.5E–10	3.4E–07	
KA3065A01	27.15	28.15	1	–	–297.96	–	–52.27	–	–	400	3.4E–11	4.5E–10	3.4E–07	
KA3065A01	28.15	29.15	1	–	–298.75	–	–52.87	–	–	400	3.4E–11	4.5E–10	3.4E–07	
KA3065A01	29.15	30.15	1	–	–298.52	–	–53.06	–	–	400	3.4E–11	4.5E–10	3.4E–07	
KA3065A01	30.16	31.16	1	–	–298.52	–	–53.17	–	–	400	3.4E–11	4.5E–10	3.4E–07	
KA3065A01	31.16	32.16	1	–	–298.59	–	–53.30	–	–	400	3.4E–11	4.5E–10	3.4E–07	
KA3065A01	32.16	33.16	1	–	–298.59	–	–53.42	–	–	400	3.4E–11	4.5E–10	3.4E–07	
KA3065A01	33.16	34.16	1	–	–297.95	–	–53.24	–	–	400	3.4E–11	4.5E–10	3.4E–07	

Results of sequential flow logging

Borehole ID	Secup L(m)	Seclow L(m)	L_w (m)	Q_1 (m^3/s)	h_{1FW} (m.a.s.l.)	Q_2 (m^3/s)	h_{2FW} (m.a.s.l.)	T_D (m^2/s)	h_i (m.a.s.l.)	Q-lower limit P (mL/h)	T_D-measl$_{LT}$ (m^2/s)	T_D-measl$_{LP}$ (m^2/s)	T_D-measl$_U$ (m^2/s)	Comments
KA3065A01	34.16	35.16	1	–	–298.04	–	–53.35	–	–	400	3.4E–11	4.5E–10	3.4E–07	
KA3065A01	35.17	36.17	1	–	–297.79	–	–53.38	–	–	400	3.4E–11	4.5E–10	3.4E–07	
KA3065A01	36.17	37.17	1	4.64E–07	–297.67	–1.06E–08	–53.58	1.9E–09	–59.01	400	3.4E–11	4.5E–10	3.4E–07	
KA3065A01	37.17	38.17	1	–	–297.48	–	–53.72	–	–	400	3.4E–11	4.5E–10	3.4E–07	
KA3065A01	38.17	39.17	1	–	–298.09	–	–54.00	–	–	400	3.4E–11	4.5E–10	3.4E–07	
KA3065A01	39.17	40.17	1	–	–298.23	–	–54.36	–	–	400	3.4E–11	4.5E–10	3.4E–07	
KA3065A01	40.18	41.18	1	–	–298.04	–	–54.56	–	–	100	3.4E–11	1.1E–10	3.4E–07	
KA3065A01	41.18	42.18	1	–	–298.02	–	–54.67	–	–	100	3.4E–11	1.1E–10	3.4E–07	
KA3065A01	42.18	43.18	1	3.22E–08	–297.85	–	–54.87	1.3E–10	–	100	3.4E–11	1.1E–10	3.4E–07	¤
KA3065A01	43.18	44.18	1	7.33E–07	–298.17	2.86E–08	–55.05	2.9E–09	–45.18	100	3.4E–11	1.1E–10	3.4E–07	
KA3065A01	44.18	45.18	1	1.58E–07	–297.51	–	–55.24	6.4E–10	–	100	3.4E–11	1.1E–10	3.4E–07	¤
KA3065A01	45.18	46.18	1	4.47E–07	–296.97	3.61E–09	–55.25	1.8E–09	–53.28	100	3.4E–11	1.1E–10	3.4E–07	*
KA3065A01	46.19	47.19	1	–	–296.65	–	–55.38	–	–	100	3.4E–11	1.1E–10	3.4E–07	
KA3065A01	47.19	48.19	1	–	–297.03	–	–55.64	–	–	100	3.4E–11	1.1E–10	3.4E–07	
KA3065A01	48.19	49.19	1	–	–297.17	–	–56.21	–	–	100	3.4E–11	1.1E–10	3.4E–07	
KA3065A01	49.19	50.19	1	–	–297.22	–	–56.41	–	–	100	3.4E–11	1.1E–10	3.4E–07	
KA3065A01	50.19	51.19	1	–	–297.23	–	–56.64	–	–	100	3.4E–11	1.1E–10	3.4E–07	
KA3065A01	51.20	52.20	1	–	–297.50	–	–56.96	–	–	100	3.4E–11	1.1E–10	3.4E–07	
KA3065A01	52.20	53.20	1	–	–297.78	–	–57.24	–	–	100	3.4E–11	1.1E–10	3.4E–07	
KA3065A01	53.20	54.20	1	–	–297.68	–	–57.50	–	–	100	3.4E–11	1.1E–10	3.4E–07	
KA3065A01	54.20	55.20	1	–	–297.32	–	–57.81	–	–	100	3.4E–11	1.2E–10	3.4E–07	
KA3065A01	55.20	56.20	1	–	–296.86	–	–57.97	–	–	100	3.5E–11	1.2E–10	3.5E–07	
KA3065A01	56.20	57.20	1	–	–296.21	–	–58.19	–	–	100	3.5E–11	1.2E–10	3.5E–07	
KA3065A01	57.21	58.21	1	–	–296.27	–	–49.12	–	–	100	3.3E–11	1.1E–10	3.3E–07	
KA3065A01	58.21	59.21	1	–	–296.87	–	–49.35	–	–	100	3.3E–11	1.1E–10	3.3E–07	
KA3065A01	59.21	60.21	1	–	–297.16	–	–49.45	–	–	100	3.3E–11	1.1E–10	3.3E–07	
KA3065A01	60.21	61.21	1	–	–296.68	–	–49.37	–	–	100	3.3E–11	1.1E–10	3.3E–07	
KA3065A01	61.22	62.22	1	–	–297.06	–	–49.51	–	–	100	3.3E–11	1.1E–10	3.3E–07	
KA3065A01	62.22	63.22	1	–	–295.35	–	–49.65	–	–	100	3.4E–11	1.1E–10	3.4E–07	
KA3065A01	63.22	64.22	1	–	–295.01	–	–49.53	–	–	100	3.4E–11	1.1E–10	3.4E–07	
KA3065A01	64.22	65.22	1	–	–295.24	–5.72E–08	–49.73	2.3E–10	–	100	3.4E–11	1.1E–10	3.4E–07	¤
KA3065A01	65.22	66.22	1	–	–295.09	–	–49.65	–	–	100	3.4E–11	1.1E–10	3.4E–07	
KA3065A01	66.22	67.22	1	–	–295.83	–	–49.70	–	–	100	3.3E–11	1.1E–10	3.3E–07	

Appendix 15.3

Results of sequential flow logging

Borehole ID	Secup L(m)	Seclow L(m)	L_w (m)	Q_1 (m^3/s)	h_{1FW} (m.a.s.l.)	Q_2 (m^3/s)	h_{2FW} (m.a.s.l.)	T_D (m^2/s)	h_i (m.a.s.l.)	Q-lower limit P (mL/h)	T_D-measl$_{LT}$ (m^2/s)	T_D-measl$_{LP}$ (m^2/s)	T_D-measl$_U$ (m^2/s)	Comments
KA3065A01	67.22	68.22	1	–	–296.09	–1.94E–08	–49.80	7.8E–11	–	100	3.3E–11	1.1E–10	3.3E–07	¤
KA3065A01	68.23	69.23	1	–	–296.20	–	–49.96	–	–	100	3.3E–11	1.1E–10	3.3E–07	
KA3065A01	69.23	70.23	1	–	–295.98	–	–50.01	–	–	100	3.4E–11	1.1E–10	3.4E–07	
KA3065A01	70.23	71.23	1	–	–296.02	–	–50.12	–	–	100	3.4E–11	1.1E–10	3.4E–07	
KA3065A01	71.23	72.23	1	–	–295.79	–	–50.25	–	–	30	3.4E–11	3.4E–11	3.4E–07	
KA3065A01	72.23	73.23	1	2.97E–06	–295.96	4.33E–07	–50.32	1.0E–08	–8.39	30	3.4E–11	3.4E–11	3.3E–07	
KA3065A01	73.23	74.23	1	1.45E–07	–295.99	–	–50.31	5.9E–10	–	30	3.4E–11	3.4E–11	3.4E–07	¤
KA3065A01	74.23	75.23	1	–	–296.25	–	–50.49	–	–	30	3.4E–11	3.4E–11	3.4E–07	
KA3065A01	75.24	76.24	1	–	–296.27	–	–50.58	–	–	30	3.4E–11	3.4E–11	3.4E–07	
KA3065A01	76.24	77.24	1	1.97E–08	–295.58	–	–50.53	8.0E–11	–	30	3.4E–11	3.4E–11	3.4E–07	¤
KA3065A01	77.24	78.24	1	–	–296.06	–	–50.64	–	–	30	3.4E–11	3.4E–11	3.4E–07	
KA3065A01	78.24	79.24	1	–	–296.06	–	–50.82	–	–	30	3.4E–11	3.4E–11	3.4E–07	
KA3065A01	79.24	80.24	1	–	–296.23	–	–50.98	–	–	30	3.4E–11	3.4E–11	3.4E–07	
KA3065A01	80.24	81.24	1	–	–296.25	–	–51.06	–	–	30	3.4E–11	3.4E–11	3.4E–07	
KA3065A01	81.24	82.24	1	4.47E–07	–296.46	4.22E–08	–51.30	1.6E–09	–25.74	30	3.4E–11	3.4E–11	3.4E–07	
KA3065A01	82.25	83.25	1	–	–296.42	–	–51.45	–	–	30	3.4E–11	3.4E–11	3.4E–07	
KA3065A01	83.25	84.25	1	2.30E–07	–296.27	2.11E–08	–51.55	8.4E–10	–26.82	30	3.4E–11	3.4E–11	3.4E–07	
KA3065A01	84.25	85.25	1	1.27E–07	–295.93	–	–51.69	5.1E–10	–	30	3.4E–11	3.4E–11	3.4E–07	¤
KA3065A01	85.25	86.25	1	–	–295.50	–	–51.83	–	–	30	3.4E–11	3.4E–11	3.4E–07	
KA3065A01	86.25	87.25	1	8.83E–07	–295.29	7.92E–08	–51.73	3.3E–09	–27.75	30	3.4E–11	3.4E–11	3.4E–07	
KA3065A01	87.25	88.25	1	5.06E–07	–294.81	2.22E–08	–51.87	2.0E–09	–40.70	30	3.4E–11	3.4E–11	3.4E–07	
KA3065A01	88.25	89.25	1	1.16E–06	–295.34	9.75E–08	–52.01	4.3E–09	–29.70	30	3.4E–11	3.4E–11	3.4E–07	
KA3065A01	89.26	90.26	1	–	–295.01	–	–52.01	–	–	30	3.4E–11	3.4E–11	3.4E–07	
KA3065A01	90.26	91.26	1	6.56E–06	–295.27	6.50E–07	–52.18	2.4E–08	–25.42	30	3.4E–11	3.4E–11	3.4E–07	
KA3065A01	91.26	92.26	1	6.25E–07	–295.03	4.75E–08	–52.24	2.4E–09	–32.27	30	3.4E–11	3.4E–11	3.4E–07	
KA3065A01	92.26	93.26	1	2.15E–07	–295.21	1.33E–08	–52.45	8.2E–10	–36.42	30	3.4E–11	3.4E–11	3.4E–07	
KA3065A01	93.26	94.26	1	9.06E–08	–295.13	6.94E–09	–52.53	3.4E–10	–32.38	30	3.4E–11	3.4E–11	3.4E–07	*
KA3065A01	94.26	95.26	1	–	–294.93	–	–52.54	–	–	30	3.4E–11	3.4E–11	3.4E–07	
KA3065A01	95.26	96.26	1	6.52E–07	–293.72	7.44E–08	–52.61	2.4E–09	–21.54	30	3.4E–11	3.4E–11	3.4E–07	
KA3065A01	96.27	97.27	1	–	–293.73	–	–52.78	–	–	30	3.4E–11	3.4E–11	3.4E–07	
KA3065A01	97.27	98.27	1	1.09E–07	–294.01	1.08E–08	–53.19	4.0E–10	–26.66	30	3.4E–11	3.4E–11	3.4E–07	
KA3065A01	98.27	99.27	1	2.45E–05	–293.59	4.00E–06	–53.30	8.4E–08	–6.31	30	3.4E–11	3.4E–11	3.3E–07	
KA3065A01	99.27	100.27	1	8.50E–08	–293.30	6.67E–09	–53.49	3.2E–10	–33.08	30	3.4E–11	3.4E–11	3.4E–07	*

Appendix 15.4

Results of sequential flow logging

Borehole ID	Secup L(m)	Seclow L(m)	L_w (m)	Q_1 (m^3/s)	h_{1FW} (m.a.s.l.)	Q_2 (m^3/s)	h_{2FW} (m.a.s.l.)	T_D (m^2/s)	h_i (m.a.s.l.)	Q-lower limit P (mL/h)	T_D-measl$_{LT}$ (m^2/s)	T_D-measl$_{LP}$ (m^2/s)	T_D-measl$_U$ (m^2/s)	Comments
KA3065A01	100.27	101.27	1	8.17E–07	–292.24	5.58E–08	–53.52	3.2E–09	–36.00	30	3.5E–11	3.5E–11	3.5E–07	
KA3065A01	101.27	102.27	1	–	–287.40	–	–53.54	–	–	30	3.5E–11	3.5E–11	3.5E–07	
KA3065A01	102.28	103.28	1	3.72E–07	–286.59	2.97E–08	–53.57	1.5E–09	–33.35	30	3.5E–11	3.5E–11	3.5E–07	
KA3065A01	103.28	104.28	1	–	–286.19	–	–53.68	–	–	30	3.5E–11	3.6E–11	3.5E–07	
KA3065A01	104.28	105.28	1	–	–285.94	–	–53.84	–	–	30	3.6E–11	3.6E–11	3.6E–07	
KA3065A01	105.28	106.28	1	1.68E–05	–286.02	1.78E–06	–54.14	6.4E–08	–26.51	30	3.6E–11	3.6E–11	3.5E–07	
KA3065A01	106.28	107.28	1	2.46E–05	–285.91	5.14E–06	–54.22	8.3E–08	7.10	30	3.6E–11	3.6E–11	3.3E–07	
KA3065A01	107.28	108.28	1	–	–287.22	–	–54.71	–	–	30	3.5E–11	3.6E–11	3.5E–07	
KA3065A01	108.29	109.29	1	1.79E–05	–286.67	1.92E–06	–54.98	6.8E–08	–27.09	30	3.6E–11	3.6E–11	3.5E–07	
KA3065A01	109.29	110.29	1	2.04E–05	–286.63	2.15E–06	–55.11	7.8E–08	–27.86	30	3.6E–11	3.6E–11	3.5E–07	
KA3065A01	110.29	111.29	1	6.50E–06	–286.69	5.39E–07	–55.46	2.6E–08	–34.56	30	3.6E–11	3.6E–11	3.5E–07	
KA3065A01	111.29	112.29	1	6.03E–06	–286.39	5.28E–07	–55.67	2.4E–08	–33.53	30	3.6E–11	3.6E–11	3.6E–07	
KA3065A01	112.29	113.29	1	7.86E–06	–286.36	3.99E–07	–55.81	3.2E–08	–43.47	30	3.6E–11	3.6E–11	3.6E–07	
KA3065A01	113.30	114.30	1	–	–285.91	–	–56.06	–	–	30	3.6E–11	3.6E–11	3.6E–07	
KA3065A01	114.30	115.30	1	2.11E–05	–286.16	1.75E–06	–56.32	8.3E–08	–35.52	30	3.6E–11	3.6E–11	3.5E–07	
KA3065A01	115.30	116.30	1	1.64E–06	–284.61	7.08E–08	–56.55	6.8E–09	–46.25	30	3.6E–11	3.6E–11	3.6E–07	
KA3065A01	116.30	117.30	1	1.28E–04	–285.27	2.97E–05	–56.85	4.3E–07	12.00	30	3.6E–11	3.6E–11	2.3E–07	**
KA3065A01	117.30	118.30	1	–	–285.32	–	–57.18	–	–	30	3.6E–11	3.6E–11	3.6E–07	
KA3065A01	118.30	119.30	1	5.81E–06	–285.48	3.63E–07	–57.62	2.4E–08	–42.43	30	3.6E–11	3.6E–11	3.6E–07	
KA3065A01	119.31	120.31	1	8.08E–05	–285.83	8.08E–06	–57.82	3.2E–07	–32.49	30	3.6E–11	3.6E–11	3.3E–07	
KA3065A01	120.31	121.31	1	8.70E–07	–285.18	7.08E–08	–58.05	3.5E–09	–37.92	30	3.6E–11	3.6E–11	3.6E–07	
KA3065A01	121.31	122.31	1	–	–284.43	–	–58.30	–	–	30	3.6E–11	3.7E–11	3.6E–07	
KA3065A01	122.31	123.31	1	8.08E–08	–283.64	5.00E–09	–58.71	3.3E–10	–43.88	30	3.7E–11	3.7E–11	3.7E–07	*
KA3065A01	123.31	124.31	1	–	–279.62	–	–58.96	–	–	30	3.7E–11	3.7E–11	3.7E–07	

* Uncertain = The flow rate Q_1 and/or Q_2 is less than 30 mL/h or the flow anomalies are overlapping or they are unclear because of noise.
** Flow rate Q_1 over the measurement limit (300,000 mL/h)
¤ T_D calculation based on assumption that flow rate Q_1 or Q_2=0 mL/h

Plotted flow rates of 1 m sections

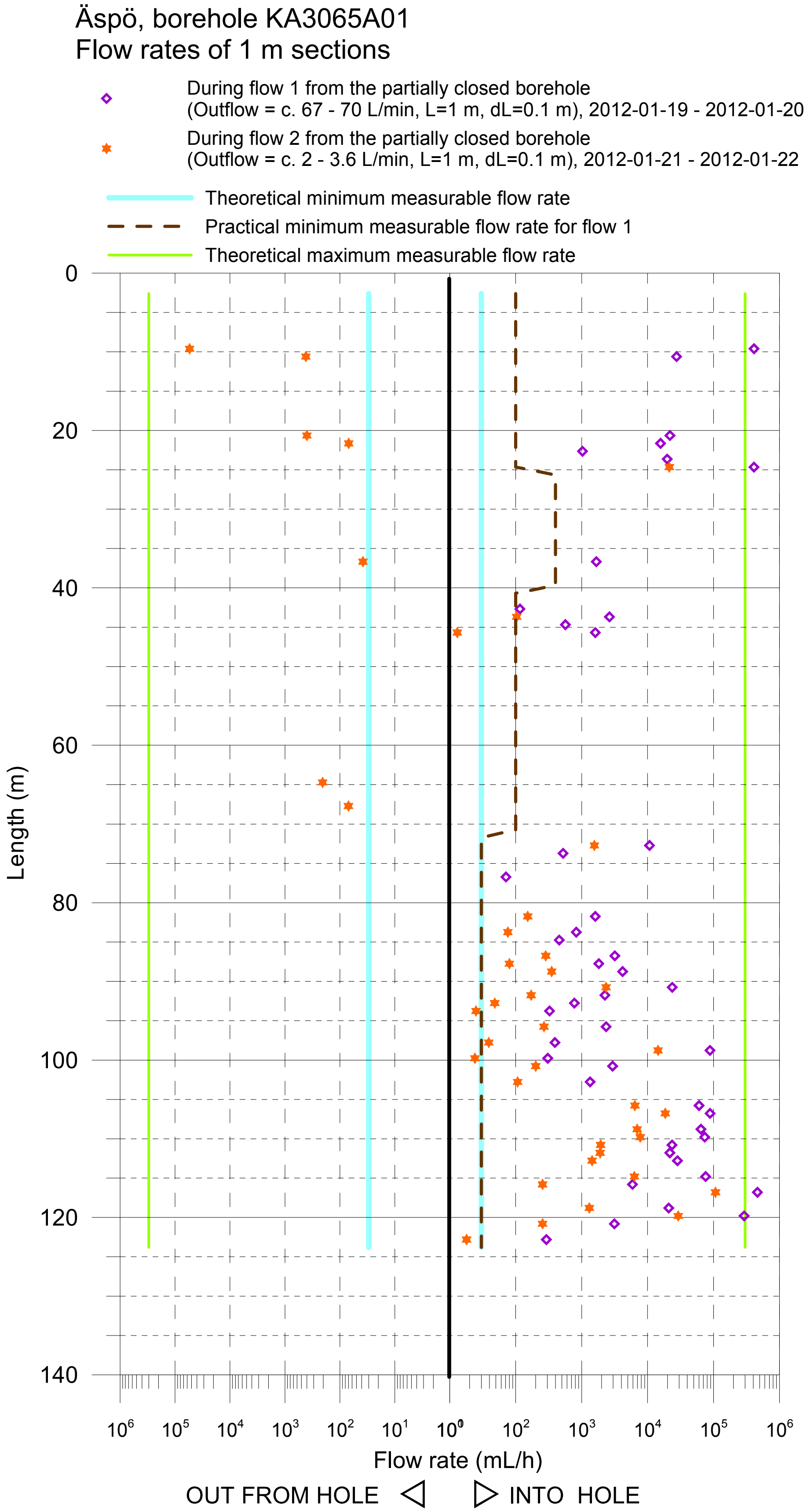

Plotted transmissivity and head of 1 m sections

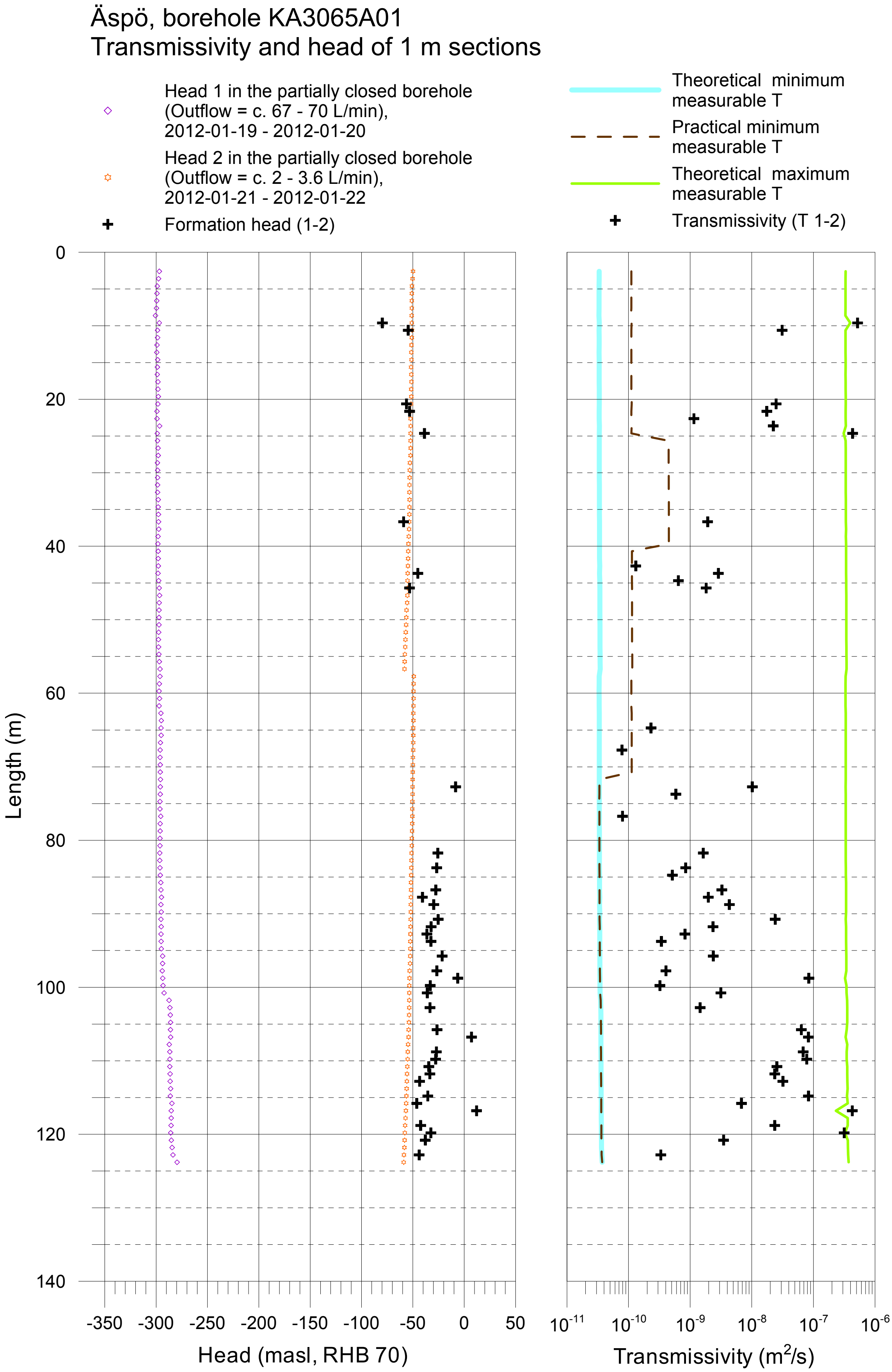

Appendix 17.1

Inferred flow anomalies from overlapping flow logging

Borehole ID	Length to flow anom. L (m)	Lw (m)	dL (m)	Q_1 (m^3/s)	h_{1FW} (m.a.s.l.)	Q_2 (m^3/s)	h_{2FW} (m.a.s.l.)	T_D (m^2/s)	h_i (m.a.s.l.)	Comments
KA3065A01	9.4	1	0.1	2.38E–06	–296.79	–1.19E–08	–50.91	9.6E–09	–52.14	
KA3065A01	10.0	1	0.1	1.12E–04	–297.65	–1.51E–05	–51.05	5.1E–07	–80.33	**
KA3065A01	10.6	1	0.1	7.28E–06	–298.64	–1.08E–07	–50.88	3.0E–08	–54.49	
KA3065A01	10.9	1	0.1	3.64E–07	–298.76	–8.06E–09	–51.06	1.5E–09	–56.42	*
KA3065A01	20.7	1	0.1	6.06E–06	–298.18	–1.11E–07	–51.78	2.5E–08	–56.21	
KA3065A01	21.3	1	0.1	3.53E–06	–298.93	–1.92E–08	–52.10	1.4E–08	–53.43	
KA3065A01	21.7	1	0.1	8.33E–07	–299.30	–	–52.15	3.3E–09	–	¤
KA3065A01	22.9	1	0.1	2.86E–07	–299.34	–	–52.27	1.2E–09	–	¤
KA3065A01	23.4	1	0.1	5.50E–06	–296.62	–	–52.11	2.2E–08	–	¤
KA3065A01	24.3	1	0.1	1.14E–04	–297.61	5.92E–06	–52.36	4.3E–07	–38.89	**
KA3065A01	24.7	1	0.1	3.78E–07	–298.93	–	–52.27	1.5E–09	–	*, ¤
KA3065A01	37.1	1	0.1	4.64E–07	–297.40	–1.06E–08	–53.60	1.9E–09	–59.02	
KA3065A01	42.7	1	0.1	3.22E–08	–297.84	–	–54.88	1.3E–10	–	*, ¤
KA3065A01	43.9	1	0.1	7.33E–07	–297.83	2.86E–08	–55.05	2.9E–09	–45.19	
KA3065A01	44.5	1	0.1	1.58E–07	–297.66	–	–55.18	6.4E–10	–	*, ¤
KA3065A01	46.0	1	0.1	4.47E–07	–296.98	3.61E–09	–55.39	1.8E–09	–53.42	
KA3065A01	64.9	1	0.1	–	–295.51	–5.72E–08	–49.74	2.3E–10	–	¤
KA3065A01	68.0	1	0.1	–	–295.93	–1.94E–08	–49.76	7.8E–11	–	¤
KA3065A01	72.7	1	0.1	2.97E–06	–295.85	4.33E–07	–50.33	1.0E–08	–8.43	
KA3065A01	73.3	1	0.1	1.45E–07	–295.68	–	–50.26	5.9E–10	–	¤
KA3065A01	77.0	1	0.1	1.97E–08	–295.02	–	–50.55	8.0E–11	–	*, ¤
KA3065A01	82.0	1	0.1	4.47E–07	–296.36	4.22E–08	–51.25	1.6E–09	–25.70	
KA3065A01	83.5	1	0.1	2.30E–07	–296.29	2.11E–08	–51.60	8.4E–10	–26.87	
KA3065A01	84.5	1	0.1	1.27E–07	–296.38	–	–51.70	5.1E–10	–	¤
KA3065A01	86.6	1	0.1	8.83E–07	–295.52	7.92E–08	–51.81	3.3E–09	–27.82	
KA3065A01	87.5	1	0.1	5.06E–07	–295.16	2.22E–08	–51.80	2.0E–09	–40.61	*
KA3065A01	88.4	1	0.1	7.92E–07	–295.18	6.50E–08	–51.87	3.0E–09	–30.11	
KA3065A01	89.2	1	0.1	3.69E–07	–295.07	3.25E–08	–52.00	1.4E–09	–28.55	*
KA3065A01	90.6	1	0.1	6.56E–06	–294.64	6.50E–07	–52.12	2.4E–08	–25.43	
KA3065A01	91.3	1	0.1	6.25E–07	–295.61	4.75E–08	–52.35	2.4E–09	–32.34	
KA3065A01	92.4	1	0.1	2.15E–07	–295.18	1.33E–08	–52.42	8.2E–10	–36.39	
KA3065A01	93.3	1	0.1	9.06E–08	–295.44	6.94E–09	–52.55	3.4E–10	–32.38	
KA3065A01	95.3	1	0.1	5.42E–07	–294.23	6.39E–08	–52.62	2.0E–09	–20.31	
KA3065A01	95.7	1	0.1	1.11E–07	–293.81	1.06E–08	–52.65	4.1E–10	–27.19	
KA3065A01	97.4	1	0.1	1.09E–07	–293.82	1.08E–08	–52.93	4.0E–10	–26.39	*
KA3065A01	98.5	1	0.1	3.00E–07	–293.56	2.14E–08	–53.21	1.2E–09	–34.76	*
KA3065A01	98.9	1	0.1	3.25E–06	–293.54	4.81E–07	–53.35	1.1E–08	–11.67	*
KA3065A01	99.1	1	0.1	2.09E–05	–293.36	3.50E–06	–53.32	7.2E–08	–5.08	
KA3065A01	99.7	1	0.1	8.50E–08	–293.17	6.67E–09	–53.45	3.2E–10	–33.05	*
KA3065A01	101.2	1	0.1	8.17E–07	–290.36	5.58E–08	–53.47	3.2E–09	–36.09	
KA3065A01	103.2	1	0.1	3.72E–07	–286.78	2.97E–08	–53.82	1.5E–09	–33.60	
KA3065A01	105.8	1	0.1	5.19E–06	–286.04	4.92E–07	–54.15	2.0E–08	–29.91	
KA3065A01	106.2	1	0.1	1.16E–05	–286.14	1.29E–06	–54.30	4.4E–08	–25.12	
KA3065A01	107.1	1	0.1	2.46E–05	–285.80	5.14E–06	–54.22	8.3E–08	7.07	
KA3065A01	108.4	1	0.1	1.79E–05	–286.76	1.92E–06	–54.83	6.8E–08	–26.91	
KA3065A01	109.4	1	0.1	6.69E–06	–286.32	6.39E–07	–55.01	2.6E–08	–30.61	*
KA3065A01	110.1	1	0.1	1.37E–05	–286.77	1.51E–06	–55.17	5.2E–08	–26.50	*
KA3065A01	110.8	1	0.1	6.50E–06	–286.70	5.39E–07	–55.47	2.6E–08	–34.57	*
KA3065A01	111.4	1	0.1	6.03E–06	–286.07	5.28E–07	–55.50	2.4E–08	–33.37	*
KA3065A01	112.4	1	0.1	7.11E–06	–286.32	3.50E–07	–55.78	2.9E–08	–43.85	
KA3065A01	112.9	1	0.1	7.47E–07	–286.57	4.92E–08	–55.85	3.0E–09	–39.60	

Inferred flow anomalies from overlapping flow logging

Borehole ID	Length to flow anom. L (m)	Lw (m)	dL (m)	Q_1 (m^3/s)	h_{1FW} (m.a.s.l.)	Q_2 (m^3/s)	h_{2FW} (m.a.s.l.)	T_D (m^2/s)	h_i (m.a.s.l.)	Comments
KA3065A01	114.6	1	0.1	2.11E–05	–286.30	1.75E–06	–56.30	8.3E–08	–35.48	
KA3065A01	115.8	1	0.1	1.64E–06	–284.62	7.08E–08	–56.56	6.8E–09	–46.26	
KA3065A01	116.3	1	0.1	1.28E–04	–285.96	2.97E–05	–56.95	4.3E–07	12.08	**
KA3065A01	118.3	1	0.1	2.61E–06	–285.75	1.61E–07	–57.35	1.1E–08	–42.33	
KA3065A01	119.1	1	0.1	3.19E–06	–285.26	2.02E–07	–57.60	1.3E–08	–42.26	
KA3065A01	119.6	1	0.1	8.08E–05	–285.56	8.08E–06	–57.76	3.2E–07	–32.45	
KA3065A01	120.4	1	0.1	8.70E–07	–285.77	7.08E–08	–58.07	3.5E–09	–37.89	
KA3065A01	122.7	1	0.1	8.08E–08	–283.92	5.00E–09	–58.68	3.3E–10	–43.83	

* Uncertain = The flow rate Q_1 and/or Q_2 is less than 30 mL/h or the flow anomalies are overlapping or they are unclear because of noise.

** Flow rate Q_1 over the measurement limit (300,000 mL/h)

¤ T_D calculation based on assumption that flow rate Q_1 or Q_2 = 0 mL/h

Plotted transmissivity and head of detected fractures

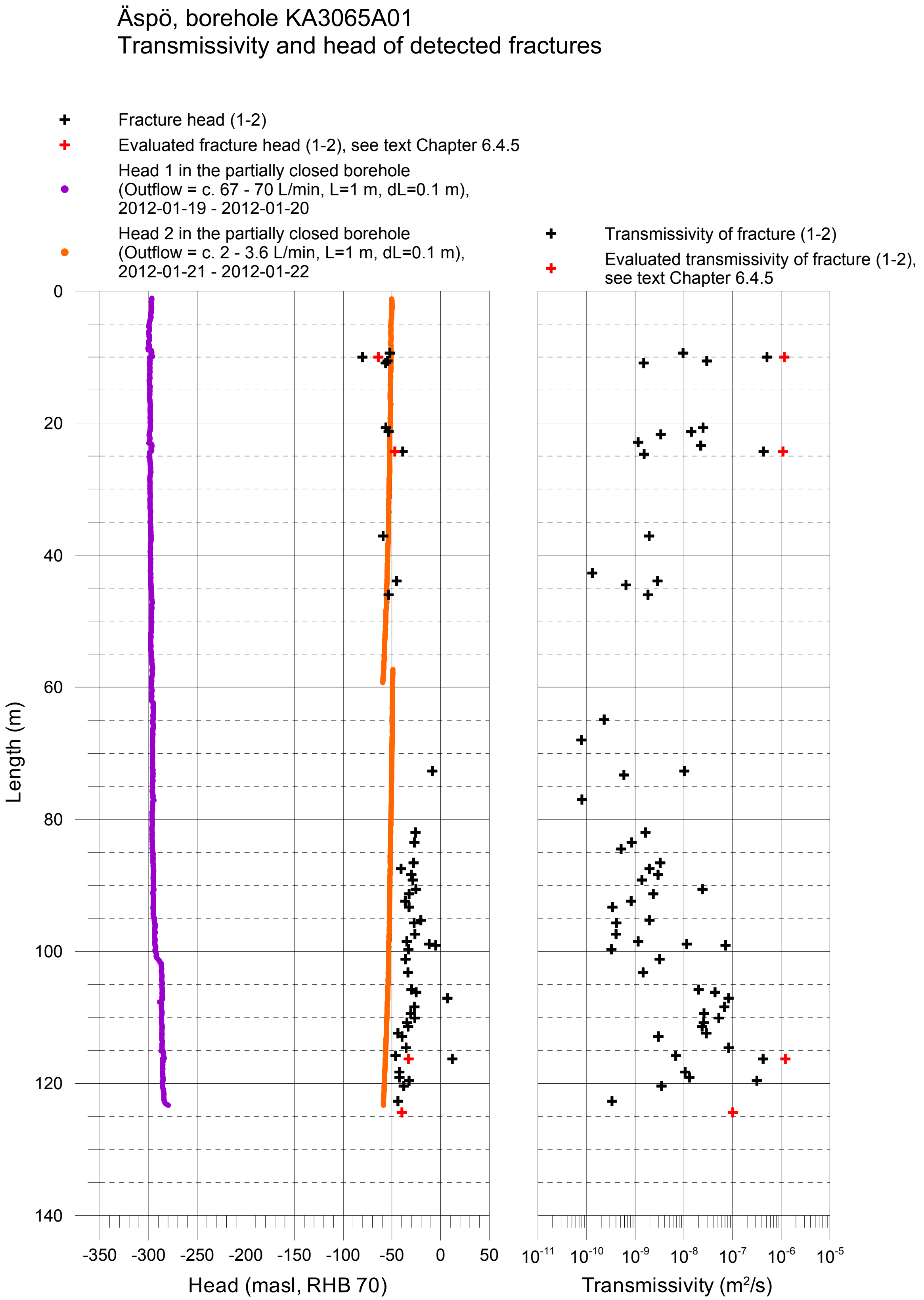

Comparison between section transmissivity and fracture transmissivity

Äspö, borehole KA3065A01
Comparison between section transmissivity and fracture transmissivity

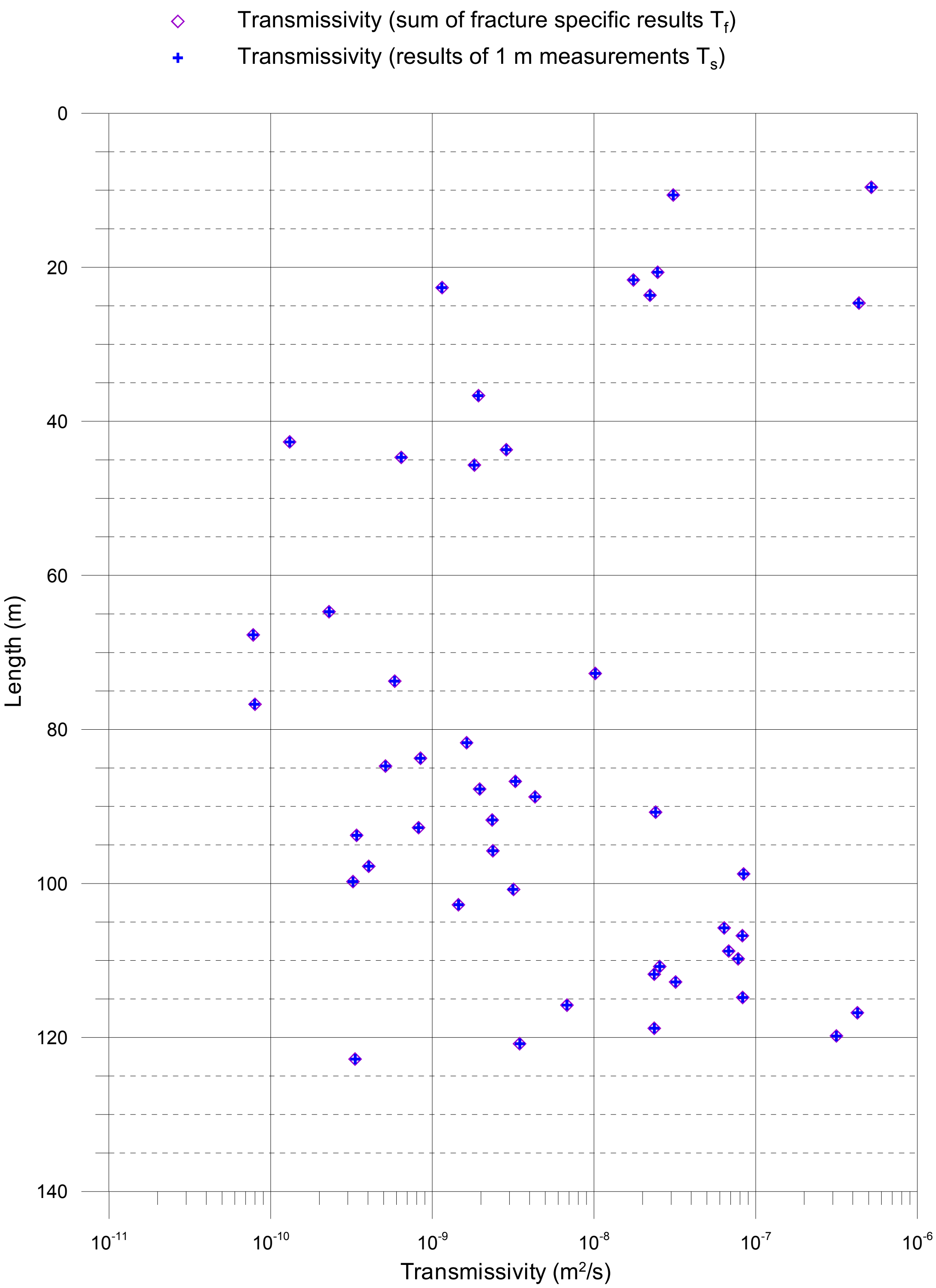

Head in the borehole during flow logging

Äspö, borehole KA3065A01
Head in the borehole during flow logging

Head(masl)= (Absolute pressure (Pa) - Airpressure (Pa) + Offset) /(1000 kg/m^3 * 9.80665 m/s^2) + Elevation (m)
Offset = 2600 Pa (Correction for absolute pressure sensor)

- Partially closed borehole, outflow c. 67 - 70 L/min, (upwards during flow logging, L=1 m, dL=0.1 m), 2012-01-19 - 2012-01-20
- Partially closed borehole, outflow c. 2 - 3.6 L/min, (upwards during flow logging, L=1 m, dL=0.1 m), 2012-01-21 - 2012-01-22

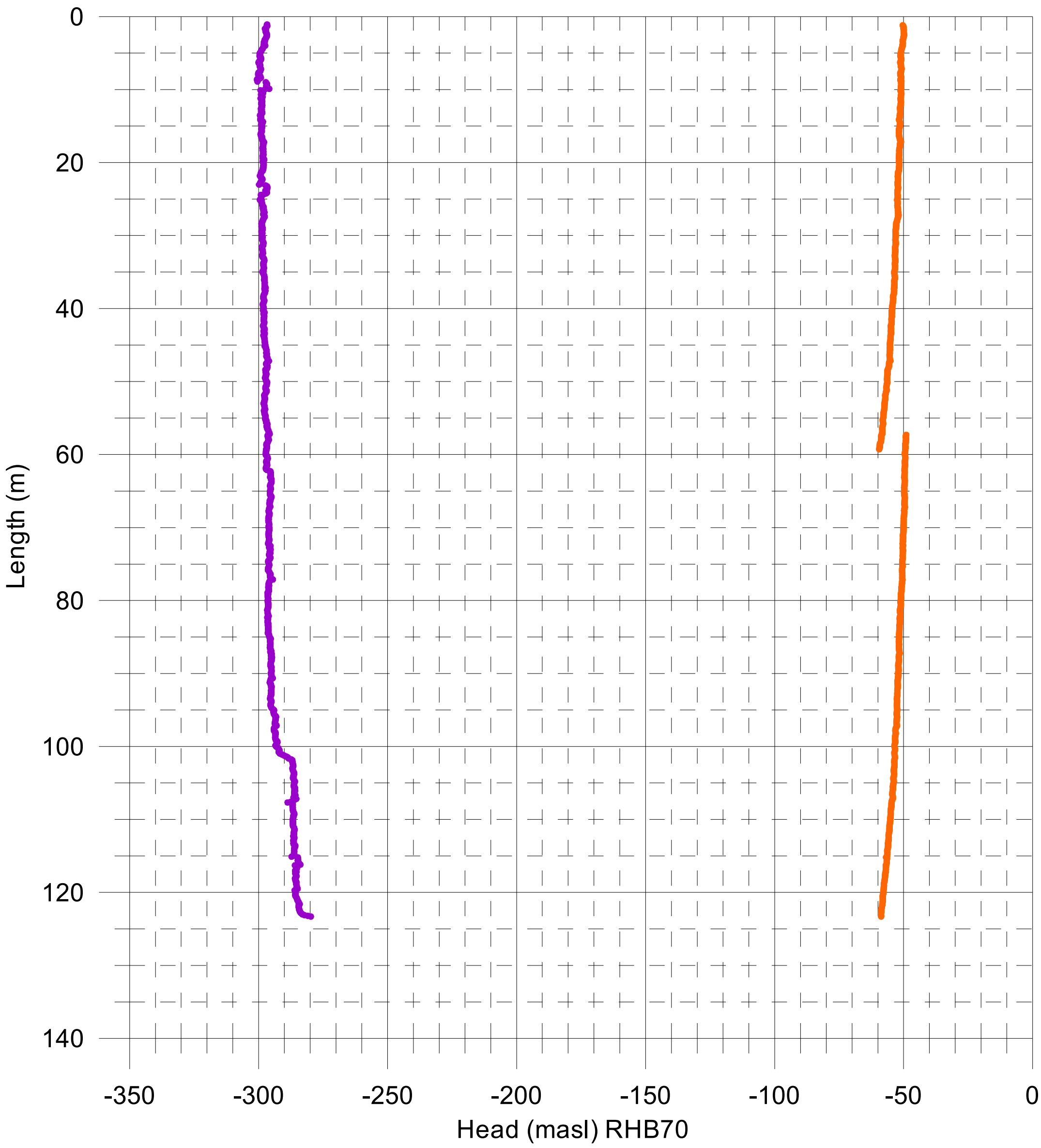

Pressure in the borehole during flow logging

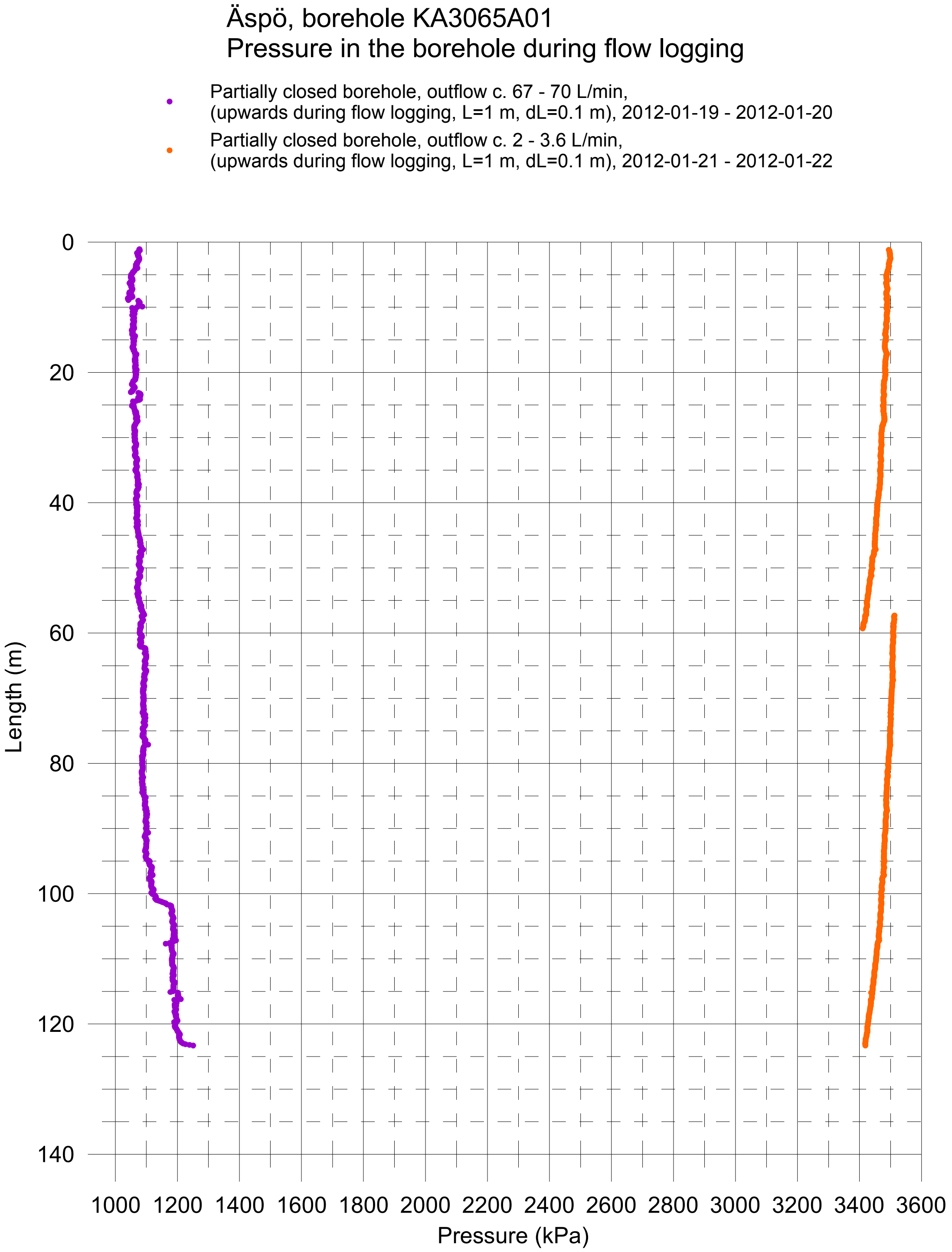

Borehole pressure and outflow from the borehole